MASTER THESIS

DESIGN OF THE ACTINARM A NOVAL PLANAR ACTIVE ARM SUPPORT FOR ASSISTING PEOPLE WITH DUCHENNE MUSCULAR DISTROPHY DURING TABLE-TOP TASKS

Eric Portema

ENGINEERING TECHNOLOGY (CTW)
DEPARTMENT OF BIOMECHANICAL ENGINEERING
BART F.J.M. KOOPMAN

EXAMINATION COMMITTEE
Joan Lobo Prat, MSc
Prof.dr.ir. Herman van der Kooij
Prof.dr.ir. Bart F.J.M. Koopman
Dr. Raffaella Carloni
Dr.ir. Arno H.A. Stienen

DOCUMENT NUMBER
BW - 492

UNIVERSITY OF TWENTE.

3 JULY 2015

Contents

General Introduction

Duchenne Muscular Dystrophy

Duchenne Muscular Dystrophy (DMD) is a progressive muscle disease. It affects mostly boys, approximately 1 in 3500 to 6000 living births, but there are also some rare cases of girls having DMD. DMD is caused by defective mutation in the Dystrophin gene on the X-chromosome. This defect result in that Dystrophin is non-existing or present in very low amounts; $< 3\%$ of the normal amount. Dystrophin is responsible for binding the F-actin at the outermost layer of myofilaments of the muscle cells to the Dystroglycan complex at the cytoskeleton, supporting the strength of the muscle cells. Without it stiffness of the muscle cell will be lower, resulting in the increase of sarcolemmal deformability and a worse mechanical stability of costameres. Also muscle fibers are easier damaged which will eventually result in degradation of muscle into fatty deposits and scar tissue.

DMD follows a certain path during the disease. As age grows the degradation of the muscle will takes place in a specific order from the larger proximal muscles, such as the hip, thigh and the shoulder muscles, towards the smaller distal muscles, such as the lower arm muscles. Also stiffness of the joints and pain will get worse with a growing age.

Usually DMD gets noticed at a young age; usually symptoms occur before the age of 5. At this age boys with DMD show a combination of symptoms like enlarged claves, the need of using the arms to stand up (Gowers sign), and difficulty with walking.

Between the ages of 6 and 12 degradation of the leg muscles continues up to the point where they become wheelchair dependent. Because of the wheelchair dependency and the muscles of the back getting weaker troubles with Scoliosis can occur. Also the shoulder muscles start to become less strong and arm movement gets more difficult.

Between 10 and 16 years of age also the larger muscles of the shoulder and upper arm are weakened quickly. With the use of assistive devices for the upper extremities some level of movement is still possible. In the next few years of the disease also the smaller distal muscles will be affected, but some hand and finger functionality is still present.

Usually around the age of 20 cardiac and respiratory muscles are also affected. Artificial ventilation at night and later on 24 hours a day is needed. In the end cardiac failure will become fatal for most people with DMD. Around half of the people with DMD will reach an age in the 30s.

At this point there are no medicines to prevent or cure DMD. Treatment is symptomatic and can consist of corticosteroid injections to reduce the speed of muscle deterioration, assistive devices to keep some level of movement and possibilities to do things themselves, and physiotherapy to keep the stiffness of the muscles lower resulting in a bigger range of motion (ROM) and less pain. Artificial ventilators can be used to help breathing.

Research Reasons and State of the Art

With increasing life expectancies for DMD men, upper extremity function becomes more important. People with DMD will live with impaired upper extremity function for over 15 years. If left unsupported DMD men may be seriously limited in upper extremity activities and restricted in social participation for the same period of time.

The limitation of functionality and activity level of the upper extremities starts around the age of 11 in a stage of the disease that can be called the late ambulatory stage. Research from Janssen et al. (2014) shows that tasks that can also be related to table top activities are giving problems in the daily life of people with DMD. In the late ambulatory and early non ambulatory stages reaching to and lifting objects is the task that creates most problems in daily life. This is followed by getting dressed and writing. When the disease progresses to the late non ambulatory stage also a shift in problematic tasks is seen. Eating and preparing food, drinking, personal hygiene, and using the computer become most problematic in daily life. Overall eating and preparing food is the activity that causes most problems in daily life due to upper extremity impairment. This is followed by getting dressed and the table top related reaching to object and writing. In every stage of the disease where upper extremities cause problems table top related tasks are a part of that.

Although people with DMD experience large impairments of the upper extremities assistive devices are barely used. The cause of this could be that there are only a limited amount of commercially available devices for supporting the upper extremities and that these few devices do not comply with the demands of the users. They do not cover the wanted range of function and activity, do not give natural support, and mostly are too visible. This is in contrast with the two big wishes of people with DMD regarding assistive devices. These wishes are that the assistive device can give natural support to the upper extremities and is inconspicuous.

Commercially available devices usually can be used in the 3D workspace that is limited by the ROM of the user. They have of the possibility to move the arm of the user in the vertical direction with passive or active support, but for the movements in the horizontal plane there is no support. In this plane the devices heavily rely on friction minimisation. The result is that they become less usable when disease progresses due to higher muscle stiffness and very weak muscles of the men and boys with DMD, and friction losses of the non-ideal components of the device. In case of actuation in the vertical direction the preload for the elastic elements can be adjusted or height can be controlled by using a switch to power the actuators. Most of these devices are clearly visible and recognisable as arm support. Examples of current commercially available devices for the upper extremities are the MAS and the WREX (Jaeco Orthopedic, USA), the Darwing, the Sling (electric) and the Top/Help (electric) (Focal Meditech B.V., The Netherlands), and the Armon Ayura (Microgravity Products B.V., The Netherlands).

To enlarge the usability of the device and to get natural arm movement for the user, external forces should be applied to the arm. Therefore active actuation for movement of the arms is needed. A big problem with this is that for active actuation the needed actuators will make the device more visible.

Next to the commercially available devices that can be used at home or on a wheelchair, there are a lot of actively actuated research and rehabilitation devices. These devices are more specific to a task or purpose and therefore differ more in design. For example the MIT-Manus is actively actuated in the horizontal plane (2DOFs) for the arms and can have a wrist extension which actuates another 3DOFs. It uses impedance control to calculate the forces given to the user by the actuators. Its purpose is training and rehabilitation and therefore it does not have to be inconspicuous and the bar linkage over the table can be clearly seen. Another rehabilitation device that also really visible, is the HapticMASTER (Moog B.V., The Netherlands). It can actively control the position of the user in the 3D workspace by using admittance control. It is a stand-alone device consisting of a series of three actuators.

A device that shows that active actuation causes a greater visibility is the WREX with active actuation. Two series elastic actuators are added to actively support shoulder and elbow movements of the user. Force input is used to control the devices and therefore the users movement. The actuators are quite large, therefore making the size of the device bigger and less inconspicuous.

Fully actuated exoskeletons for the upper extremities, to assist arm movement, can support every movement of the arm in every direction. Usually six or more DOFs are actively actuated and can be controlled with force or EMG input of the user. Problems with the user can occur if the joints of the exoskeleton and the user are not properly aligned. The linkage and actuators cause the exoskeleton to be clearly visible.

An active assistive device that is close to commercial availability and is already a lot more inconspicuous than the fully actuated assistive devices, is the McArm (Focal Meditech, The Netherlands). It is an exoskeleton type of device that supports all movements in the 3D workspace. Several more DOFs are available for alignment issues. The user needs to put the arm in an arm cup, where the force of user is measured and an appropriate amount of force is added by the actuators to make the movement as natural as possible. The device can be mounted to wheelchair and although it is a lot more inconspicuous, it is still as clearly visible as the non-actuated commercially available devices.

It can be concluded that none of the discussed devices comply with both of the wishes of people with DMD. Therefore a new device will be developed, which is called the ActInArm.

Design of the ActInArm is part of the Flextension project. The Flextension project is there to develop an inconspicuous assistive device that gives natural support to the upper extremities. It is a body worn passively actuated exoskeleton that can be worn underneath clothes, therefore making it inconspicuous. After the passively actuated device an actively actuated device was the next step. A one degree of freedom elbow device for assisting eating and drinking is already made. This device is actively actuated and multiple types of control to let the device give natural support to the arm are researched. To extend this research a two degree of freedom actively actuated device that gives natural support in the 2D horizontal plane is the next step.

Design of the ActInArm - a novel planar active arm support for assisting people with Duchenne Muscular Dystrophy during table-top tasks

Eric Portema[1], Joan Lobo-Prat[1], Herman van der Kooij[1,2], Bart F.J.M. Koopman[1], Raffaella Carloni[3] and Arno H.A. Stienen[1,4]

[1]Department of BioMechanical Engineering, University of Twente, Enschede, The Netherlands

[2] Biomechanical Engineering, TU Delft, Delft, The Netherlands

[3] Robotics and Mechatronics, University of Twente, Enschede, The Netherlands

[4] Department of Physical Theraphy and Human Movement Science, Northwestern University, Chicago (IL), USA

Email: e.portema@student.utwente.nl

***Abstract*—Men and boys with Duchenne Muscular Dystrophy (DMD) suffer from a progressive muscle disease causing the skeletal, respiratory, and cardiac muscles to deteriorate, leading to loss of independent ambulation, loss of upper extremity function, and breathing and heart problems. The loss of movement of the upper extremities causes a lot of problems in daily life and table top related tasks make up a big part of this.**

A big wish from boys and men with DMD is have an inconspicuous assistive device that can give natural arm support. Current commercially available devices do not comply with these wishes and do not cover the complete range of function and activities.

The main goal of the novel device, the ActInArm, is to give active arm support in a planar surface from an inconspicuous device so that boys and men with DMD can move their arms again.

The ActInArm is an inconspicuous device that consists four big parts: a hollow table, the actuators, an arm cart, and a magnetic coupling. Inside the hollow table the two actuators that move an end effector in the horizontal plane are positioned. On top of the table's surface there is an arm cart in which the user can lay their arm in. The movements of the end effector of the actuators and the user's arm are coupled over distance by the magnetic coupling. One magnet is attached to the end effector and one to the arm cart. Movement of the arm cart is controlled by the user's own intention, giving a natural feeling.

Implementation of the ActInArm concept showed that a user could move its own arm intentionally over a workspace of $410mm \cdot 260mm$ with very little muscle effort. By hiding the actuators inside the table and replacing the table many boys and men with DMD already have on their wheelchair, the ActInArm can be considered to be inconspicuous.

I. Introduction

Duchenne Muscular Dystrophy (DMD) is the most common muscular dystrophy affecting 1 in 3500-6000 living male births [1]. DMD is caused by the absence or defect of the dystrophin protein [1]. Defective mutations in the dystrophin gene result in progressive degeneration of skeletal, respiratory and cardiac muscles leading to loss of independent ambulation in the early teens, followed by the development of scoliosis and loss of upper extremity function. The life expectancy of boys with DMD has improved substantially due to improvements in care, drugs and the introduction of home care technology. As a result, currently there is a considerable group of adult DMD patients living with severe physical impairments and a strong dependency on care [2].

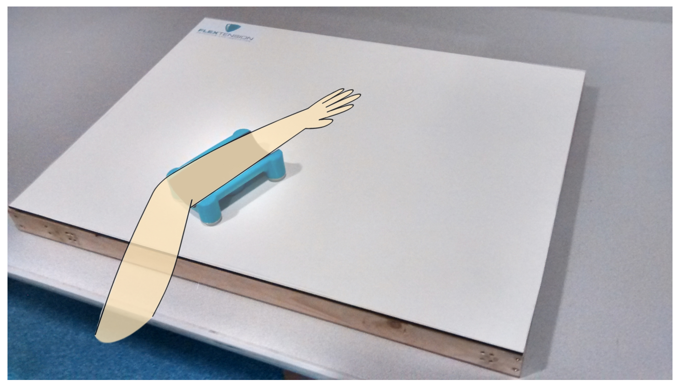

Fig. 1: The ActInArm, a novel design of an actively actuated inconspicuous arm support.

A special characteristic of DMD is that patients lose the ability to move their arms due to the weakening of proximal muscles, while distal muscles, such as hand and finger muscles, remain less affected [3]. Therefore, DMD patients can benefit from devices that support the arm movement taking advantage of the user's residual hand function and proprioception.

Commercially available assistive devices, like the Top/Help, the SLING (both Focal Meditech B.V., The Netherlands [4][5]), and the MAS (Jaeco Orthopedic, USA[6]), have the capability to move in the 3D space. They support the weight of the arm with elastic elements, but mostly are non-actuated in the 2D horizontal plane and therefore heavily rely on friction minimization. Because of this these devices become insufficient at the last stages of the disease, when patients can barely produce any force to overcome the friction with their muscles [7][8].

Therefore, adult DMD patients can potentially benefit more from active arm supports, which are able to provide the assistance that adult patients need for the performance of basic activities of daily living.

However current actively actuated devices, such as the MIT-Manus [9] and research exoskeletons (e.g. WREX, Jaeco Orthopedic, USA[10]), are simply not usefull in daily life due to their size. Also they are not used by boys and men with DMD because of their presence.

In an international survey [11] it was concluded that for boys and men with DMD table top related activities, like reaching to objects, writing, and using the computer, belong to activities that caused most problems in daily life. The same research also concluded that effective and adequate aids as well as attention for pain and stiffness in therapeutic management could help to reduce upper extremity activity limitations and restrictions in social participation.

A big wish from boys and men with DMD is inconspicuous of these assistive devices [12][13]. The earlier stated examples are not inconspicuous and therefore do not comply with this wish.

The main goal is to actively support the arm movement of boys and men with DMD in a planar surface so they can move their arms again.

The novelty of this assistive device, the ActInArm (Fig. 1), is that it will actively support the arm movements and does comply with the big wish of boys and men with DMD, to have an inconspicuous assistive device.

II. Requirements and Implications

A. Workspace and Degrees of Freedom

The required workspace can be determined with anthropometric data [14][15] and workspace analysis (human linkage) [14]. With this data the normal working area (NWA) the area you can easily sweep with your hand can be determined. Tasks like writing using the computer are conducted within this area. The area of reaching tasks can be described by the zone of convenient reaching (ZCR) (Table I). For boys and men with DMD the NWA and ZCR will be a bit smaller due to stiffer joints.

To move an arm over the planar workspace at the endpoint 3 degrees of freedom are needed. Two for the position in the plane and one for the orientation of the forearm, because the orientation of the fore arm is a unique solution of the position of the shoulder and the lengths of the arm segments.

TABLE I: An approximation of the dimensions for the different application areas for two arms. Origin is at the crossing point of the midian plane of the human body with the table's edge.

Area	X-direction		Y-direction	
	min	max	min	max
NWA	-500mm	500mm	0mm	400mm
Writing task	-250mm	250mm	50mm	300mm
Reaching task (ZCR)	-800mm	800mm	0mm	550mm

B. Inconspicuousness

As stated earlier, one of the key aspects of the device is its inconspicuousness. This is a big wish for people with DMD [12][13]. To make this device inconspicuous actuators need to be hidden or really small. Also the human machine interface, where the arm is connected to the device, needs to be barely visible. This puts a boundary on the dimensions of the necessary parts. Also the thickness of the table needs to be as small as possible.

Because boys and men with DMD are wheelchair bounded the maximum width of the device is limited to the dimensions of the wheelchair and the dimension of everyday obstacles one will interact with, like doors and hallways. Therefore the maximum width of the device may not be larger than 800mm.

C. Power

To actively assist the movement of the users arm a source of force is needed. This force is will generate a movement and thus a velocity. The maximum needed force is determined by dynamic data from heathy subjects and is set to 10N. The maximum velocity will be set to 100mm/s for safety reasons.

D. Safety

Safety is an important requirement of the machine and should always be guaranteed. Because the users have high skin sensitivity and cannot generate enough force by themselves to detach from the machine the acceleration should be smooth, and the maximum force and velocity should be limited. Also there should be a possibility to limit the workspace so the joint extremities of the user cannot be reached. Finally the user should be able to stop the machine at all times with an emergency stop button.

III. Conceptual Design

The concept of the ActInArm consists of a hollow table in which all the active components, such as the actuators and the controller, will be placed to get the desired level of inconspicuousness. The end effector describes a planar workspace and is actuated by two perpendicular actuators. On top of the table's surface there is an arm cart where the user can lay their arm in. The movements of the actuators and the arm cart are coupled to each other with two magnets. One at the end effector of the actuators and one on the arm cart at the user's side (Fig.2).

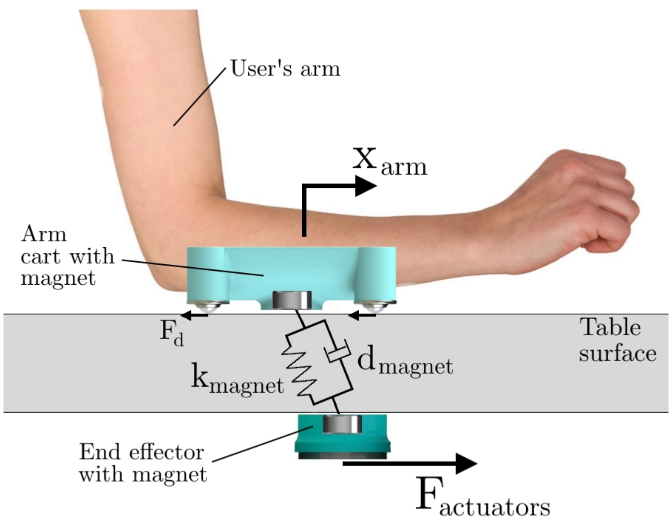

Fig. 2: The concept of arm movement with the ActInArm. The actuators exert a force ($F_{actuators}$) on the end effector with the magnet that will start moving. This causes the conceptual line through the magnets centers to be under an angle, resulting in a force component acting on the arm cart in the direction of the end effector's movement. Before the arm cart with the user's arm starts moving (x) drag force (F_d) of the arm cart on the table has to be overcome. The stiffness (k_{magnet}) and damping (d_{magnet}) of the magnetic coupling are dependent on the distance between the magnets at the arm cart and the end effector.

A. Arm placement

Placement of the arm in the arm cart it is important for a correct working of the complete device. To give enough support and stability to the arm, and to be comfortable for the user, the radius of the arm cup corresponds with the radius of the users forearm and the length is such that the fore arm stays horizontal. Placement of the fore arm in the arm cart is such that the centre of mass of the arm lies inside the boundaries of the arm cart (Fig. 3).

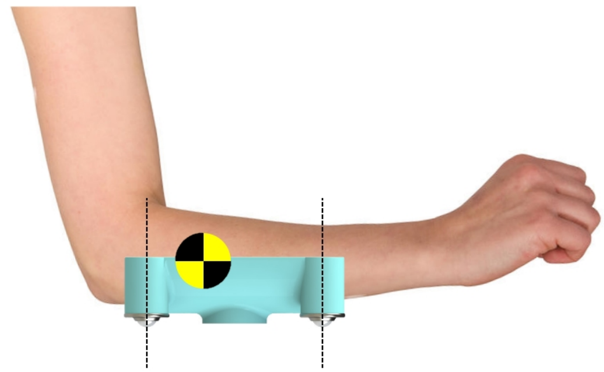

Fig. 3: The center of mass of the arm should be between the wheels of the arm cart (depicted by the striped lines).

B. Magnetic coupling

The magnetic coupling couples the users arm and the actuators below the table surface with two magnets. It releases the rotational degree of freedom and therefore the orientation of the arm is always correct and does not have to be controlled. It is important that the stiffness between the two is high enough so the arm stays coupled to the actuators while moving. To enlarge the interaction between the two magnets, cups of high permeability material are made to redirect the magnetic field through the cups rather than through the air. An advantage of shaping the magnetic field is that the field can be contained in a smaller area so interaction with ferromagnetic materials and electronics will be reduced significantly and the device will be safer to use (Fig. 4).

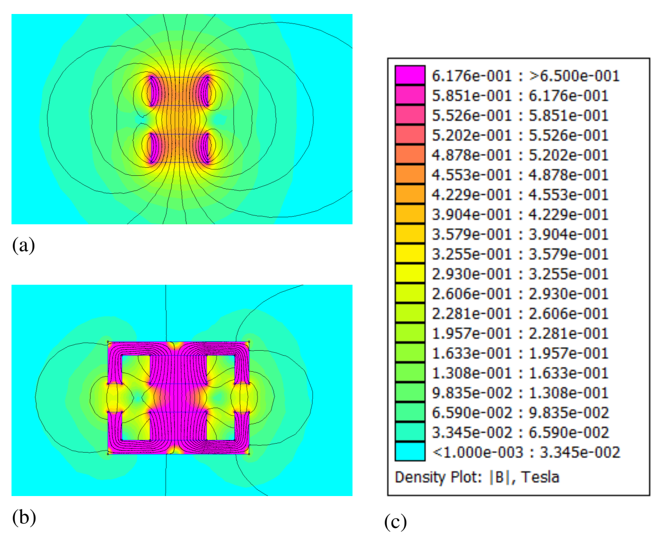

Fig. 4: An example of the difference in field shape and strength between two magnets without and with cups of high permeability material (a & b). Colors (c) are representing the field strengths [T]. The pictures are generated using Femm4.2 [16].

IV. Implementation

The designed assistive device can be divided into four main parts; 1. The table, 2. The Actuators, 3. The magnetic interface, and 4. The arm cart (Fig. 5).

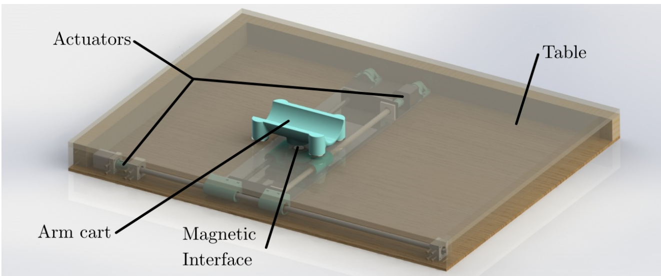

Fig. 5: A 3D CAD impression of the ActInArm concept. The table top and two wooden frame parts have been made transparent to make the actuators below the table top visable.

A. Mechanics and actuation

To make movement of the end effector in the horizontal plane possible two actuators that are perpendicular to each other are used (Fig. 6). Each actuator consists of a stepper motor (Oriental Motors PKP223D15A-L, Oriental Motors Co. Ltd., Japan) that drives a lead spindle (Tr12x3). The lead spindle and stepper motor are connected to each other with a 3d printed flexible coupling. The dimensions of the lead spindle are determined using the critical speed calculations [17] of the spindle and the maximum force the stepper motors could deliver.

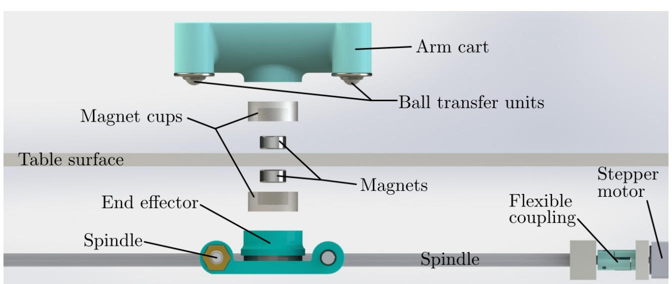

Fig. 6: A 3D CAD impression of the drivetrain of the ActIn-Arm prototype.

The arm cart is an arm cup that is supported by four ball transfer units (515-0-14, Alwayse Enginering Ltd., England). The diameter of the cup is 70mm, has a length of 120mm, and is padded with a soft foam material. The arm cart holds a permanent magnet at the bottom's center to be coupled with the permanent magnet that is attached at the end effector of the actuators. Both magnets have a steel cup around them to redirect the magnetic field. This makes the stiffness of the couple higher and reduces the risk of attracking metal objects.

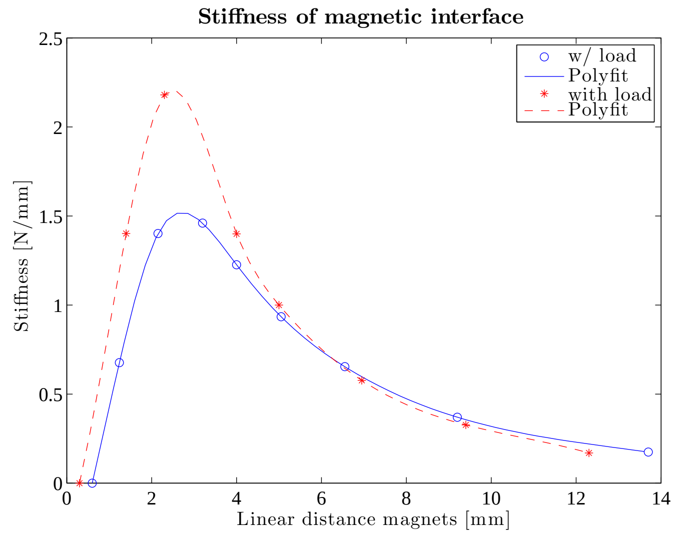

Fig. 7: The measured stiffnesses of the magnetic interface with (dashed red line) and without (solid blue line) a load of 2kg in the arm cart. The distance, is the horizontal distance between the two magnets.

The stiffness of the magnetic interface is maximally 2.2N/mm (Fig. 7).

B. Sensors

To sense the position of the end effector at the actuator side, potentiometers (X-direction: SP-L-0500-103-3%-ST, Y-direction: SP-L-0400-103-3%-ST, Spectra Symbol, USA) in combination with wipers(WP-M6-01-03-014-DI, Spectra Symbol, USA) are used. For sensing the user intention an Olimex EKG/EMG shield (SHIELD-EKG-EMG, Olimex Ltd., Bulgaria) is used in combination with snap connector EKG/EMG cables (SHIELD-EKG-EMG-PRO, Olimex Ltd., Bulgaria) and gel electrodes. All the sensors send their analog signal to a microcontroller (Arduino Mega2560, Arduino Project, Italy) where it is digitalized with a sampling frequency of 100Hz into a 10-bit value .

C. Control

EMG control, from each muscle the raw EMG signal is filtered to get a smooth control signal. Filtering is done by using a digital second order high pass Butterworth filter at 3Hz, retification of the signal, and using a second order low pass Butterworth filter at 20Hz.

From one muscle pair the signals are subtracted and normalized with the maximum voluntary isometric contraction (MVIC). This signal is the input for a virtual model to get the desired velocity and direction. The desired velocity is expressed as a frequency of pulses where every pulse

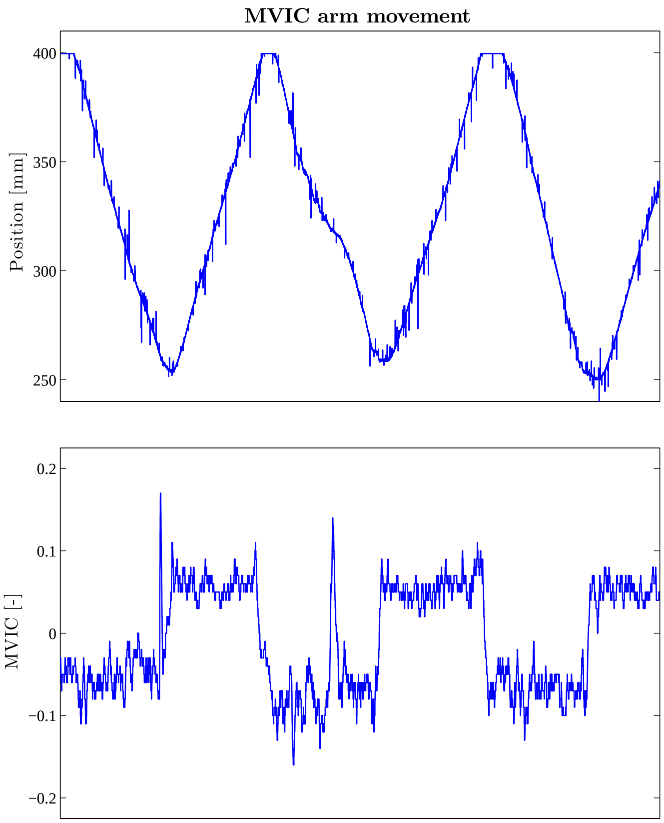

Fig. 8: The result of the validation. Plotted are the position of the end effector (top) and the normalized EMG signal, MVIC (bottom). Targets were positioned at 250mm and 400mm.

represents one step. The stepper motor driver (Big Easy Driver v1.2, Schmalz Haus LLC, USA) controls the step resolution of the stepper motor. With this type of control the arm of a healthy subject could be moved with little effort (Fig. 8).

To measure the bandwidth of the ActInArm prototype a sinusoidal input as desired velocity is chosen. The position output is logged with the potentiometers and differentiated once to get the output velocity. Transfer function is from desired velocity to output velocity.

V. Validation

A. Workspace

The actively supported workspace of the end effector is 410mm by 260mm. This workspace is larger than is needed for table top related tasks like writing and using the computer. Also for tasks like reaching for objects the workspace is large enough, because the fore arm and hand of the user are enlarging the workspace of the assistive device.

B. Inconspicuousness

Although the outer dimensions of the device are quite large, $800mm \cdot 600mm \cdot 55mm$ (width · depth · thickness), and the table is clearly visible, it can be said that it is inconspicuous. This because the table most people with DMD have on their wheelchair is also quite large and will be replaced by the ActInArm which is of approximately the same size. Also the actuators of the device are hidden, giving the user the idea that they make the movement themselves because the only moving things are the arm and arm cart. This also makes the device more inconspicuous.

C. Power

Although the intended maximum velocity and the maximum force are not met with the implemented materials ($F_{max} = 7.8N \pm 0.8N, v_{max} = 28.8mm/s$) the power of the device supports movements of a user (Fig. 8). Movements using less than 0.5MVIC can be considered to be easy to execute, where the MVIC using the ActInArm stayed below 0.1. The maximum force is measured at the arm cart. The magnetic coupling, which is the dominant factor in the stiffness and maximum force, reduces the maximum force applied to the user.

D. Safety

The implemented magnetic coupling is the dominant factor in the maximum force the user could experience. The arm cart will decouple from the actuators at forces exceeding $F_{max} = 7.8N \pm 0.8N$. With a maximum acceleration and deceleration of around $100mm/s^2$ in normal working conditions, the force acting on the users arm will stay well below the maximum force.

It was measured that with the magnetic cups at the magnetic coupling the area in which attraction of metal objects occurred stayed within the outer dimensions of the arm cart.

E. Bandwidth

The bandwidth of the ActInArm prototype is around 3Hz (Fig. 9). Healthy humans require a control bandwidth of $1-2Hz$ newly introduced actions, repetative actions a bandwidth of $2-5Hz$ [18]. For people with DMD a bandwidth of 3Hz should be enough to make newly introduced and repetative movements using the ActInArm prototype.

VI. Conclusions and Future Work

Combining all the results from the implementation and validation it can be concluded that the conceptual idea of the

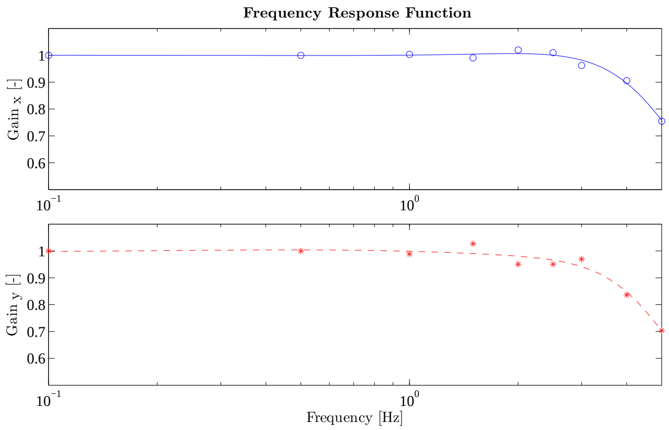

Fig. 9: The frequency response functions (FRF) of the assistive device in the X- and Y-direction ($Gain_x$ & $Gain_y$). The FRFs are the open loop functions from the desired velocity to the measured velocity and are measured without a load in the arm cart.

ActInArm works. The device can be considered inconspicuous and actively supports movements of the arm in two degrees of freedom over a workspace of 410mm by 260mm. This could be seen by the low amount of muscle activation during the movement (Fig. 8). With a measured bandwidth of 3Hz, newly introduced and some repetative action could be performed by a user using the ActInArm.

However, the drivetrain used in the prototype was causing a few problems like non smooth movements due to missed steps, sound issues, and a lower than expected velocity due to the needed amount of pulses per second from the microcontroller. These issues can all be tackled when the stepper motors are replaced by permanent magnet DC motors.

Verification of the ActInArm prototype is done with a healthy subject. To be sure that the device actually works for men and boys with DMD there should be clinical testing with this target group. Within this test multiple control methods as proposed by Lobo-Prat [19] can be tested to have the most suitable control for this device.

References

[1] A. E. Emery, "The muscular dystrophies," *The Lancet*, vol. 359, no. 9307, pp. 687–695, 2002.

[2] B. Bartels, R. F. Pangalila, M. P. Bergen, N. A. Cobben, H. J. Stam, and M. E. Roebroeck, "Upper limb function in adults with duchenne muscular dystrophy," *Journal of rehabilitation medicine*, vol. 43, no. 9, pp. 770–775, 2011.

[3] E. M. Yiu, A. J. Kornberg *et al.*, "Duchenne muscular dystrophy," *Neurology India*, vol. 56, no. 3, p. 236, 2008.

[4] F. Meditech, "Sling." [Online]. Available: http://www.focalmeditech.nl/nl/content/sling

[5] ——, "Top/help." [Online]. Available: http://www.focalmeditech.nl/nl/content/tophelp

[6] Jaeco Orthopedic, "Standard mas." [Online]. Available: http://jaecoorthopedic.com/products/products/Standard-MAS-w%7B47%7D-Adjustable-Mount.html

[7] T. Rahman, R. Ramanathan, S. Stroud, W. Sample, R. Seliktar, W. Harwin, M. Alexander, and M. Scavina, "Towards the control of a powered orthosis for people with muscular dystrophy," *Proceedings of the Institution of Mechanical Engineers, Part H: Journal of Engineering in Medicine*, vol. 215, no. 3, pp. 267–274, 2001.

[8] A. Kumar and M. F. Phillips, "Use of powered mobile arm supports by people with neuromuscular conditions," *Journal of rehabilitation research and development*, vol. 50, no. 1, pp. 61–70, 2013.

[9] N. Hogan, H. I. Krebs, J. Charnnarong, P. Srikrishna, and A. Sharon, "Mit-manus: a workstation for manual therapy and training. i," in *Robot and Human Communication, 1992. Proceedings., IEEE International Workshop on*. IEEE, 1992, Conference Proceedings, pp. 161–165.

[10] Jaeco Orthopedic, "Wrex: Wilmington robotic exoskeleton arm." [Online]. Available: http://jaecoorthopedic.com/products/products/WREX%3A-Wilmington-Robotic-EXoskeleton-Arm.html#

[11] M. M. Janssen, A. Bergsma, A. C. Geurts, and I. J. de Groot, "Patterns of decline in upper limb function of boys and men with dmd: an international survey," *Journal of neurology*, vol. 261, no. 7, pp. 1269–1288, 2014.

[12] A. Dunning and J. Herder, "A review of assistive devices for arm balancing," in *Rehabilitation Robotics (ICORR), 2013 IEEE International Conference on*. IEEE, 2013, Conference Proceedings, pp. 1–6. [Online]. Available: http://ieeexplore.ieee.org/xpls/abs_all.jsp?arnumber=6650485&tag=1

[13] T. Rahman, S. Stroud, R. Ramanathan, M. Alexander, R. Alexander, R. Seliktar, and W. Harwin, "Consumer criteria for an arm orthosis," *Technology and Disability*, vol. 5, no. 2, 1996.

[14] S. Pheasant and C. M. Haslegrave, *Bodyspace: Anthropometry, ergonomics and the design of work*. CRC Press, 2005.

[15] TU Delft, "Dined anthropometric database." [Online]. Available: http://dined.io.tudelft.nl/dined/

[16] D. Meek, "femm4.2," 2013. [Online]. Available: http://www.femm.info/wiki/HomePage

[17] Kruger Ventilation, "Critical speed of shafts," pp. 1–5, 1998. [Online]. Available: http://www.krugerfan.com/brochure/publications/Tbn017.pdf

[18] B. van Ninhuijs, L. van der Heide, J. Jansen, B. Gysen, D. van der Pijl, and E. Lomonova, "Overview of actuated arm support systems and their applications," in *Actuators*, vol. 2, no. 4. Multidisciplinary Digital Publishing Institute, 2013, pp. 86–110.

[19] J. Lobo-Prat, P. N. Kooren, A. Q. Keemink, M. I. Paalman, E. E. Hekman, P. H. Veltink, A. H. Stienen, and B. F. Koopman, "Design and control of an experimental active elbow support for adult duchenne muscular dystrophy patients," in *Biomedical Robotics and Biomechatronics (2014 5th IEEE RAS EMBS International Conference on*. IEEE, 2014, Conference Proceedings, pp. 187–192.

General discussion

Benefits for people with Duchenne Muscular Dystrophy

With the ActInArm people with DMD have an assistive device with active actuation that is inconspicuous and gives natural support to the upper extremities during table top related activities. Because of this, drawbacks other devices have, like unnatural arm support and a high visibility, do not longer exist. Therefore, the ActInArm is more likely to be accepted and used in daily life.

Although it cannot be concluded that the ActInArm works at people with DMD, it can be discussed that the result of moving with little muscle force using a healthy subject is also applicable for the target group of the device. The target group of the ActInArm are people with DMD that are in the later non ambulatory stages of the disease where active support of arm movement is beneficial. But, also people with DMD that are in the earlier stages of the disease can use the device. The ActInArm can be used by people with different arm sizes without many changes to the device. For comfort reasons the arm cart could have different dimensions. Also the control type and controller gain, how much support will be given by the ActInArm, is adjustable.

The type of control is adjustable, because it is still unknown what type of control is best and because the best type of control is dependent on the users feeling. Next to the already implemented EMG-input for the controller, the ActInArm is also suitable to use user force as a control input to the device. However, using force as an input could be problematic with users that can only produce low forces because friction of the arm cart with the table must be overcome before the active assistance is applied to the users movement.

The custom sized arm cart, and the adjustable control type and controller gain are there to maximize the sensation of natural arm support experienced by the user and to make the devices usability as high as possible.

The inconspicuousness of the device and the sensation of natural support should allow for a higher acceptance and more frequent usage of the ActInArm. Arm movement of people with DMD can be seen as therapeutic. Therefore, as a result of more frequent usage of the device the effects of the deterioration of the upper extremity muscles could have a little bit less influence on the daily lives of boys and men with DMD. This means that there could be some positive benefits regarding pain, stiffness of the joints, and the range of motion of the upper extremities.

With the ActInArm some of the activities that give the most problems like reaching to objects, writing, using the computer, playing video games/control

TV/using telephone, and using books can be performed again. The part of the people with DMD saying that one of these activities causes the most problems in daily life is around one third of the total DMD population. Also other activities like play and crafts, and controlling the wheelchair are table top related activities and these can also be performed again by the men and boys with DMD themselves.

The inconspicuousness of the ActInArm and the regained ability of the boys and men with DMD to move their arm and performing activities again by themselves, take some social limitations away. By taking some of these social limitations away, social participation can be greater which could have a positive effect on the well-being and quality of life of boys and men with DMD.

Comparison to the State of the Art

Compared to commercially available and the state of the art in assistive devices for the upper extremities the ActInArm differs in a number of points.

Two of the features of the ActInArm that are new to assistive devices are the combination of active actuation with inconspicuousness of the device and the magnetic coupling between the actuators and the arm of the user.

In the current commercially available devices and state of the art, active actuation results in a device that can be easily noticed. The other way around is that the existing inconspicuous assistive devices only have passive actuation at most, not giving enough arm support at the later stages of the disease. To achieve active actuation with the ActInArm in an inconspicuous way meant that the actuators needed to be hidden and could not be directly fixed to a mechanism that is directly attached to the arm. This resulted in the replacement of a fixed coupling by a flexible coupling based on magnetics. Such an implementation of a magnetic coupling between the actuators and the users arm in the assistive devices application has not been done before.

Although the ActInArm is quite large ($800 \cdot 610 \cdot 55mm$) in comparison with the other devices and can be seen quite easily, the positioning of it and the hidden actuators makes it inconspicuous. The ActInArm replaces an existing table most boys and men already have on their wheelchair. Therefore, it looks like there is no visible external force acting on the users arm. All the other assistive devices are an addition to the wheelchair and the arm of the user. Therefore, these devices can be regarded as conspicuous.

Regarding degrees of freedom and workspace the ActInArm has less DOFs and a smaller workspace than most other assistive devices for the upper extremities. The ActInArm has two actively actuated DOFs for the movement in the horizontal plane and one passive DOF for the orientation of the users arm. The arm cart of the ActInArm is actuated over a workspace of $410mm \cdot 260mm$. However, the reach of the user is bigger than this workspace because of how the forearm of the user is positioned in the arm cart. Other devices usually have the possibility to move the arm in a 3D space and use at least 3DOF for movement in this space and more DOFs to account for alignment and orientation purposes. Workspaces of the devices are usually limited by the users ROM or safety features for the user in case of active actuation.

Comparing actuation of the commercially available assistive devices with the ActInArm it shows that the ActInArm and the McArm are the only devices with active actuation in the horizontal plane. They both actuate an endpoint in this plane, so alignment of the arm segments does not have to be controlled. The other commercially available devices are non-actuated in this plane and rely on friction elimination. From the research and rehabilitation devices most of the actively actuated ones have actuation in horizontal plane. The exoskeleton types actuate the joints of the user wearing the device resulting in assistance of movement in any direction. The actuation power of the drivetrain as implemented in the ActInArm is less than most of the other actively actuated devices.

The ActInArm can be controlled by either user force or the implemented EMG of the users muscles. With this input a set point velocity and direction of movement are determined. In other actively actuated assistive devices several types of control are used, such as admittance control, impedance control, EMG-control, and joystick control. The control inputs for these systems include forces applied by the user, movement of the arm, activation signals of the muscles (EMG), and joystick movement.

Appendices

Contents

A Introduction

Duchenne Muscular Dystrophy (DMD) is a progressive muscular disease with a prevalence of 1 for every 3500 male births [1]. Girls can be a carrier of the gene mutation that causes DMD and there are some rare cases that girls also have DMD. DMD is caused by a gene mutation at the Xp21 Locus of the X-chromosome which is responsible for the production of Dystrophin [2]. The result is that little or no functional Dystrophin is produced which causes the muscles to deteriorate. Between the age of 6 and 10 years muscle power decreases progressively [3]. This decrease of muscle power will first occur at the bigger proximal muscles e.g. upper legs, upper arms, shoulders than proceed toward the smaller distal muscles e.g. wrist, fingers and also the respiratory muscles and the heart will be affected [1]. Most boys will be wheelchair dependent at the age of 14 years [3]. When the shoulders and upper arms muscles are weakened that much that the patient cant perform activities of daily living (ADL), the patient will be dependent on caretakers and assistive devices.

An assistive device that gives the patient more freedom and independency of caretakers will improve the quality of life [1] [3]. This can be done with an assistive device that supports the arm such that the patient can use the arms again for ADL. Such an assistive device is called an orthotic device. There are some assistive devices available for the arm. These devices can be divided into several groups: 1) robotic manipulators, 2) passive orthoses (non-powered), 3) active orthoses (powered) and 4) functional electrical stimulation (FES) [1] [4]. For DMD patients only of assistive devices are useful. The devices of the first group that have been developed and are commercially available are devices that are usually mounted on the wheelchair of the patient and act as an extra arm that can be controlled by means of a remote control. These devices wont give the user a sensation of using their own arm again. Users prefer an inconspicuous device that gives a natural support and also a wearable device is preferred for assistance in ADL [1]. The devices of the second group arent extremely useful if the patient is in the stage where muscle deterioration is so bad that the patient cant even use residual strength to easily position their arms towards a desired position. The commercially available devices of the third group are rare and for most of these devices flexion and extension of the elbow isnt actuated or needs to be actuated by means of a remote control [1] [3].

To give DMD patients more independence an active two degree of freedom assistive device that supports the arm in the horizontal plane is going to be developed, designed and implemented. Application of this device is to support the arm of the patient for writing and drawing purposes. Such an active assistive device could also help the patient reaching the arm to grasp something on a nearby desk or to easily hover over a keyboard such that for example typing a letter becomes easier. The ability to write and draw again could give the patient the feeling of a better quality of life.

A.1 Main Goal of the Thesis

Main goal of the research is to support the movement of the arms of people with Duchenne Muscular Dystrophy (DMD) in the 2dimensional horizontal plane over an area of 400mm by 250mm.

This will be done through the development of an actively actuated assistive device that will actively actuate two degrees of freedom (2 DOF). The actuators of the assistive device amplify the force the user can generate. Result is an easier, less fatiguing movement for the user.

A.1.1 Research questions

To reach the main goal of the thesis, the following research questions can be asked.

- What is Duchenne Musclular Dystrophy?
- How can the daily life of people with Duchenne Musclular Dystrophy be improved?
- How are the arms of people with Duchenne Muscular Dystrophy affected?
- What is the State-of-the-Art in assistive devices?
- What is the workspace of an arm?
- What are critical requirements for assistive devices?
- How to make the assistive device suitable usable for people with DMD?
- What kind of functionality does the device need to have?
- What kinds of user interfaces are suitable?

A.2 Theory

A.2.1 Duchenne Muscular Dystrophy

Duchenne Muscular Dystrophy is a progressive muscle disease, that affects approximately one in 3500 male births. It is a genetic mutation of the Dystrophin gene, located at the x-chromosome at location Xp21.2-p21.1. Because it is located at the x-chromosome the mother is the carrier of the disease. The genetic mutation causes that verry little or no dystrophin is produced. Dystrophin is a protein located between the outer layers of the myofilaments(myofiber) and the cell membrane(sarcolemma) and is a structural component of muscle tissue.

A healthy skeletal muscle consists of a bundle of Fascides, which are a bundle of muscle cells. Each muscle cell consists of a sarcolemma and within this sarcolemma there are a number Myofibrils surrounded by sarcoplasmic recticulum and mitochondria. A sarcomere part of the myofibril concists of three parts; a thin filament (made primarily from actin), a elastic element (made from titin), and a thick filament (made primarily from myosin). 1.

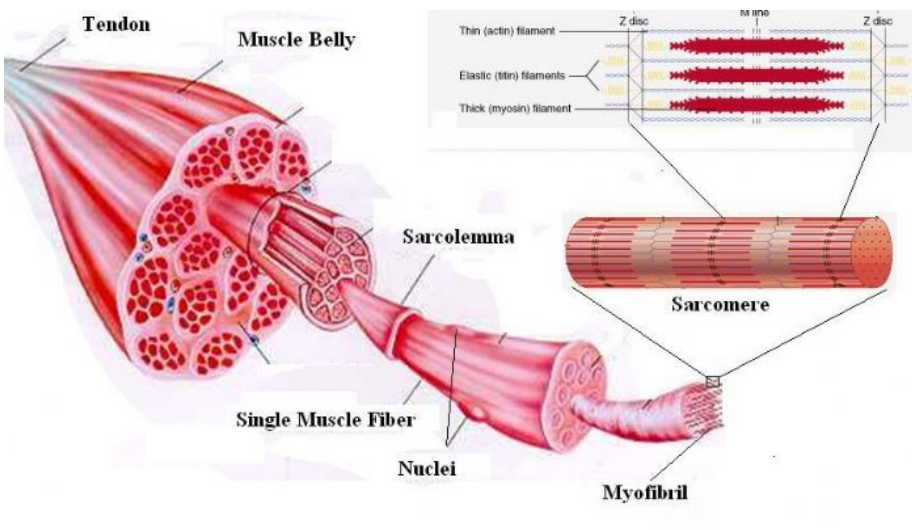

Figure 1: A 3D rendering of a skeletal muscle fiber [5]

When looked closer at the Dystrophin-Glycoprotein complex, a part of muscle cell, it can be seen that the outer layers of the myofilaments(myofiber), through F-actin, and the cell membrane(sarcolemma) are connected by Dystrophin 2, a structural component of the muscle tissue. It is needed to maintain cell structure and without it the muscle cells will not operate properly, suffer from progressive damage and will eventually die causing scarr tissue. Besides that Dystrophin is needed to connect the myofiber to the sarcolemma, it also responsible for the reduction of muscle stiffness.

Fig. 1. Schematic diagram showing relation between the cytoskeletal protein dystrophin, the dystrophin-associated protein complex in the membrane, and the extracellular matrix. (A) Normal muscle. (B) Dystrophic muscle. (Adapted from Davies & Nowak 2006.)

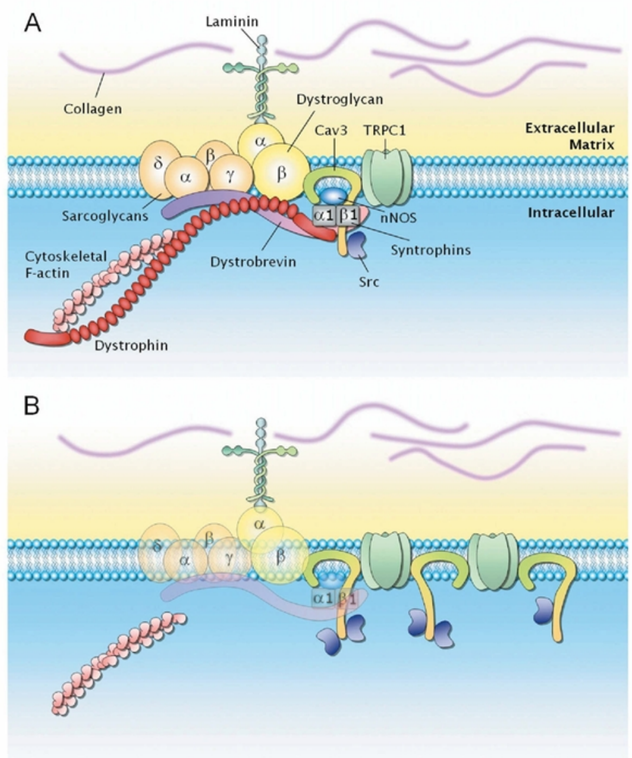

Figure 2: The difference between a healthy muscle cell (A) and a muscle cell of someone with DMD (B). It can be seen that when there is no Dystrophin the F-actin of the myofiber is not attached to the sarcolemma. [6]

Knowing this it is easy to see that the lack of Dystrophin at people with DMD results in the loss of muscle strength, deteriorating muscles, and higher stiffness of the muscles and thus difficult or no voluntairy movement at all.

A.2.2 Development of Duchenne Muscular Dystrophy

As stated before Duchenne Muscular Dystrophy is a disease that has a progressive character. It starts at the large proximal muscles, e.g. the legs, the shoulders and upper arm, and continuous with the smaller distal muscles. At later stages of the disease ventilation and is needed 4.

Usually DMD can be detected at young ages, i.e. diagnosis of the disease is up to the age of 7. Typical signs are:

- Hard time lifting the head or having a weak neck
- When standing up, shows the Gower's maneuver (Fig.3)
- Has enlarged calves, i.e. pseudohypertrophy
- Not walking by 15months
- It is hard to walk, run, or climbing the stairs
- Walks with the legs apart
- Walks on the toes and waddles
- Walks with a pointed out chest

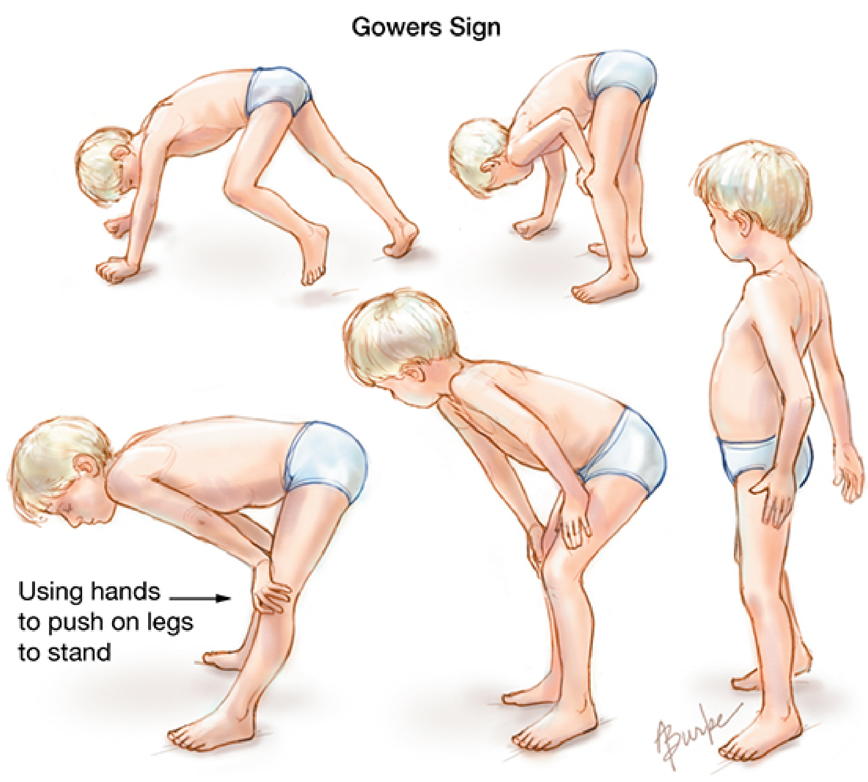

Figure 3: A typical example of Gowers' sign [7]

In the transition stage of the disease, i.e. between the ages of 6 and 9, the muscles of the person with DMD will get weaker. It will become harder to walk and to keep balance. Most will still have use of their arms and hands, but it could become more difficult to lift objects. Also fatiguing can become an issue, what results in the need for support for moving over longer distances.

The continuously weakening muscles cause the next big step in the disease, i.e. the loss of ambolation and therefore becoming wheelchair bound. This happens to most people with DMD around the age of 13. Also the upper arms and trunk may need some kind op support. For most DMD patients the fingers can still be used and therefore they can still write and use a computer. The weak back muscles and being seated most of the day can result in scoliosis symptoms.

When people with DMD reach their adult stage, the disease is usually progressed to the heart and the respiratory muscles, i.e. the lungs. This results in ventilation is needed. First only at night and it progresses to 24 hours per day. The heart gets enlarged which is dangerous. These two types of complications are usually the reason for the death of people with Duchenne.

In the last few decades better medicine and improved cardiac and respiratory machines have caused the life expactancy of people with DMD to grow. Reaching the age of 30 is becomming more normal and there are even known cases of persons that are making it into their 40s and 50s [8] [9].

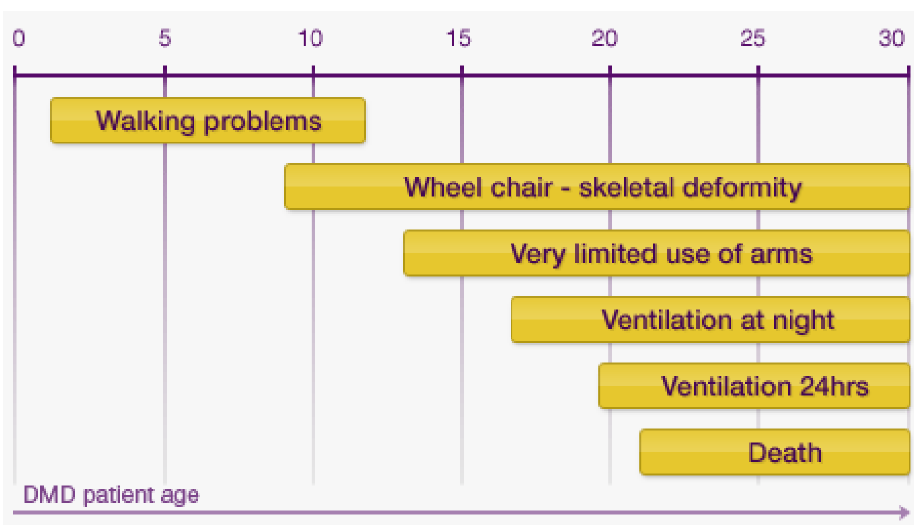

Figure 4: A timeline of the different stages of Duchenne Muscular Dystrophy. [10]

A.2.3 Treatment of Duchenne Muscular Dystrophy

Until now treatment of DMD is symptomatic, meaning that there is no cure for this disease. Only thing that is working right now is corticosteriod (i.e. Prednisolone, Deflazacort) injections. This only makes the disease progress slower. Other (experimental) treatment can consist of:

- Physical theraphy helpful to maintain muscle strength flexibility function

- Non jarring movements (e.g. swimming) are encouraged for muscle flexibility

- Respiratory support to support breathing is important at later stages of the disease

- Use of orthopedic appliances to improve mobility and ability self care

- Beta blockers to help the heart relax

- Beta2-agonist to increase muscle strength

- Exon skipping to 'skip' the DMD exon that is missing and to couple the remaining exons again to make a milder form of muscle dystrophy (e.g. Becker).

- Stem cell transplant

- Replacement gene therapy with Ataluren (PTC124) or Eteplirsen (AVI-4658)

A.3 Workspace analysis

To determine what the range of motion (ROM) for the to be designed assistive device should be, a workspace analysis of the intended user's should be made. The intended user's are people with Duchenne Muscular Dystrophy who can be put in Brooke scale 5 and 6. These are the stages where the arm can't be moved but the finger still can. Normally these scores on the Brooke scale are reached in later stages of DMD. Ages of people with DMD Brooke scale 5 and 6 range from the beginning teens up to adults. Therefore for the workspace analysis anthropomorphic data for adult males [11] is used.

Within the user's ROM certain areas can be distinguised. First the zones of convinient reach, i.e. everything within arm's length, can be determined by the arm length of the user (Fig. 5). The other area is the normal working area of the arms and is dependent not only on arm length, but also on table height, i.e. vertical distance between the shoulder and table surface. This normal working area is the area that can be described by a comfortable sweeping moment of the upper limb around the shoulder with a elbow flexion of 90^o or a little less (Fig. 6).

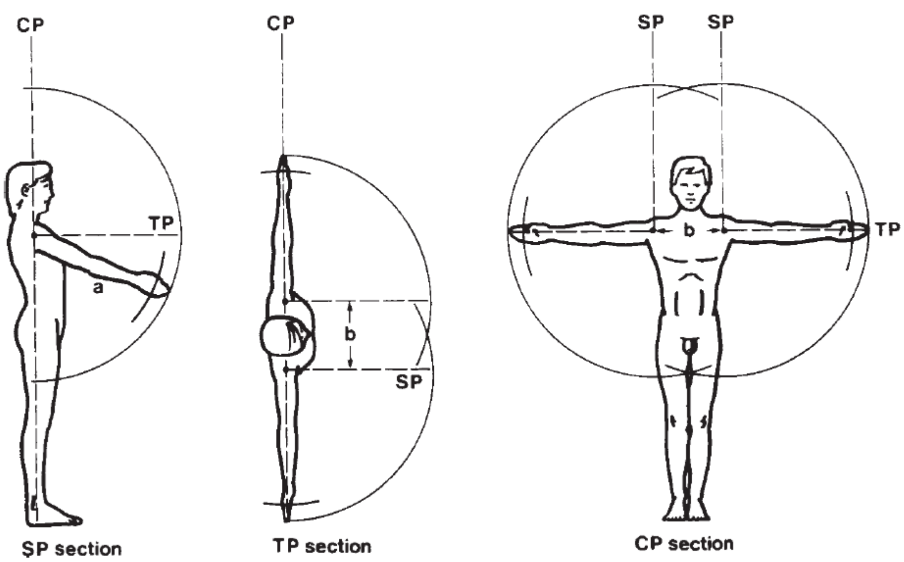

Figure 5: Zones of convenient reach (ZCR) [11]

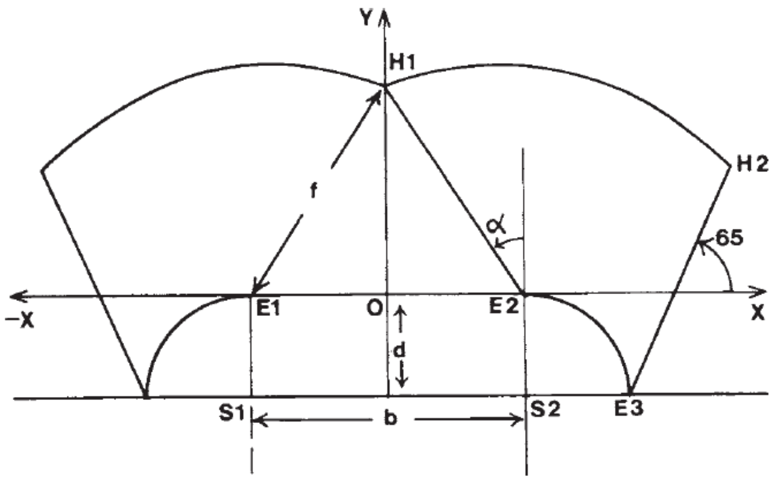

Figure 6: Construction of the normal working area (NWA) [11]

With the anthropometric data of adult males 1 the dimesions of the convinient reach zone and the normal working on the table surface can be determined.

Table 1: Estimates of anthropometric data of Dutch adults aged 20-60 used in the calculation of the normal working space. Measurements are in mm.

	Male		
Dimension	P5	P50	P95
Sitting shoulder height	570	620	670
Upper limb length	750	805	860
Biacromial shoulder breadth	385	410	445
Abdominal depth	245	310	375
Shoulder-elbow length	340	375	405
Elbow fingertip length	455	490	525
Shoulder grip length	635	685	735
Hand length	180	195	210

To estimate the elbow grip length, not given in [11], 2/3 of the hand length is subtracted from the elbow fingertip length. The estimated elbow grip length than is 335mm (P5), 360mm (P50), 385mm (P95). When looked at the DINED data of the elbow grip length [12] the made estimation is good enough.

The zone of convenient reach is determined by the shoulder grip length, and the horizontal and vertical distance between the shouder and the table surface. The horizontal distance between the shoulder and the table is taken as half of the abdominal depth. The vertical distance between the shoulder and the table is approximately 300mm. The coordinates of the zone of convenient reach can be calculated as follows:

$$
\begin{aligned}
X_{ZCR} &= l_{shoulder-grip} \cdot cos(\theta) \cdot sin(\beta) + \frac{1}{2} l_{bia.\ breadth} \\
Y_{ZCR} &= l_{shoulder-grip} \cdot cos(\theta) \cdot cos(\beta) - l_{abd.\ depth}
\end{aligned}
$$

Where

$$
\begin{aligned}
\theta &= arcsin\left(\frac{d_{shoulder-table}}{l_{shoulder-grip}}\right) \\
\eta_1 &= arcsin\left(\frac{l_{bia.\ breadth}}{2l_{shoulder-grip}}\right) \\
\eta_2 &= arccos\left(\frac{l_{abd.\ depth}}{l_{shoulder-grip}}\right) + \eta_1 \\
\beta &= -\eta_1 \dots \eta_2
\end{aligned}
\tag{1}
$$

The normal working area is determined by the elbow-grip length, the biacromial shoulder breadth, and the abdominal depth. The shoulder rotates through 90^o, i.e. the upper arm in front of the user towards the side of the user. The comfortable outward rotation of the forearm is limited from 25^o to 90^o flexion of the elbow. This result in that the angle of the forearm is bounded at 65^o from the table edge. In the normal working area the forearm is parallel to the table surface. The coordinates of the normal working area can be calculated as follows:

$$
\begin{aligned}
X_{NWR} &= \frac{1}{2} l_{abd.\ depth} \cdot sin(\beta) - l_{elbow-grip} \cdot sin(\alpha - \gamma) + \frac{1}{2} l_{bia.\ breadth} \\
Y_{NWR} &= \frac{1}{2} l_{abd.\ depth} \cdot cos(\beta) + l_{elbow-grip} \cdot sin(\alpha - \gamma) - \frac{1}{2} l_{abd.\ depth}
\end{aligned}
$$

Where

$$
\begin{aligned}
\alpha &= arcsin\left(\frac{l_{bia.\ breadth}}{2l_{elbow-grip}}\right) \\
\beta &= 0 \dots \frac{\pi}{2} \\
\gamma &= \frac{2}{\pi}\beta\left(\alpha + \frac{5}{36}\right)
\end{aligned}
\tag{2}
$$

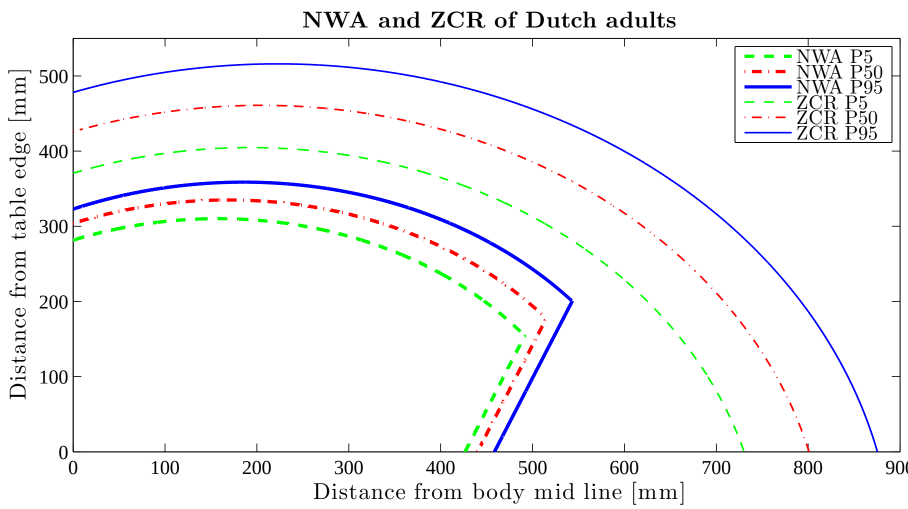

Figure 7: The normal working area (NWA) and zone of convenient reach (ZCR) over the table surface of the 5^{th}, 50^{th}, and 95^{th} percentile of Dutch adult males.

The calculated areas (figure 7) are for healthy people. People with Duchenne Muscular Dystrophy probably have a smaller normal working area and a smaller zone of convenient reach due to stiffer muscles and contractures at the extremities of the shoulder and elbow joints of the arm.

A.4 Excisting research and designs

There are quite a lot of assistive devices on the market to help movement of the arm [1] [4]. As stated before in subsection A on page 19 these devices can be categorised in several groups; robotic manipulators, passive orthoses (non-powered), active orthoses (powered), and functional electrical stimulation (FES). On their turn the passive orthoses can be devided in non-actuated and passively actuated devices.

Most devices do not actively help with extension and flexion of the elbow joint, but reseach [13] [14] shows that this could be beneficial for people with DMD. Devices that acitive help flexion and extension of the arm are the Darwing, McArm,

Focus here is more on the passive and active orthosis because robotic manipulators are more of an extra arm and do not give the user's arm a natural support and FES is not working well and can be painfull for the user. In the non-powered and powered orthosis several types can be distinguished.

Figure 8: The Focal Meditech sling [15].

The sling type assistive devices consist of a sling where the user can put their arm in. This sling is attached to cables that run through an overhead arm that can rotate in the base. For the vertical support there are non actuated, passively actuated and actively actuated systems that make raising and lowering the user's arm easier. For the movement in the horizontal plane friction is minimized or eliminated. Sling type support devices are not inconspicuous and quite large. Examples of sling type devices are the passively and actively actuated Sling of Focal Meditech [15][16] (Fig. 8, the non actuated Nitzbon's Mobility Arm[17], and the Swedish Help Arm [18].

Figure 9: The MAS of Jaeco Orthopedic [19].

The most commercially available assistive devices are the bar mechanism types. Examples of theis type of assistive devices are the Jaeco Mobile Arm Support (MAS) [19] (Fig. 9, the TOP or TOP/Help of Focal Meditech [20], the Dynamic arm support [21], the Neater Arm Support(NAS[22], and supports like the Ergoarm [23].

Bar mechanism type orthosis consist of a linkage system that support the arm in vertical direction with an arm cuff. If they are actively actuated, it is mostly in the vertical direction (i.e. height). The assistive devices that do not have active atuation in the horizontal plane the focus is on minimising or eliminating friction in this plane. Therefore movement in this direction could still be verry hard for people with Duchenne Muscular Dystrophy, although the gravity support makes movement easier than without it.

The exoskeletal type orthoses are mostly actively actuated and will support every arm movement if needed, but in general these devices are bulky, not commercially available, and not usable in daily life. Exoskeletal types of support devices have body worn linkages with joints that have to be aligned with the joints of the user to minimize unwanted joint forces and moments. Actuation to support the user's movement is mainly done at the joints. The actuation can either be passive, i.e. with springs, or active, i.e. with actuators.

Figure 10: Prototype of the Flextension orthosis [24].

An example of a passively actuated exoskeleton that is inconspicuous and small is from the Flextension A-Gear Project [24] (Fig. 10. Examples of bulkier passively actuated types are the Wilminton Robotic EXoskeleton Arm (WREX) [25] (also as active powered type) and the wearable Cable Driven Exoskeleton [26]. Actively actuated systems are for example the LIMPACT [27] and the 7 DOF powered exoskeleton of the University of Washington [28].

Types of revalidation devices that could be changed to support devices are the Technalia Arm Support[29] and the well-known MIT-MANUS[30]. The Technalia Arm Support is a cart like structure where the user can lay their arm in. To be able to move in any direction on the table it uses three omnidirectional wheels. To train arm movement motion is made more difficult by braking the omnidirectional wheels. The MIT-MANUS consists of a four bar mechanism with two motors is the base to make the user's planar arm movement more difficult.

A.4.1 Useful steering signals

An overview of the most used user input signals for actively actuated assistive devices is given here. These signals are the input for the control system of the device. The decribed input signals are still measurable at people that have Duchenne Muschular Dystrophy and can be put in Brooke scale 5 or 6, although some signals are easier to produce for them than others.

One of the most used input signals in assistive devices is a joystick signal.

The user needs to move a stick like manipulator. The device will move in the direction the manipulator is moved to and the amplitude will determine the acceleration, velocity, or force/torque the device will apply to the user.

User force can also be used as an input signal. The force the user applies to the device will than be measured by a force sensor. The direction the user applies the force will be the direction the assistive device will move to. The amount of force is a measure for acceleration of the end point of the device. Force as an input can be combined with several control strategies. For example proportional control or admittance control can be used. With proportional control the force applies is a measure for the amount of acceleration. With admittance control the measured force is fed through an admittance model, i.e. a virtual model where mass and damping can be added/determined, and where a reference position or velocity will be send to the controller of the assistive device.

Another usefull input signal could be an electromyography(EMG) signal. This is the electric activity produced by the skeletal muscles. Although in the later stages of Duchenne skeletal muscles are deteriorated this signal could still measured at one person that was 22 years old and in a late stage of DMD [31]. The EMG signal is used to estimate the joint torque. To make the EMG signal from the user useful it needs to be processed. There are many types of classifiers used for the estimation of muscle joint torques like the Hill type model [32], artificial neural-networks [33], and fuzzy logic [34]. Lenzi [35] has showed that is also possible to do a simpler proportional torque estimation because the human controller is highly adaptable and therefore can compensate for errors in the torque estimation. With the estimated torque a desired acceleration, velocity, or position can be determined.

Acquiring sonomyogram (SMG) signals looks a bit like the acquisition of EMG signals. Both measure signals produced by the muscles. The difference is that EMG measures the electric signals and SMG measures the change in muscle thickness using ultrasound. As with EMG, SMG signals can be used to estimate joint torque. The estimated torque can be used to determine a reference acceleration, velocity, or position.

To use displacement as an input signal for the controller the user first need to move their arm with the attached assistive device before assistance is provided. This means that friction needs to be very low or not present for people with DMD to use the device. With displacement as input a force or torque to support the movement of the user is determined by the controller. Displacement as control input is mostly used for rehabilitation devices.

B Method

B.1 Function analysis

To determine all the functions the assistive device needs to cope with. This is done with a black box approach. The inputs - the user's arm, the wheelchair, and energy - and the output - a moving arm in the horizontal plane - are known and everything within the black box are steps to accomplish the output with the inputs. A flowchart of the black box model is shown on page 36.

The functions of the black box can be devided into three systems, namely the mechanical system, the control system, and an energy system. The mechanical system on its turn can be devided into four subsystems - the arm-machine interface, the attachment, the configuration, and the drivetrain.

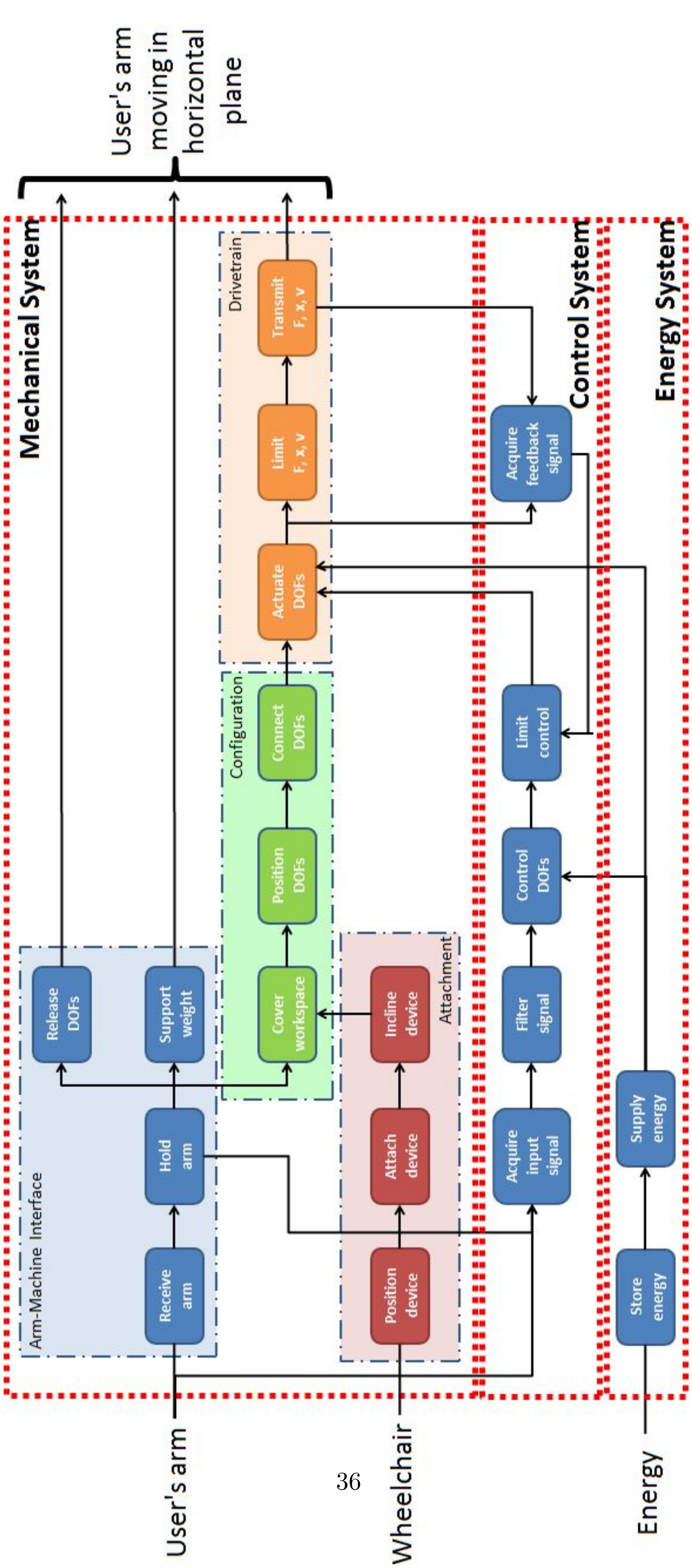

User's arm
Wheelchair
Energy
User's arm moving in horizontal plane
Mechanical System
Control System
Energy System
Arm-Machine Interface
Receive arm
Hold arm
Release DOFs
Support weight
Configuration
Cover workspace
Position DOFs
Connect DOFs
Drivetrain
Actuate DOFs
Limit F, x, v
Transmit F, x, v
Attachment
Position device
Attach device
Incline device
Acquire input signal
Filter signal
Control DOFs
Limit control
Acquire feedback signal
Store energy
Supply energy

B.2 Program of requirements

The requirement are devided into two parts. A section with only the critical requirements are stated and one with all the other requirements. The critical requirements are the requirements that are really important for the design of the assistive device. Without these requirements a good design will be compromised. Of course more requirements and wishes for the design of a assistive device can be thought of.

B.2.1 Critical requirements

No.	Requirement	Explanation	Target	Evaluation
		Generic		
1.	Target group	People with DMD Brooke scale 5 and 6 need to be able to use the assistive device	Brooke scale 5 and 6	Test with people who are in Brooke scale 5and 6
		Range of Motion (ROM)		
2.	Cover workspace	The end effector of the device will need to cover this workspace. A piece of paper and the pen or pencil will be within this workspace	Everything within a radius of 510mm from the shoulder in the horizontal plane	Test if the end effector of the device is able to move within this radius
3.	Pronation & supination need to be possible	Pronation and supination of the forearm are used when writing and drawing and picking up a pen(cil)	Approximately needed: $20°$ - $70°$ forearm pronation	Test with subject if a reasonable amount of forearm pronation is possible
4.	Flexion & extension of the elbow joint need to be possible	Flexion and extension of the elbow is needed to move the hand in the horizontal plane	Approximately needed: $15°$ - $100°$ elbow flexion	Test with subject if a reasonable amount elbow flexion is possible
5.	Rotation of the shoulder joint needs to be possible	Rotation of the shoulder (Glenohumeral joint) is needed to move the hand in the horizontal plane	Approximately needed: 0 - $45°$ abduction* $10°$ extension - $60°$ flexion 0 - $90°$ medial rotation	Test with subject if a reasonable amount of shoulder rotation is possible
		Functional		
6.	Technical feasibility	To ensure the device is reliable during usage, components and concepts that have proven themselves to be reliable are used	Reliable working prototype	Use components and concepts that have proven to be reliable
		Cosmetics		
7.	Inconspicuous	Users say that the device should be inconspicuous	Users think the device is inconspicuous	Ask users and caregivers if they think the device is inconspicuous
		Control		
8.	No play at end effector	Play can cause troubles for the control of the device. (For example unwanted force / acceleration / velocity peaks)	Zero play at the end effector	Look at sensor data if force / acceleration / velocity peaks occur when moving the device, without user's arm attached

Safety			
9. Limit velocity	A software limit. Don't want to hurt the user	$V_{max} = 0.1m/s$	Set the limit in software and look at sensor data if velocity stays within this limit
10. Limit force / torque	Limit the force or torque applied by the assistive device on the user's arm in software. Don't want to hurt the user	$F_{max} = 10N$ (at end effector) $T_{max} = 2.5Nm$ (on user's joints)	Set the limit in software and look at sensor data if velocity stays within this limit
11. Limit displacement	At the limits of the user's range of motion, co-contraction can occur easily. This is unwanted. Don't want to hurt the user.	$X_{max} \leq$ Range of motion (ROM) user	Set a limit in software and test if end effector stays within this limit
12. Emergency stop	Users and caregivers need to be able to stop the device in case of an emergency	Emergency stop buttons on device	Check if emergency stop works
Comfort			
13. Fatigue	It should be easy to use the assistive device. The muscles shouldn't get fatigued when using the device for daily use. Tune the device such that it's possible	$>$ 8hours without fatiguing	Look at EMG levels for fatigue / if subject can use the device $>$8h continuously without fatiguing
14. Small distance between hand and writing surface	It's more comfortable and gives a better posture to have the hand as close as possible to the surface of the table	$<$ 25mm between hand and writing surface	Measure distance between hand and writing surface

B.2.2 Other requirements and Wishes

- **Functional**
- Needs to fit different arm sizes
- Stiffness of the device needs to be high
- The device needs to have a low weight
- Working time of the device need to be ¿8h without recharging or likewise
- Device need to mimic normal arm movement
- Device needs to be quiet
- Device needs to be corrosion resistant
- **Usability**
- Device does not make wheelchair bigger
- Control of the device needs to be intuitive
- Device needs to be comfortable
- Device needs to be easy to clean
- Device needs to be easy to transport
- **Safety**
- A smooth acceleration profile is needed
- Device has no sharp edges
- No unintended movements are possible
- Device needs to be back drivable
- Device doe not have gaps where clothes can get stuck
- **Cost**
- Production costs need to be low

- **Environmental**
- No hazardous materials will be used
- **Wishes**
- No lubrication is needed
- Device can be mounted to multiple types of wheelchair/tables/other surface
- Lifespan of the device is ¿10years
- Maintenance is low
- Device should be easy to manufacture
- Parts of the device should be easily replaceable
- Device has low environmental impact
- Device should satisfies with law requirements

B.3 Morphological chart

A morphological chart is a chart in which for every function, found in the function analysis, solutions are found. To create a concept from such a chart one or more solutions for every function are chosen and combined into one solution/concept. The chosen combination of solutions needs to be sequacious to produce sensible concepts which probably will work. The morphological chart for this project can be found on the nexr pages.

Function	Solution 01	Solution 02	Solution 03	Solution 04
Mechanical system				
Arm machine interface				
• Receive arm	Cuff	Bracelet	Bars	Sling
• Hold arm	Exact fitting	Strap(s)	Elactic band(s)	Magnet(s)
• Release degrees of freedom (DOFs)	Flexible element	Rotational joint	-	
• Gravity support	Device itself	Magnet(s)	Cable(s)	Ball(s)
Configuration device				
• Cover workspace	2x Rotational (RR) in series	RR in parallel	2x Prismatic (PP) in series	PP in parallel
• Position DOFs	User's joints (in horizontal plane)	User's joints (exoskeleton)	Best position to cover workspace	Around wrist
• Connect DOFs	Fixed frame	Links that can change length	Cable(s)	
Drivetrain				
• Actuate DOFs	Electric motors	Linear actuators	Pneumatic artificial muscles (PAM)	Shape Memory Alloy (SMA)
• Limit F, v	Brakes	Shear (break pin)	Actuator choice	Magnetic coupling
• Limit x	Length device	Length user's arm	Physical boundaries	
• Transmit F, x, v	Direct drive	Worm wheel with anti-backlash nuts	Capstan gear(s)	Harmonic drive
Attachment wheelchair				
• Position device	Underneath worktable	Side of wheelchair behind user	Side of wheelchair underneath forearm	Side of worktable
• Attach device	Tube clamps	Bolts	Vacuum	Magnetic
• Incline device	Rotational joint	Tube clamps under an angle	Agonist – antagonist with flexible and rigid elements	-
Control system				
Control device				
• Acquire input signal	EMG	MMG	Force	Displacement
• Filter signal	Threshold	Pattern recognition	Intention detection	Low pass filter
• Control DOFs	EMG + Admittance control	EMG + Impedance control	Admittance control	Impedance control
• Limit control signal	Limit force in model	Limit velocity in model	Limit position in model	Limit acceleration in model
• Acquire feedback signal	Force	Absolute position	Incremental position	Velocity
Energy system				
Energize device				
• Store energy	Battery	Pressurised air	Fluid	Flywheel
• Supply energy	Electric wires	Air hose	Pipeline	Friction wheel

Solution 05	Solution 06	Solution 07	Solution 08	Solution 09
Mechanical system				
Felcro	Friction	-		
Wheel(s)	-			
RP	Cart			
Electro-active polymer	Piezo motors	Elastic nanotube actuator		
Slip clutch	-			
Cable(s)	Spring(s)	Redundant gears	Timing belt with zero backlash gears	Pull-push bar(s)
Top of worktable	Bottom of worktable	On top of worktable	Above worktable	
Friction	Form-retaining connection	Glue	Elastic bands	Straps
Control system				
Joystick	Eye movement	Voice		
Kalman filter	Threshold	-		
Force control	Position control	MMG + Admittance control	MMG + Impedance control	
Limit output signal				
Acceleration				
Energy system				
Potential	Elastic (springs)			
Cables				

B.4 Morphological chart rating

All the solutions are graded within the range 1-5. A score of 5 points is the highest score, 1 point the lowest. In the graded morphological chart the scores are represented by colors. Table 2 shows the complete range of scores and colors.

Table 2: The points and colors for grading the solutions

Points	Color	Explaination
5		Very good solution
4		Good solution
3		Average solution
2		Bad solution
1		Very bad solution

Function	Solution 01	Solution 02	Solution 03	Solution 04
Mechanical system				
Arm machine interface				
• Receive arm	Cuff	Bracelet	Bars	Sling
• Hold arm	Exact fitting	Strap(s)	Elactic band(s)	Magnet(s)
• Release degrees of freedom (DOFs)	Flexible element	Rotational joint	-	
• Gravity support	Device itself	Magnet(s)	Cable(s)	Ball(s)
Configuration device				
• Cover workspace	2x Rotational (RR) in series	Cart	2x Prismatic (PP) in series	PP in parallel
• Position DOFs	User's joints (in horizontal plane)	User's joints (exoskeleton)	Best position to cover workspace	Around wrist
• Connect DOFs	Fixed frame	Links that can change length	Cable(s)	
Drivetrain				
• Actuate DOFs	Electric motors	Linear actuators	Pneumatic artificial muscles (PAM)	Shape Memory Alloy (SMA)
• Limit F, v	Brakes	Actuator choice	Magnetic coupling	Shear (break pin)
• Limit x	Length device	Length user's arm	Physical boundaries	
• Transmit F, x, v	Direct drive	Worm wheel with anti-backlash nuts	Capstan gear(s)	Harmonic drive
Attachment wheelchair				
• Position device	Underneath worktable	Side of wheelchair behind user	Side of wheelchair underneath forearm	Bottom of worktable
• Attach device	Tube clamps	Bolts	Vacuum	Magnetic
• Incline device	Rotational joint	Tube clamps under an angle	Agonist – antagonist with flexible and rigid elements	-
Control system				
Control device				
• Acquire input signal	EMG	Joystick	Force	Displacement
• Filter signal	High pass + rectify + low pass	Pattern recognition	Intention detection	Low pass filter
• Control DOFs	Admittance control	Impedance control	Force control	Position control
• Limit control signal	Limit force in model	Limit velocity in model	Limit position in model	Limit acceleration in model
• Acquire feedback signal	Force	Absolute position	Incremental position	Velocity
Energy system				
Energize device				
• Store energy	Battery	Pressurised air	Fluid	Flywheel
• Supply energy	Electric wires	Air hose	Pipeline	Friction wheel

Solution 05	Solution 06	Solution 07	Solution 08	Solution 09
Mechanical system				
Felcro	Friction	-		
Wheel(s)	-			
RP	RR in parallel			
Electro-active polymer	Piezo motors	Elastic nanotube actuator		
Slip clutch	-			
Cable(s)	Spring(s)	Redundant gears	Timing belt with zero backlash gears	Pull-push bar(s)
Top of worktable	Side of worktable	On top of worktable	Above worktable	
Friction	Form-retaining connection	Glue	Elastic bands	Straps
Control system				
MMG	Eye movement	Voice		
Kalman filter	Threshold	-		
Velocity control				
Limit output signal				
Acceleration				
Energy system				
Potential	Elastic (springs)			
Cables				

B.5 Concepts

Per function category - arm machine interface, configuration, actuation, attachment, control, and energize - concepts were made, which can be seen in the morphological chart with the lines of the concepts on the next few pages. Each line represents a concept. These concepts are than combined into logical combinations to make a complete concept for the whole assistive device.

Function	Solution 01	Solution 02	Solution 03	Solution 04
Mechanical system				
Arm machine interface				
• Receive arm	Cuff	Bracelet	Bars	Sling
• Hold arm	Exact fitting	Strap(s)	Elactic band(s)	Magnet(s)
• Release degrees of freedom (DOFs)	Flexible element	Rotational joint	-	
• Gravity support	Device itself	Magnet(s)	Cable(s)	Ball(s)
	1		2	3
Configuration device				
• Cover workspace	2x Rotational (RR) in series	Cart	2x Prismatic (PP) in series	RP
• Position DOFs	User's joints (in horizontal plane)	User's joints (exoskeleton)	Best position to cover workspace	Around wrist
• Connect DOFs	Fixed frame	Links that can change length	Cable(s)	
	1 2 3	4	5	
Drivetrain				
• Actuate DOFs	Electric motors	Linear actuators	Pneumatic artificial muscles (PAM)	Shape Memory Alloy (SMA)
• Limit F, v	Brakes	Actuator choice	Magnetic coupling	Shear (break pin)
• Limit x	Length device	Length user's arm	Physical boundaries	
• Transmit F, x, v	Direct drive	Worm wheel with anti-backlash nuts	Capstan gear(s)	Harmonic drive
	1	2	3	4
Attachment wheelchair				
• Position device	Underneath worktable	Side of wheelchair behind user	Side of wheelchair underneath forearm	Bottom of worktable
• Attach device	Tube clamps	Bolts	Vacuum	Magnetic
• Incline device	Rotational joint	Tube clamps under an angle	Agonist – antagonist with flexible and rigid elements	
			1	2 3 4 5

Solution 05	Solution 06	Solution 07	Solution 08	Solution 09
Mechanical system				
Felcro	Friction	-		
Wheel(s)	-			
4				
PP in parallel	RR parallel			
Electro-active polymer	Piezo motors	Elastic nanotube actuator		
Slip clutch	-			
Cable(s)	Spring(s)	Redundant gears	Timing belt with zero backlash gears	Pull-push bar(s)
5				
Top of worktable	Side of worktable	On top of worktable	Above worktable	
Friction	Form-retaining connection	Glue	Elastic bands	Straps

Function	Solution 01	Solution 02	Solution 03	Solution 04
Control system				
Control device				
• Acquire input signal	EMG	Joystick	Force	Displacement
• Filter signal	High pass + rectify + low pass	Pattern recognition	Intention detection	Low pass filter
• Control DOFs	Admittance control	Impedance control	Force control	Position control
• Limit control signal	Limit force in model	Limit velocity in model	Limit position in model	Limit acceleration in model
• Acquire feedback signal	Force	Absolute position	Incremental position	Velocity
	1 2	3 4		
Energy system				
Energize device				
• Store energy	Battery	Pressurised air	Fluid	Flywheel
• Supply energy	Electric wires	Air hose	Pipeline	Friction wheel

Solution 05	Solution 06	Solution 07	Solution 08	Solution 09
Control system				
MMG	Eye movement	Voice		
Kalman filter	Threshold	-		
Velocity control Limit output signal				
Acceleration				
Energy system				
Potential Cables	Elastic (springs)			

B.5.1 Mechanical concepts

The mechanical concepts are generated from the function categories ‘Arm machine interface’, ‘Configuration device’, and ‘Attachment wheelchair’.

Concept 1 - *’Bar mechanism’*
The ’Bar mechanism’ concept is a combination of line 1 of the function category ’Arm machine interface’, line 4 of ’Configuration device’, and line 4 of ’Attachment wheelchair’. Figure 11 gives an impression how this concept will look like.

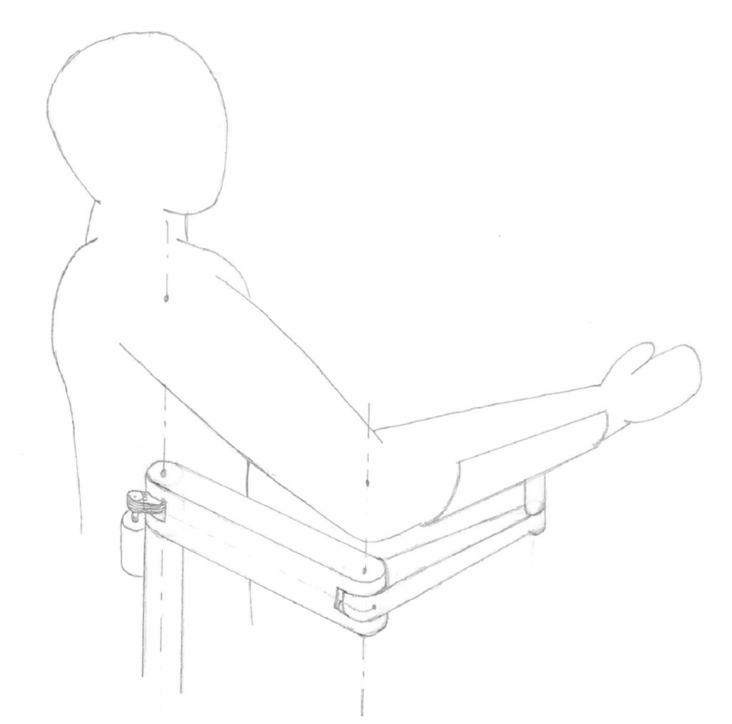

Figure 11: An impression of the ’Bar mechanism’ concept.

The arm of the user is put in an exact fitting cuff that is attached to the device with a rotational joint which can rotate around the vertical (z-axis). The arm is gravity supported by the device itself. The device cover the planar field by two rotational joints that are in series with each other. These joints are positioned at the projected joints of the user in the same planar field of the devices rotational joint. Seen from above the joints of the device are at the same position as those of the user. To ensure that each person can use this device the rotational joint of the device are connected with each other by links of which the length can be changed by two sliding elements. The device will be attached to the bottom of the worktable by bolts. The device won't need a method to change the inclination with respect to the table top because it's attached to the table.

This concept scores 49 (20+14+15) points.

Concept 2 - *'XY Table'*
The 'XY Table' concept is a combination of line 3 of the function category 'Arm machine interface', line 1 of 'Configuration device', and line 2 of 'Attachment wheelchair'. Figure 12 gives an impression how this concept will look like.

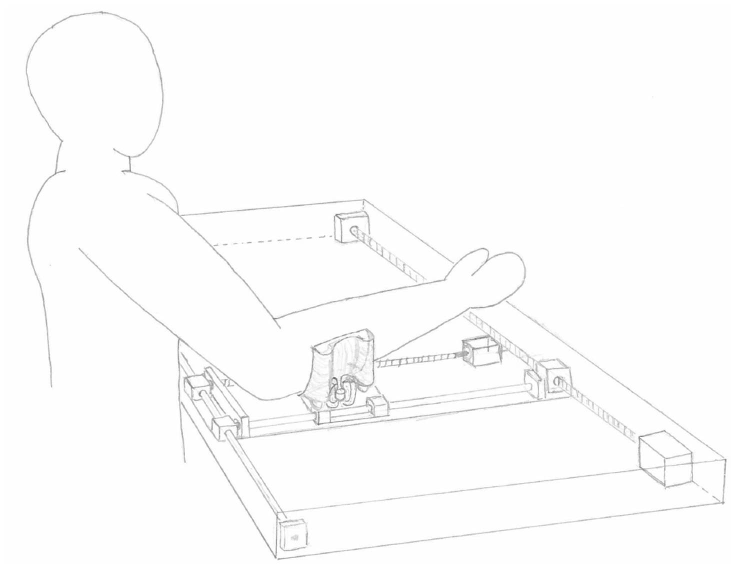

Figure 12: An impression of the 'XY-Table' concept.

The XY-Table consists of two parts. One part is the table itself that replaces the existing table of the wheelchair. The second part is the arm cart that will roll on top the table surface. The two are coupled with two magnets. One at the end effector of the XY manipulator - two prismatic joints in series - and one at the bottom of the arm cart. The arm cart that recieves the arm of the user, is an arm cuff on hemispherical wheels. The magnetic interface causes the rotation around the vertical to be free. The prismatic joints are positioned in a way to cover the maximum workspace of the table.

This concept scores 50 (20+15+15) points.

Concept 3 - *'Haptic master type'*
The 'Haptic master type' concept is a combination of line 1 of the function

category 'Arm machine interface', line 2 of 'Configuration device', and line 1 of 'Attachment wheelchair'. Figure 13 gives an impression how this concept will look like.

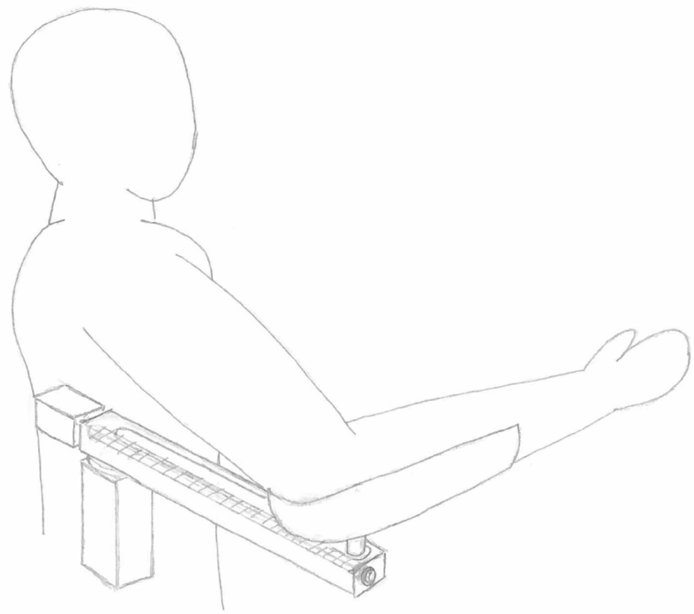

Figure 13: An impression of the 'Haptic master type' concept.

As with the 'Bar mechanism' concept, this 'Haptic master' concept uses the same arm machine interface. A exact fitting cuff which is connected with the mechanism by a rotational joint to release the rotation around the vertical. The mechanism provides the gravity support. The workspace is covered by a rotational joint and rigidly connected to that is a prismatic joint. This device is positioned at the side of the wheelchair at the position that the maximal workspace is covered without interfering with the user. The device is attached to the wheelchair with tube clamps.

This concept scores 45 (20+13+12) points.

Concept 4 - *'Arm cart'*
The 'Arm cart' concept is a combination of line 4 of the function category 'Arm machine interface', line 3 of 'Configuration device', and line 5 of 'Attachment wheelchair'. Figure 14 gives an impression how this concept will look like.

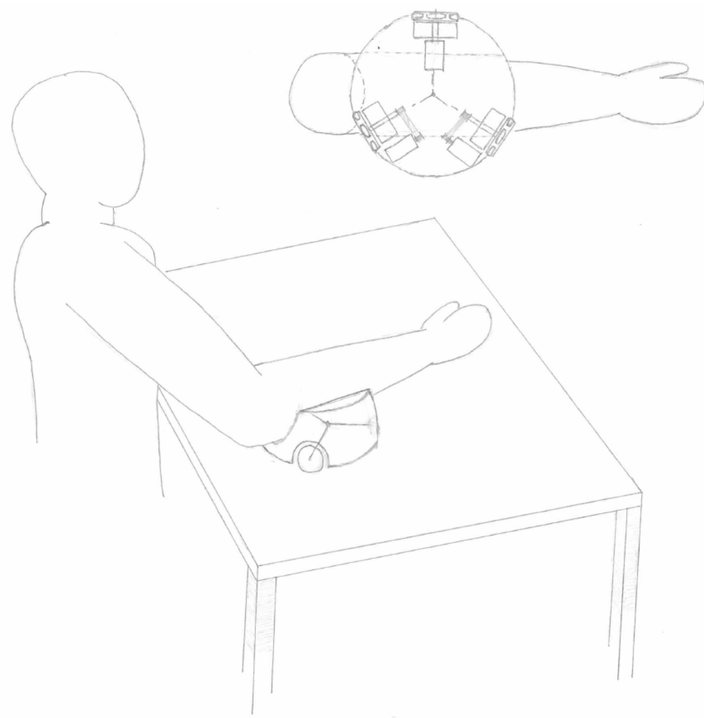

Figure 14: An impression of the 'Arm cart' concept.

The 'Arm cart' concept is a cart supported by three omni-directional wheels that are on the same radius so independent of orientation the cart can move in any direction on the planar surface. The arm is recieved by an arm cuff and is held in the arm cuff by friction. This concept can be placed on any table surface and be used by the user.

This concept scores 44 (18+14+12) points.

Concept 5 - *'Exoskeleton'*
The 'Exoskeleton' concept is a combination of line 2 of the function category 'Arm machine interface', line 5 of 'Configuration device', and line 3 of 'Attachment wheelchair'. Figure 15 gives an impression how this concept will look like.

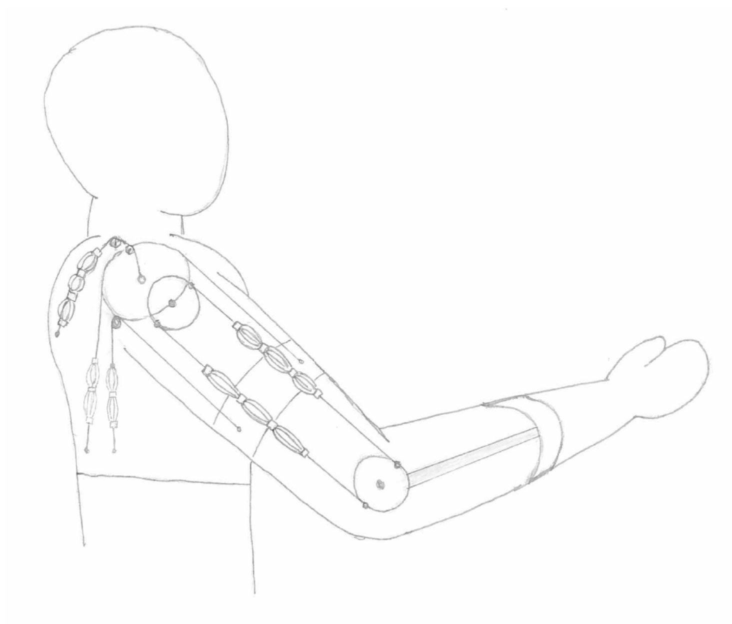

Figure 15: An impression of the 'Exoskeleton' concept.

The 'Exoskeleton' is attached to the arm by elastic bands on the fore arm and upper arm. Gravity support is done by applying the right amount of pressure to the pneumatic artificial muscles. The joints of the exoskeleton must be alligned with the user's joints to achieve a good movements. The ROM of the device is little bit smaller than the ROM of the user for safety.

This concept scores 43 (18+12+13) points.

B.5.2 Actuation concepts

The mechanical concepts are generated from the function categories 'Drivetrain' from the mechanical system, and 'Energize device' from the energy system.

For the 'Bar Mechnanism' concept the most logical combination for the actuation is a system with electric motors (line 3). Mechanical safety of the user is guarenteed by choosing a motor that isn't strong enough to hurt the user and as an extra safety a break pin that will break when the transmitted force is to high is added. Position will be limited by the device itself. The range of motion (ROM) of the device will be smaller than the ROM of the user. Force and velocity from the motor will be enlarged and transmitted by capstan gears and cables to the joints of the device. The motors will be powered by electrical power which comes from the battery pack of the wheelchair.

For the 'XY-Table' concept the logical choice is to combine it with electrical actuation (line 2), because it has a good size to torque ratio. The torque of the motors will be transmitted through lead spindles to the end effector. Displacement will be limited by the ROM of the device. Other safety is guaranteed by actuator choice and the magnetic coupling between the magnet on the end effector side - below the table top - and the magnet attached to the cart on the user side - on top of the table. The motors will be powered by electrical power which comes from the battery pack of the wheelchair.

Also for the 'Haptic master type' concept it's the obvious choice to use electrical motors to actuate the degrees of freedom (line 1). One of the motors is directly driving the rotational degree of freedom. The other, for the prismatic degree of freedom, is attachted to a lead spindle. The force and velocity will be mechanically limited by the chosen actuators and the maximum displacement is limited by the user's arm length. The motors will be powered by electrical power which comes from the battery pack of the wheelchair.

For the actuation of the degrees of freedom in the 'Arm cart' concept electric motors in combination with harmonic drives that drive the three omni-directional wheels will be used (line 4). Also here to energize the system electrical energy will be used. Displacement is mechanically bounded by the length of the arm of the user. The force and velocity are limited by actuator and gearbox choice.

In the 'Exoskeleton' concept pneumatic artificial muscles (PAMs) are used to actuate the degrees of freedom (line 5). The most common pneumatic artificial muscles are balloon shaped membranes with stiff pleating or braiding, and are used to mimic real muscles [36]. When a pneumatic artificial muscle is pressurised by air it contracts. To actuate one degree of freedom two pneumatic artificial muscles - agonist and antagonist - are needed. To get an 2D movement of the hand three degrees of freedom need to be actuated - two in the shoulder and one in the elbow - when no degrees of freedom are coupled. Because three degrees of freedom are actuated also a 3DOF movement of the hand is possible. Force and velocity are limited by the actuator and maximum air pressure. The range of motion is limited by the user and the maximum contraction of the pneumatic artificial muscles.

B.5.3 Control concepts

In the four produced control concepts two different control methods can be distinguished, namely admittance and impedance control. These are the two types of control used for human-machine interfaces. The concepts mainly differentiate from each other by input signal. In the generated concepts Electromyography

(EMG) (line 4) and force (line 3) signals are used in combination with an admittance controller, and joystick (line 1) and displacement (line 2) are used as an input for the impedance controller. All four concepts are limiting the same signals - force generated by the motors, and velocity and displacement of the endeffector - for safety of the user.

Admittance controlled system - *'Force input'*
In this concept force of the user is used as an input to the system. The force is going to be measured by a 2 degree of freedom force sensor that measures the force in X and Y direction. This force sensor is put at the end effector of the robot. Therefore the orientation - angle in the planar field - of the arm inside the arm cuff doesn't need to be known for control purposes.

Because the raw signal from the force sensor could be noisy the signal needs to be filtered. First a notch filter at 50Hz is used to filter the noise introduced by the electrical mains. Further a low pass filter with a low cut-off frequency could be used to get a smooth signal that is introduced by the user.

As a feedback signal for the low level controller the absolute position of the end effector - therefore also the position of the user's arm - is used. This signal will be put in a PID controller, with the desired position coming from the user - through the admittance block - as the reference.

The cotrol scheme of this controller is showed in figure 16.

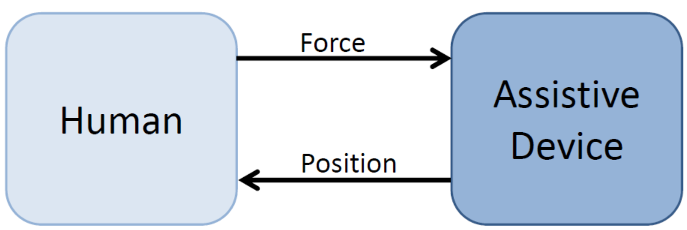

Figure 16: The interface of admittance control between the human and the controlled device. The device measures a force given by the user with it's sensors and the actuators make a movement according to this force.

Admittance controlled system - *'EMG input'*
The admittance controller with the EMG input is similar to the admitance controller with the force input. The difference lies obviously in the way the input signal is obtained and also the way the signal is filtered. For movement of a joint EMG signals of an agonist and an antagonist muscle need to be measured. For the elbow joint the Biceps and Triceps muscles are a good choice. For the shoulder the Pectoralis Major and the Trapezius muscle are a good choice. The

electrodes are placed according to the SENIAM recommondations [37] to get the best EMG signals from the independent muscles.

These signals from these muscles are than put through a high pass filter - with a cut-off frequency of 3Hz - to filter the static deviation with the zero. After that rectified, and than put through a low pass filter - cutoff frequency 20Hz - to get a smooth signal. Noise introduced by the electrical mains is filtered by a notch filter at 50Hz. The filtered signal is than proportionally amplified to get an estimation of the force vector at the arm machine interface. Absolute position of the end effector is used as a feedback signal for the low level controller. See figure 17 for a control schematic of the admittance with the EMG input signal.

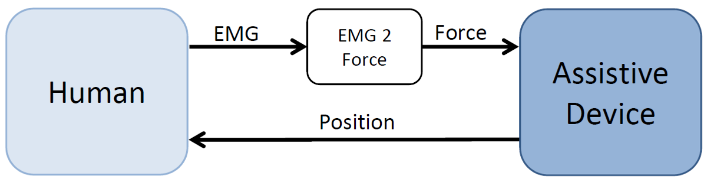

Figure 17: The interface of admittance control between the human and the controlled device. The device measures an EMG signal of the user's muscles. The EMG signal of the user's muscles is translated into a force and used to determine the desired movement of the actuators.

Impedance controlled system - *'Displacement input'*
This concept is a typical impedance controller. Displacement of the end effector is the input signal. Therfore the user needs to exert a force to make a displacement possible. This displacement is measured by sensors and put through an impedance controller and a block to calculate how much force is needed for the robotic manipulator. These two forces added to each other results in the reference force the motors need to generate. Actuation force generated by the motors is measured for the low level controller. The difference between the reference force and the actual actuation force is put in a PID controller to generate a control signal for the actuators. The actuators than generate a force that is delivered to the robot and the user's arm. For the control schematic see figure 18.

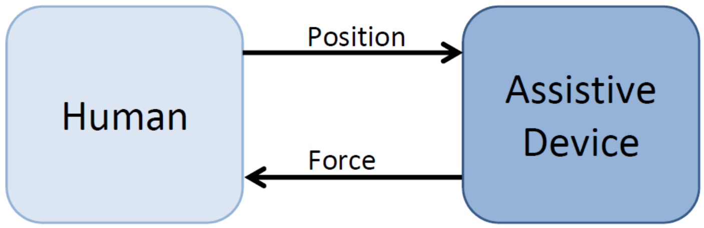

Figure 18: The interface of impedance control between the human and the controlled device. The device measures a position change with it's sensors and gives a force back to the user.

Impedance controlled system - *'Joystick input'*
For the second impedance controlled system concept, a joystick is chosen to be the input signal. This could be a 'normal' joystick, but also systems like the Powerglove [38] can be used as a joystick system, because most users of the target group can still move their fingers.

The joystick is 'adding' a virtual displacement to the robot's position that results in an actuation force and therefore movement, instead of adding a real displacement. Therefore position measurement is only needed for boundary issues and safety features. See figure 19 for the schematic.

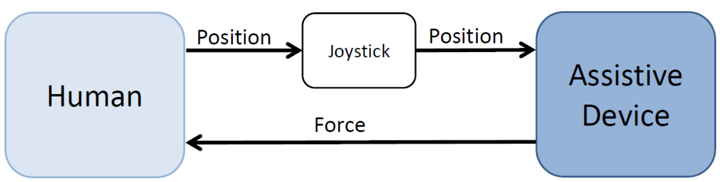

Figure 19: The user gives the input by moving a joystick. The joystick signal is than used to give a force back to the user.

B.6 Concept rating

It can be seen that concept 3 - 'Haptic master type', concept 4 - 'Arm cart', and concept 5 - 'Exoskeleton' have lower scores than concept 1 - 'Bar mechanism' and concept 2 - 'XY table'. Another important reason why concept 3 - 'Haptic master type' is not chosen is beacause it is a sort of copy of the MOOG Haptic Master [39]. Also concept 4 - 'Arm cart' looks like the Technalia ArmAssist [29] and is therefore not chosen. The 'Exoskeleton' concept 5 is not chosen because it is much harder to control the degrees of freedom of it than for the other concepts.

Now the choice has to be made between the two remaining concepts, concept 1 - 'Bar mechanism' and concept 2 - 'XY table'. They both have about the same score when looking at the graded morphological chart at page 49. A good reason to choose for concept 1 is that the bar mechanism is widely used and has proven itself in non actuated assistive devices. A good reason to choose concept 2 is that it is an innovative solution to the problem and that it therefore could give new insights into useable solutions for assistive devices. To be sure the best solution is chosen both the concepts will be assessed by how well they comply with the critical requirements.

Requirement	Bar mechanism concept	Score	XY-table concept	Score
		Generic		
Target group	Force that people with DMD can generate will decrease if they get in a later stage of DMD	4	EMG signals of people with DMD that are in a late stage of life are still good measurable	5
		Range of Motion (ROM)		
Cover workspace	Easily done by using right linkage lengths and drivetrain	5	Easily done by right actuator choice	5
Pronation & supination need to be possible	Released in cuff	5	Released in bracelet	5
Flexion & extension of the elbow joint need to be possible	Isn't constrained by cuff or bar mechanism	5	Isn't constrained by bracelet	5
Rotation of the shoulder joint needs to be possible	Isn't constrained by cuff or bar mechanism	5	Isn't constrained by bracelet	5
		Functional		
Technical feasibility	All separate components have proven themselves in orthotics and other applications	5	The magnetic coupling between the actuator and the arm hasn't been done for such a device	4
		Cosmetics		
Inconspicuous	The whole manipulator can be seen	3	Only the bracelet around the user can be seen	5
		Control		
No play at end effector	Zero play at the end effector is no problem. But, Cable driven gearbox may get bulky, or motors need to be big to get enough torque at the joints.	4	Use anti-backlash nuts, Magnetic coupling can be seen as stiffness	5
		Safety		
Limit velocity	Can be done in software and by actuator choice	5	Can be done in software and by actuator choice	5
Limit force / torque	Can be done in software, by actuator choice and with a shear (break pin)	5	Can be done in software, by actuator choice and with the magnetic coupling	5
Limit displacement	Can be done in software and by mechanical end stops	5	Can be done in software, by actuator choice and by end stops	5
Emergency stop	Multiple emergency stop buttons can be added for both user and caregivers	5	Multiple emergency stop buttons can be added for both user and caregivers	5
		Comfort		
Fatigue	It's harder for the people with DMD that are in a late stage to produce force. This means more muscle activation (earlier fatigue) or higher gains (worse signal-noise ratio) are needed.	4	EMG signals, especially in the later stage of DMD, are more suitable as an input signal for the control of the device because they deteriorate less than the force produced by the person with DMD.	5
Small distance between hand and writing surface	Bar mechanism underneath the forearm causes the hand to be some distance above the writing surface	4	Support by bracelet allows hand to be close to the writing surface	5
Total Score		64 (= 91.4%)		69 (= 98.6%)

Of the maximum score of 70points the 'Bar mechanism' concept scores 64 points (i.e. 91.4%) and the 'XY table' concept scores 69 points (i.e. 98.6%). Biggest difference between the two is in the score at the requirement to be inconspicuous. This is a important requirement given by the intended users.

The control concepts do not have a big difference in scores. This is mainly because of the safety features, i.e. limiting the force, the velocity, and the position within the controller. These are counted separately because they are three limiters in series, a redundant system. For all control concepts these are the same and therefore already have 14 points, almost half of the maximum score of 30 points. What can be seen is that the impedance controllers score less than the admittance controllers.

B.7 Definitive choice

As can be seen in the rating of concepts 'Bar mechanism' and 'XY table' the XY-table concept is chosen to be the best mechanical concept. The chosen and most obvious actuation concept for the 'XY table' concept is with the lead spindles that are driven by electric motors. The chosen controller is an admittance controller. The type of input is force, because it is easier to implement it with the 'XY table' concept. There is no need to measure the angle of the cart in the XY plane, because the force sensor can be placed underneath the table surface. The forces than can be measured in the X- and Y-direction and are independent of the orientation of the cart. With EMG as input signal it is necessary to measure orientation of the cart, because the force vector calculated from the EMG signals is dependant on arm orientation.

C Design

C.1 XY table

The XY table consists of the following elements; 1. The Table, 2. The Actuators, 3. The magnet assembly, and 4. The arm cart (figure 20 and Appendix E).

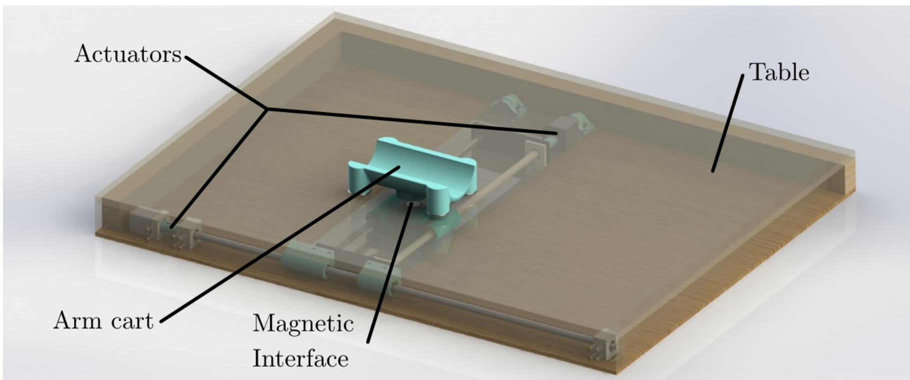

Figure 20: A 3D CAD impression of the final design of the XY-table concept. The table surface and two wooden frame parts have been made transparent to make the manipulator below the table surface visable. The parts are 1. The Table, 2. The Actuators, 3. The magnet assembly, and 4. The arm cart

C.1.1 The Table

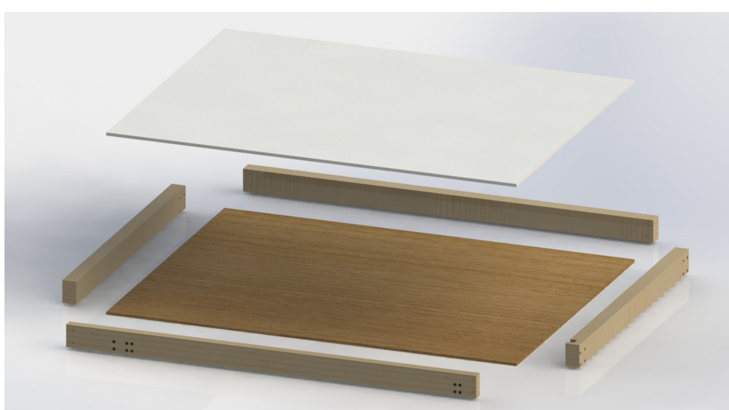

Figure 21: An exploded view of the table

The table will hold or support all the other parts of this concept. It is 800mm wide, 610mm deep, and 60mm thick. The size of the table is chosen to be a bit bigger than the normal working area of one arm. The width is kept to 800mm. This dimension is maximum one can easy go through a door, that are in general 900mm wide. The thickness is needed to house all the actuation parts in it. It consists of multiple materials. The bottom plate is a 6mm thick piece of oak. The beams on top of that are pine with a thickness of 44mm. The table surface is made of 10mm thick High Pressure Laminate (HPL). HPL is a laminate that is made out of multiple layers of impregnated paper which are fused under high temperature and high pressure. HPL is mostly used as decorative covering and furnature material.

C.1.2 The Actuators

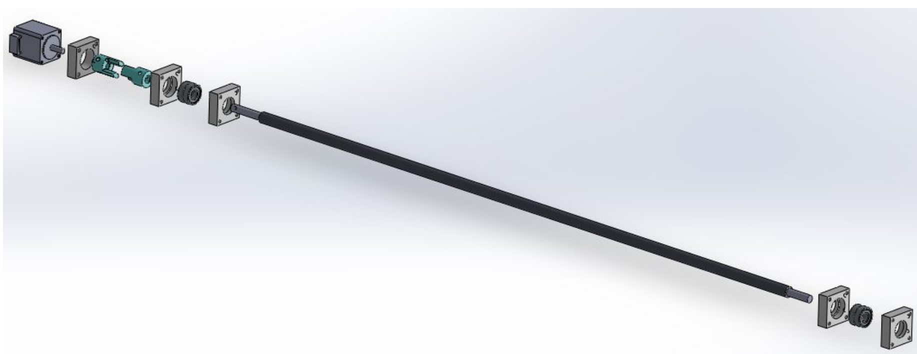

Figure 22: An exploded view of the manipulator for the x-direction

The actuator for the x-direction will take care of movement for the user's arm in the left and right direction. It is also a platform to connect the actuator for the Y-direction too. The actuator in the X-direction consists of a few parts, a stepper motor, a lead spindle, a flexible coupling between the spindle and the motor, and bearings and mounting blocks to connect the assembly to the frame.

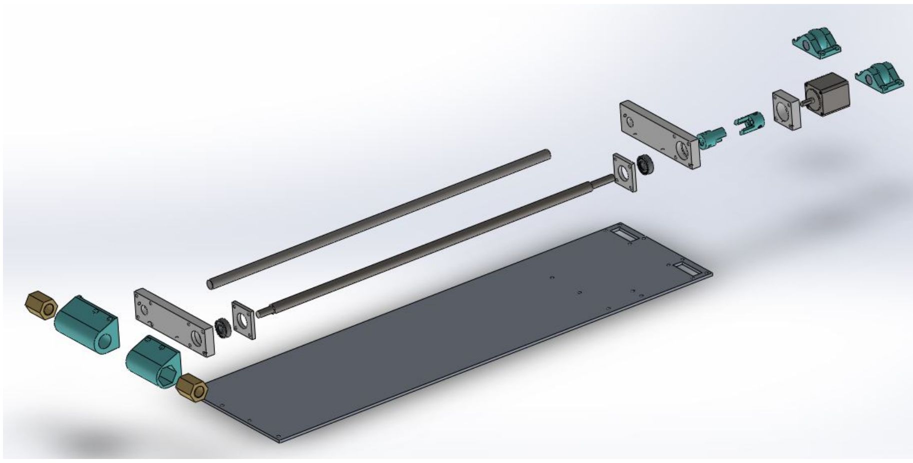

Figure 23: An exploded view of the manipulator for the y-direction

The actuator in the y-direction will take care of the forward and backward movement of the arm of the user. The magnet assembly will be attached to the lead spindle and the linear guidance this assembly. The movement is produced by a stepper motor. These parts with the bearings and mounting blocks are connected to a mounting plate, i.e. a 3mm thick aluminium sheet. This is connected to the actuator for the movement in the X-direction with two lead spindle nuts, which are separated by 150mm.

C.1.3 The magnet assembly

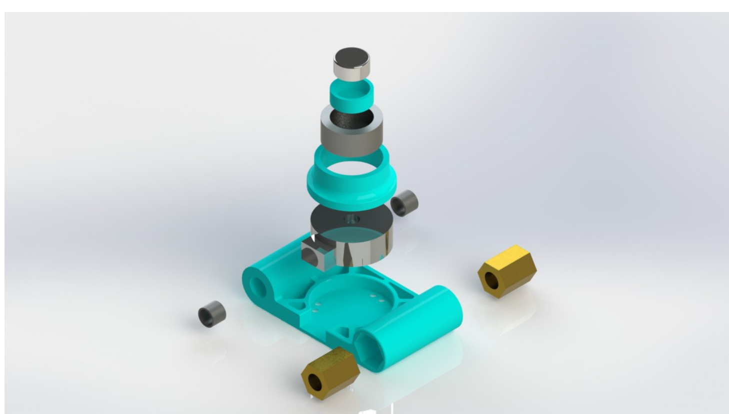

Figure 24: An exploded view of the magnet assembly

The magnet assembly is attached to the actuator for the Y-direction. It consists of a 3D-printed frame where a lead nut and two linear bearings are attached to. The 3D-printed frame also holds the force sensor and the magnet for the coupling with the arm cart that rolls on top of the table surface. To be sure that the magnetic field only affects the arm cart a cup of 5mm thick steel is placed around the magnet.

C.1.4 The arm cart

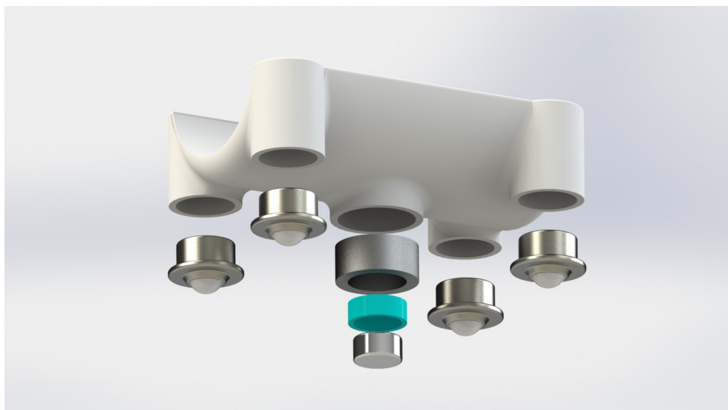

Figure 25: An exploded view of the arm cart

The arm cart is modelled of an existing arm cuff (UR5). The radius of the cart where the arm needs to be placed is 35mm. At the four corners of the arm cart there is a ball transfer unit. A ball transfer unit is a hemispherical ball bearing that is free to roll in any direction. In the middle at the bottom of the cart the same magnet, as at the magnet assembly, with the steel cup is placed.

C.2 Calculations

C.2.1 Motor and spindle calculation

In this section the required specifications of the motor and the spindle are determined. Specifically the diameter and lead, forward movement per revolution, are determined as is the needed torque of the stepper motor.

C.2.2 Spindle

In this case the most important requirements that determine the diameter and lead of the spindle are the required maximum linear velocity, 0.1m/s, and the force required to accelerate the arm towards a certain velocity. A very important limiting factor on the spindle is the so called critical spindle speed. This critical spindle speed is mainly determined by the root diameter of the spindle, the unsupported spindle length, the Young's modulus of the used spindle material, and the way the spindle is supported as can be seen in figure 26 [40]. Manufacterers of lead screw spindles advise to stay below 75%-80% of the critical spindle speed [40, 41, 42].

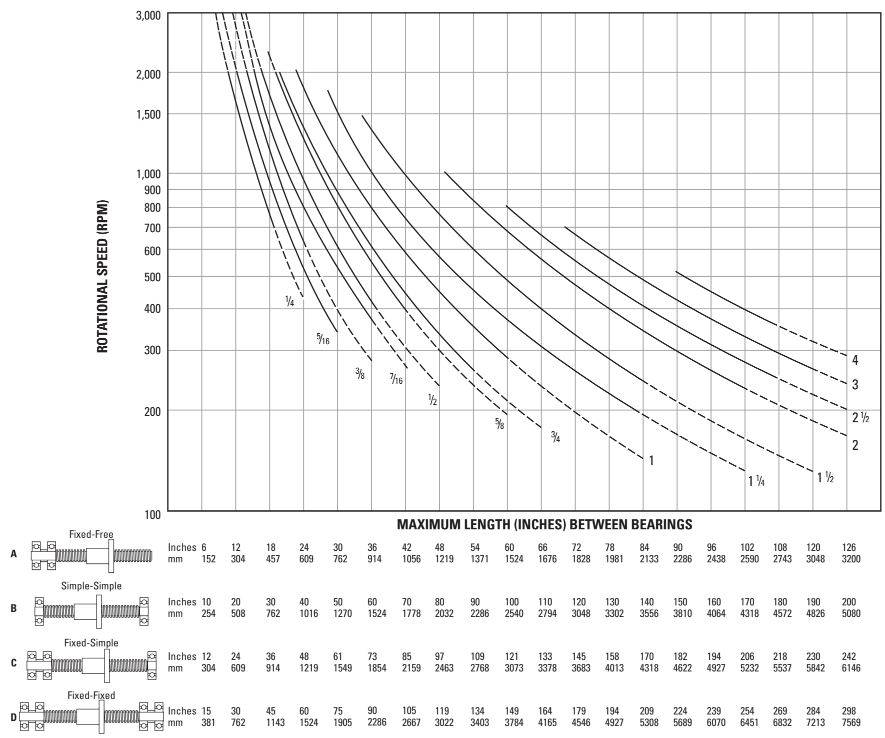

Figure 26: A typical critical spindle speed chart. The x-axis shows the unsupported length for different types of spindle support. A, B, C, and D represent the different types of support. The y-axis shows the rotational speed in revolutions per minute. The different root diameter are shown inside the graph underneath the lines and is given in inches.[40]

The spindle with the longest unsupported length is the spindle that will move the Y-table. The unsupported length of this spindle is 640mm, the other one has an unsupported length of 390mm. To move with a maximum linear speed of 0.1m/s with a spindle lead of 3mm, it is necessary to have a maximum rotational speed of 2000 revolutions per minute (rpm). With these two parameters - the unsupported length and the maximum rotational speed - a spindle diameter and the needed bearing support can be chosen. A spindle diameter of 12mm with a fixed-fixed bearing support is chosen for the spindle in the X-direction. The 80% critical spindle speed for this configuration is approximately 2500rpm. For the spindle in the Y-direction the same diameter is chosen with a simple-simple bearing support. The 80% critical spindle speed for this configuration is approximately 3500rpm, so the needed maximum rotational speed of both configurations are below the 80% critical spindle speed.

The critical spindle speed can also be calculated with the Rayleigh-Ritz equation which is the following formula [43];

$$n_c[rpm] = \frac{30}{\pi}\sqrt{\frac{g}{\delta_{st}}} \tag{3}$$

Where $\frac{30}{\pi}$ is a constant to convert rad/s into rpm, g is the gravitational acceleration in m/s^2, and δ_{st} is the total maximum static deformation in meters. When this formula is used with the deflections calculated in subsection C.4.1 on pages 81 - 85 the 80% critical spindle speed is 5350rpm for the x-spindle and 2480rpm for the y-spindle. Which way of determining the critical spindle speed is best won't be reviewed, but the latter one looks more accurate because it also takes the load on the spindle into account. Fact is that in both cases the needed rotational speed stays below the 80% critical spindle speed.

C.2.3 Stepper motor

To calculate the motor torque that is required to move the arm, the forces that are occuring during movement are identified. In the drivetrain there are friction losses at the bearings supporting the spindle. Also the ball transfer units at the arm cart have some friction and there is force needed to accelerate the Y-table, the cart with the arm of the user, and the spindle. See figure 27 for an overview of the forces.

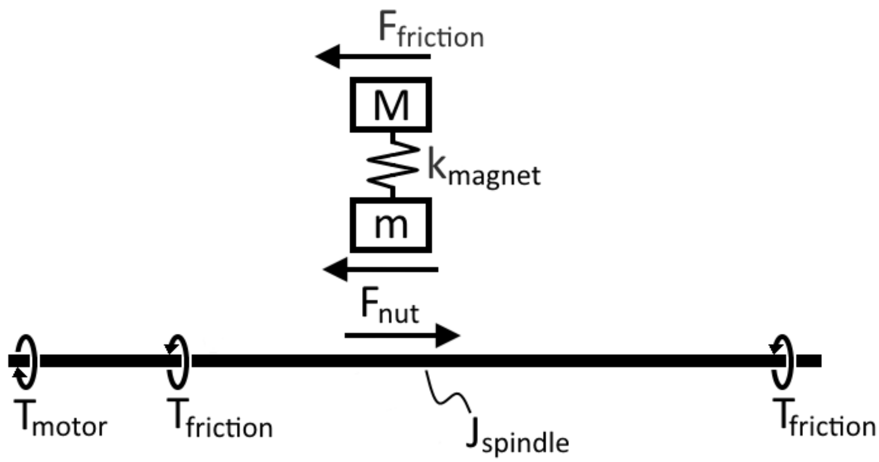

Figure 27: The forces the stepper motor needs to overcome. The spindle and the Y-table and arm with cart are decoupled, with F_{nut} being the interaction force between the two. The forces at the spindle include friction forces at the ball bearings of the spindle, acceleration of the spindle, and the nut force. The nut force includes acceleration of the Y-table and the arm with cart, and friction forces of the ball transfer units of the cart.

In a pulling test (Appendix A), that was conducted with healthy subjects (3f/1m), a static frition force of around 2 Newton was measured. When the arm with the cart are considered as a pure mass, an acceleration of $1m/s^2$ maximally adds 9 Newton. With anthropomorphic data [44] and weight distribution [45] it shows that with an arm mass of 8kg 95% of the US male population is included. The weigth of the armrest cart is 0.5kg.

The weight of the Y-table with the magnet assembly is 1.3kg. To accelate this with $1m/s^2$ a force of 1.3Newton is needed. These forces need to be converted to a motor torque that is needed to move the arm. The efficiency of the spindle and and nut is around 48% [46, 47]. Equation 4 comes from [41] and shows the amount of torque needed to accelerate the arm with $1m/s^2$.

$$\begin{aligned} T &= \frac{F[N] \cdot lead[mm]}{2\pi \cdot \eta} \\ &= \frac{12N \cdot 3mm}{2\pi \cdot 0.48} \\ &= 12mNm \end{aligned} \tag{4}$$

The chosen lead for the spindle is 3mm. This results in a torque of 12mNm. It is recommended by manufacterers that the nominal needed motor torque is approximately half of the pull out torque of the motor. Therefore we should look at stepper motors that have a pull out torque of 24mNm or higher over the complete rpm-range. The motor should also have a small frame size so the table thickness will be as thin as possible.

C.3 Magnet calculation

C.3.1 Magnet force

To overcome the static friction - around 2Newton in the horizontal plane - measured with the pull test (appendix A), interaction force between the magnets should be large enough. This static friction causes a dead-band in the cart movement and should be as small as possible. This can be done by making the friction coefficient smaller, by enlarging the magnetic interaction force or by making the gradient, the angle with the vertical, of the magnetic field larger.

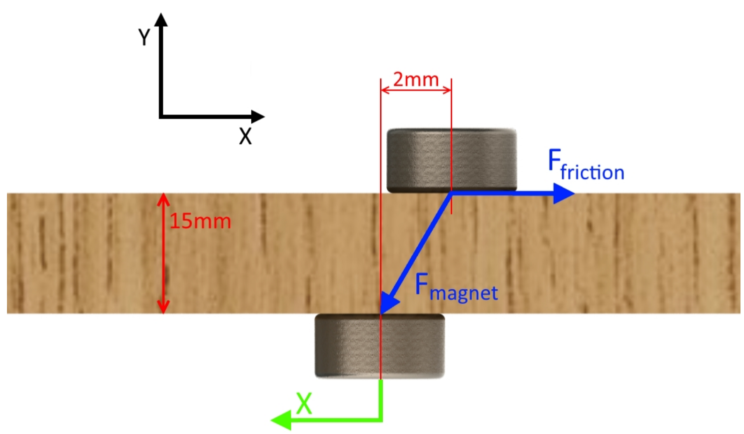

Figure 28: Relevant dimensions and forces acting on the magnets. The distance between the magnets in the y-direction is 15mm, the allowed dead-band is 2mm. The bottom magnet is moved in the x-direction and at the the maximum dead-band distance the x-component of the magnet force should be larger than the friction.

A dead-band of 2mm is seen as acceptable. With an air gap between the to magnets of 15mm, the result is that the pulling force between the magnets should be equal to or higher than 15Newton. See figure 28 for a representation of the described situation. With this force an approximation of the minimally required magnetic flux density, B, can be determined. Under the assumption that the field between the two magnets is uniform, the following formula can be used [48];

$$F[N] = \frac{B^2[T] \cdot A[m^2]}{2\mu_0[H/m]\mu_r[1]} \tag{5}$$

From this follows that the following also should hold, resulting in the minimally needed magnetic flux density;

$$\begin{aligned} B[T] &= \sqrt{\frac{2F[N]\mu_0[H/m]\mu_r[1]}{A[m^2]}} \\ &= \sqrt{\frac{2 \cdot 15N \cdot 4\pi \cdot 10^{-7}H/m}{\frac{\pi}{4} \cdot 0.02^2 m^2}} \\ &= 0.35T \end{aligned} \tag{6}$$

With the use of K&J Magnetics' calculator [49] that can calculate the magnetic flux density between two magnets, using a finite element method (FEM), a pair of magnets has been found that have a flux density at the center of the air gap of 0.35T between them. A validation test with the same magnets did confirm that the magnets were stong enough - 3.5N was measured - to overcome the friction force of 2N. The magnets have a diameter of 20mm, a thickness of 10mm, and are of grade N42 [50]. The grade resembles the maximum energy product (BH_{max}) and is equal to the maximum value of the flux density, B, times the field strength, H. It is measured in kilojoule per cubic meter (kJ/m^3) or Mega-Gauss-Oersted ($MGOe$). So a magnet with grade N42 has a maximum energy product of $40 - 42MGOe$ or $318 - 334kJ/m^3$. In general it can be said that the higher the maximum energy product is the stronger the magnet is [50].

To make the interaction force between the magnets larger the magnetic field can be redirected by using high permeability materials, like steel, iron, and mu-metal. With this redirection of the field also interaction between the two magnets is better. There will be a higher magnetic flux density between the magnets and the interaction area is larger. This results in a higher pulling force between two magnets and a lower dead-band on the arm cart side.

A small test conducted with the two chosen magnets showed an increase of maximal horizontal force from 3.5Newton to 6Newton by adding a steel sheet of 2mm on top of one magnet and below the other (see figure 29). This is an increase of 70% in horizontal force.

(a) 3 - 3.5 Newton (b) 4.5 - 5 Newton (c) 6 - 6.5 Newton

Figure 29: The three scenarios that were tested during the magnetic pull test. In subfigure a) the magnets were free. In subfigure b) both magnets have a 2mm steel sheet attached to them. In subfigure c) one magnet is free and the other has a 4mm steel sheet attached to it. The maximum horizontal forces up to the point where the two magnets still had interaction with eachother are stated underneath each subfigure.

C.3.2 Magnetic field deformation

The shape magnetic field can be changed by creating an easier path for the field to go through. Different materials have different permeabilities. A material with a higher permeability means that it is easier for the field to travel through that material than through materials with a lower permeability. The total permeability can be stated as:dd

$$\mu = \mu_0 \cdot \mu_r \tag{7}$$

With μ_0 being the permeability of free space (vacuum) and μ_r being the relative permeability of the specific material. Five types of magnetic material can be distinguished, namely diamagnetic, paramagnetic, ferromagnetic, antiferromagnetic, and ferrimagnetic. These types all have their own range of typical relative permeabilities. Diamagnetic, paramagnetic, and antiferromagnetic materials have a relative permeability of around 1. Ferrimagnetic materials of 2 to 100, and ferromagnetic materials 5000 to 200 000. [51].

The permeability is also dependent on the flux density and the field strength, as permeability can also be defined as:

$$\mu = \frac{B}{H} \tag{8}$$

So, the permeability of the material, when subjected to a magnetic field, can be derived from the manetisation curve. An example of such a magnetisation curve can be seen in figure 30.

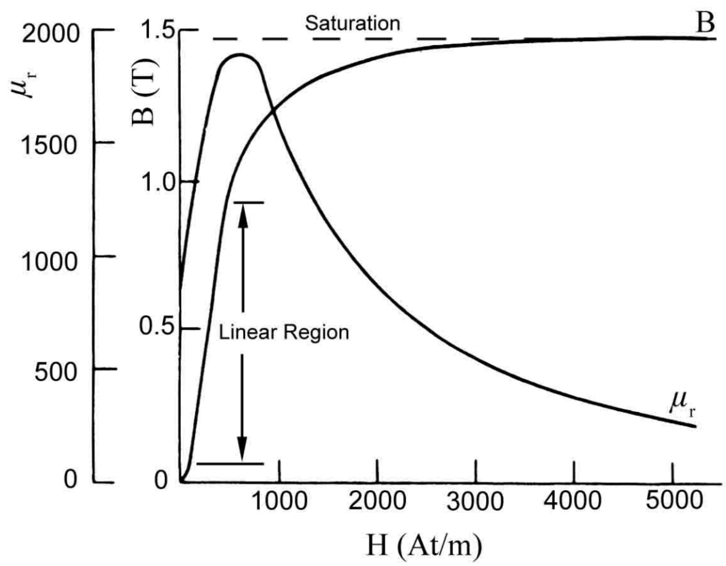

Figure 30: A typical relation between the relative permeability μ_r and the magnetisation of ferromagnetic material [52].

In figure 30 it can be seen that the permeability changes when either the flux density or the field strength changes up to the point where the material is magnetically saturated. When the material is saturated the permeability is equal to zero and additional field won't go through the material.

From testing with the used magnets, to redirect all magnetic field a steel plate with a thickness of 5mm is needed. Also see figure 31 for an example of the difference between field shape and strength of a free magnet and a magnet that is attached to a 5mm thick steel sheet. These figures are made with the FEM calculator of K&J Magnetics [53] [54].

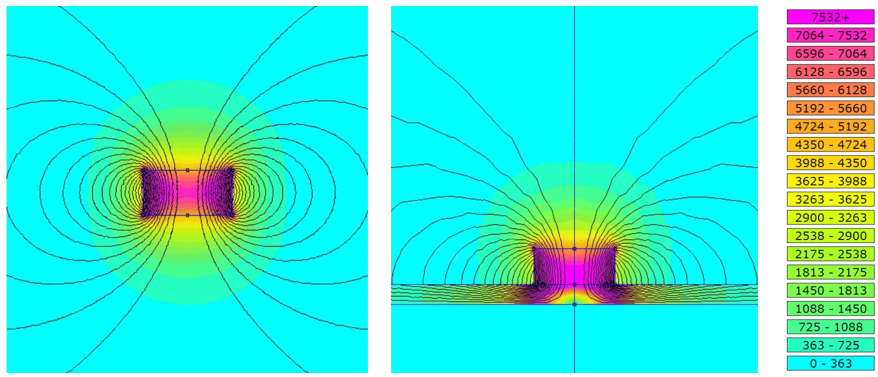

(a) A free magnet

(b) Magnet with 5mm steel sheet

(c)

Figure 31: The difference in field strength and shape of the field beteen a) a free magnet and b) a magnet attached to a steel sheet that is thick enough to redirect all of the field through the sheet material. The colors in a) and b) correspond to the colors and field strengths in c). Pictures are made with K&J Magnetics' FEM calculator

An exploded view of the magnetic interface is shown below (Fig.32. The magnetic interface consist of two magnets - one attached to the end effector of the actuators underneath the table surface and one above it, attached to the arm cart - and their shielding to make it safe. With this shielding the magnetic field can be shaped so the interaction between the two magnets is stronger and can be kept within a small distance ($\leq 25mm$) from the magnet center (Fig. 33). The result is that the risk of attacting large metal objects or damaging electronics is very low. The only way to collect metal objects with the device is by rolling over the object itself. Another positive about the magnetic redirection is that electronics won't get affected by the device's magnetic field. Also with the use of magnets the rotational DOF around the magnets center is released, allowing rotation of the arm around this point.

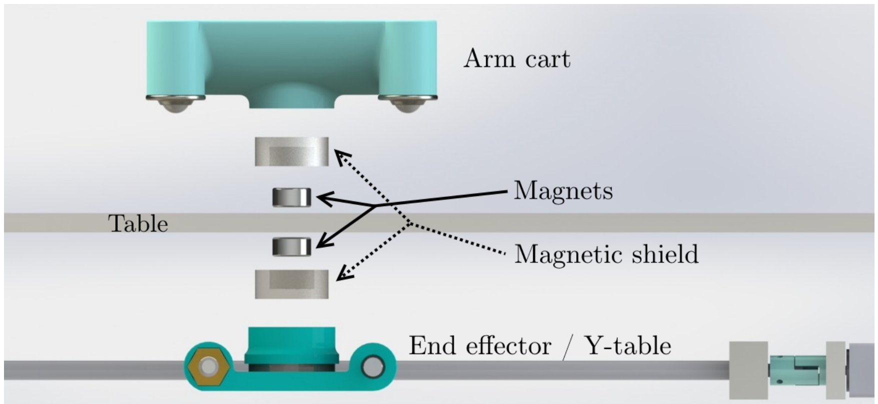

Figure 32: An exploded view of the magnetic interface. At both sides of the table top - the Arm cart and the Y-table side - there is a magnet with magnetic shield. With this interface movement of both parts is connected.

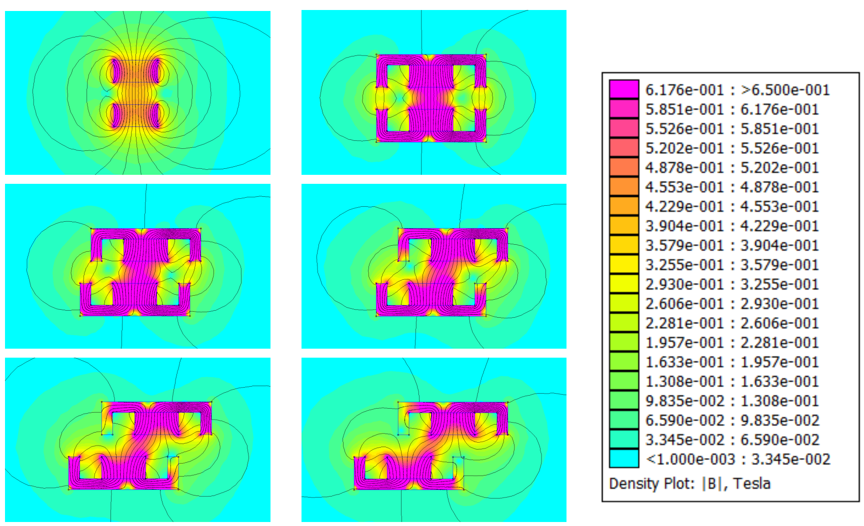

Figure 33: The difference in field between two magnets without and with magnetic shield (a & b), and the attractor field shapes of the magnets with shielding at cener distances of 5mm (c), 10mm (d), 15mm (e), and 20mm (f). Colors are representing the field strengths in Tesla (g). The pictures are generated using Femm4.2 [55].

C.4 Deformations of table components

Here the deformation of some important parts is calculated. These parts are the spindle and linear guidance who support the Y-table and magnet assembly and are responsible for movement in the x-direction, the Y-table with the spindle and linear guidance that supports the magnet assembly and is responsible for movement in the y-direction, and the table top that supports the arm cart with the arm. Also if the balls of the arm cart will cause permanent deformation of the table top is calculated.

C.4.1 Spindle deformation

Due to the weight of the carriege and the magnetic forces the spindles and the linear guindances for movement in the x- and y-direction will deflect up or down. In this section an appoximation of how much deformation will occur is calculated.

The x-direction spindle will experience the weight of the Y-table and the magnet assembly, and the magnetic pull force of the magnets. The pitch diameter of the used spindle and diameter of the linear guidance shaft are the same, therefore it can be said that the second moment of area is the same. Also own weight of the spindle has influence on the deformation. Figure 34 shows the two types of bending that are used to calculate the deformation of the x-direction spindle.

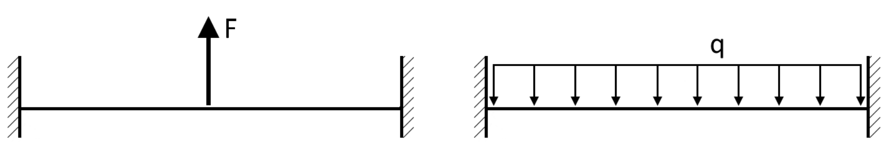

(a) $w = \frac{1}{192}\frac{Fl^3}{EI}$ (b) $w = \frac{1}{384}\frac{ql^4}{EI}$

Figure 34: Two types of bending that are used to calculate the deformation of the spindle and also the linear guidance. (a) shows the deflection due to the force of the magnet and the weight of the Y-table and magnet assembly.
(b) shows the deflection caused by the spindle's own weight. The sum of the two deflections is the total deflection of the spindle.

$$
\begin{aligned}
F &= \sum F_z \\
&= 20N - 1.27kg \cdot 9.81m/s^2 = 7.6N
\end{aligned}
$$

$$
\begin{aligned}
I_{spindle} = I_{shaft} &= \iint y^2 dA \\
&= \frac{\pi}{4} r^4 \\
&= \frac{\pi}{4} 5^4 mm^4 = 491mm^4
\end{aligned}
\tag{9}
$$

$$
\begin{aligned}
w_F &= \frac{1}{192} \frac{Fl^3}{EI} \\
&= \frac{1}{192} \frac{7.6N \cdot 639^3 mm^3}{200\ 000 N/mm^2 \cdot 2 \cdot 491mm^4} \\
&= 0.053mm \\
w_q &= \frac{1}{384} \frac{ql^4}{EI} \\
&= \frac{1}{384} \frac{7.5 \cdot 10^{-3} N/mm \cdot 639^4 mm^4}{200\ 000 N/mm^2 \cdot 491mm^4} \\
&= 0.033mm \\
w_{x-stage} &= w_F - w_q \\
&= 0.053mm - 0.033mm = 0.020mm
\end{aligned}
\tag{10}
$$

The maximum total deflection of the x-direction spindle and the linear guidance is 0.020mm in the upward direction.

The y-direction spindle experience the weight of the magnet assembly and the magnetic pull force of the magnets. Most deformation occurs when the magnet is half-way the range of the y-direction spindle. This deformation consists of two components; the deformation of only the y-direction spindle with the linear guidance and the total deformation of the y-table.

To determine the deflection of the Y-table, first the neutral axis should be found. With the neutral axis the bending stiffness of the Y-Table can be calculated (see figure 35).

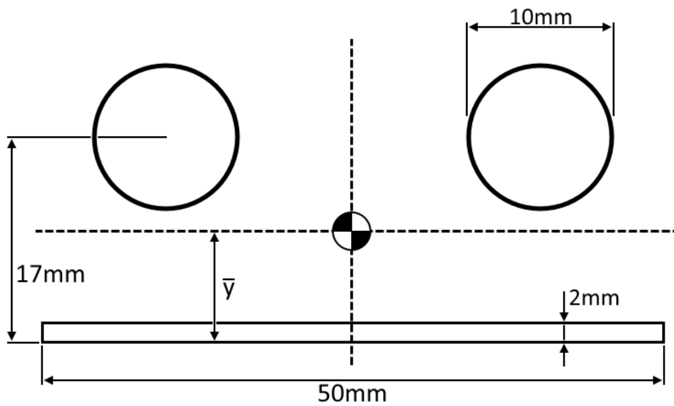

Figure 35: Cross-section of the Y-table, with the spindle and the guidance shaft being both $\phi 10mm$ and the mounting plate below that has dimensions 50mm x 2mm. $\bar{y}$ represents the distance between the neutral line and the bottom of the mounting plate.

$$\begin{aligned}\bar{y} &= \frac{\sum \bar{y} dA}{\sum dA} \\ &= \frac{17mm \cdot \frac{\pi}{4} 10^2 mm^2 + 1mm \cdot 50mm \cdot 2mm}{\frac{\pi}{4} 10^2 mm^2 + 1mm \cdot 50mm \cdot 2mm} \\ &= 8.04mm\end{aligned} \tag{11}$$

$$\begin{aligned}I_{y-table} &= \iint y^2 dA \\ &= 2 \cdot \sum (I_{xx} + A d_y^2) \\ &= 2\left(\frac{\pi}{4} r^4 + A_{spindle} \cdot d_{spindle}^2 + \frac{b \cdot t^3}{12} + A_{sheet} \cdot d_{sheet}^2\right) \\ &= 2(491mm^4 + 6\ 308mm^4 + 67mm^4 + 6\ 462mm^2) \\ &= 26\ 653mm^4\end{aligned} \tag{12}$$

$$\begin{aligned}I_{y-spindle} &= 2 \iint y^2 dA \\ &= 2\frac{\pi}{4} r^4 = 2\frac{\pi}{4} 5^4 mm^4 = 982mm^4\end{aligned} \tag{13}$$

With the bending stiffness of the Y-table being determined, the deflections of all components can be calculated. The bending situations of the complete Y-table ,and the spindle and linear guidance are shown in figure 36. To simplify the calculation of the total deflection it is assumed that the centre of the Y-table lines up with the centre of the spindle and linear guidance. The centre is where the largest deflection should occur. The case is that these two centers lay 20mm apart from each other. So the simplification will show a higher deflection than in the real world case.

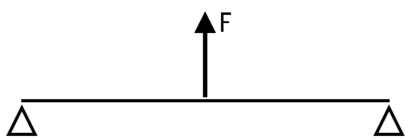

(a) $w = \frac{1}{48}\frac{Fl^3}{EI}$

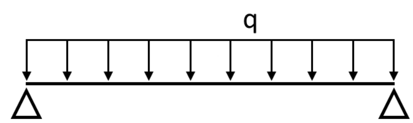

(b) $w = \frac{5}{384}\frac{ql^4}{EI}$

Figure 36: Two types of bending that are used to calculate the deformation of the spindle and also the linear guidance. (a) shows the deflection due to the force of the magnet and the weight of the magnet assembly. This is applicable for both the spindle and linear guidance as for the Y-table deflection calculations. (b) shows the deflection caused by the spindle's own weight. The sum of the deflections is the total deflection of the spindle.

$$\begin{aligned} F &= \sum F_z = F_{magnet} - m_{magnet} g \\ &= 20N - 0.23kg \cdot 9.81m/s^2 = 17.8N \end{aligned} \tag{14}$$

$$
\begin{aligned}
w_{y-table} &= \frac{1}{48}\frac{Fl^3_{y-table}}{EI_{y-table}} \\
&= \frac{1}{48}\frac{17.8N \cdot 530^3mm^3}{200\ 000N/mm^2 \cdot 26\ 653mm^4} \\
&= 0.010mm
\end{aligned}
$$

$$
\begin{aligned}
w_{F,y-spindle} &= \frac{1}{48}\frac{Fl^3_{y-spindle}}{EI_{y-spindle}} \\
&= \frac{1}{48}\frac{17.8N \cdot 397^3mm^3}{200\ 000N/mm^2 \cdot 982mm^4} \\
&= 0.118mm
\end{aligned} \tag{15}
$$

$$
\begin{aligned}
w_{q,y-spindle} &= \frac{5}{384}\frac{ql^4_{y-spindle}}{EI_{y-spindle}} \\
&= \frac{5}{385}\frac{7.5 \cdot 10^{-3}N/mm \cdot 397^4mm^4}{200\ 000N/mm^2 \cdot 982mm^4} \\
&= 0.025mm
\end{aligned}
$$

$$
\begin{aligned}
w_z &= w_{y-table} + w_{F,y-spindle} - w_{q,y-spindle} \\
&= 0.010mm + 0.118mm - 0.025 = 0.103mm
\end{aligned}
$$

The maximum total deformation of the Y-table, and the spindle and linear guidance is 0.103mm. The total deflection of the whole X- and Y-stage is 0.123mm in the upward direction.

C.4.2 Table top deformation

To see how much the table top will bend under the given load, a calculation under the worst case situation will be done. The worst case situation is when the cart is at the middle of the table. To calculate how much deformation occurs the Kirchhoff-Love method for thin plate bending will be used. The total deflection consists of deformation caused by a load and deformation caused by own weight.

The used material is High Pressure Laminate (HPL) which is a highly compressed plastic. Manufacturers guarantee a Young's modulus of $\geq 9\ 000N/mm^2$ [56, 57, 58]. The dimension of the used HPL plate is $800mm \times 610mm \times 10mm$ ($L_x \times L_y \times t$). The poisson ration (ν) of HPL is approximately 0.32 [59] and the terms used in x- and y-direction (m and n) for numerical solving the equation are both 32.

It is assumed that the load, that is distributed through four ball transfer units, acts like a point load. The table top is simply supported at all four edges by a frame that consists of three 27mm wide beams and one 18mm wide beam. See figure 37 for the bending situation. The deformation, w, can be calculated as seen in equation 16 [60].

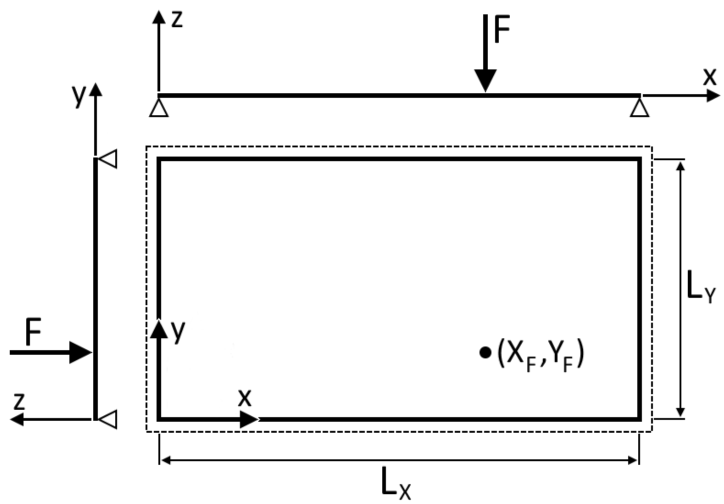

Figure 37: The situation of bending under the weight of the arm plus cart and the magnet force. 'F' represents the total force of the previous stated components. All four edges are simply supported.

$$w(x,y) = \frac{4F}{\pi^4 L_x L_y D} \sum_m^\infty \sum_n^\infty \frac{\sin\left(\frac{m\pi x_0}{L_x}\right)\sin\left(\frac{n\pi y_0}{L_y}\right)\sin\left(\frac{m\pi x}{L_x}\right)\sin\left(\frac{n\pi y}{L_y}\right)}{\left\{\left(\frac{m}{L_x}\right)^2 + \left(\frac{n}{L_y}\right)^2\right\}^2} \quad (16)$$

Where D, the flexural modulus, is;

$$\begin{aligned} D &= \frac{Et^3}{12(1-\nu^2)} \\ &= \frac{200\ 000 N/mm^2 \cdot 10^3 mm^3}{12(1-0.32^2)} \\ &= 18.57 \cdot 10^6 Nmm \end{aligned} \quad (17)$$

The largest deflection is at the middle of the plate, position $(x_0, y_0) = (\frac{L_x}{2}, \frac{L_y}{2})$ and is equal to 0.41mm;

$$\begin{aligned} w(x_0, y_0) &= \frac{4F}{\pi^4 L_x L_y D} \sum_m^\infty \sum_n^\infty \frac{\sin^2\left(\frac{m\pi x_0}{L_x}\right)\sin^2\left(\frac{n\pi y_0}{L_y}\right)}{\left\{\left(\frac{m}{L_x}\right)^2 + \left(\frac{n}{L_y}\right)^2\right\}^2} \\ &= \frac{300N}{7.62 \cdot 10^{14} Nmm^3} \sum_{m=1}^{32} \sum_{n=1}^{32} \frac{\sin^2\left(\frac{m\pi}{2}\right)\sin^2\left(\frac{n\pi}{2}\right)}{\left\{\left(\frac{m}{746mm}\right)^2 + \left(\frac{n}{565mm}\right)^2\right\}^2} \\ &= 0.413mm \end{aligned} \quad (18)$$

The deformation caused by the HPL plate's own weight can be calculated as in equation 16 [61] and the bending situation can be seen in figure 38.

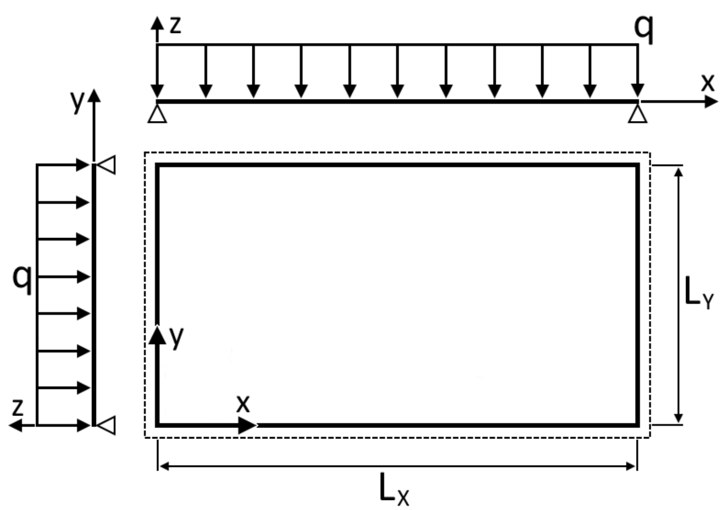

Figure 38: The situation of bending under own weight. All four edges are simply supported. 'q' represents the own weigth of the HPL plate.

$$w(x, y) = \frac{16q}{\pi^6 D} \sum_m^\infty \sum_n^\infty \frac{\sin\left(\frac{m\pi x}{L_x}\right)\sin\left(\frac{n\pi y}{L_y}\right)}{mn\left\{\left(\frac{m}{L_x}\right)^2 + \left(\frac{n}{L_y}\right)^2\right\}^2} \quad (19)$$

Where q is the distributed load, which is equal to the plate's weight per square meter, $14.0kg/m^2$ [56], times the gravitational acceleration, $9.81m/s^2$, and the flexural rigidity D is the same as with the point load.

$$\begin{aligned} w(x_0, y_0) &= \frac{16q}{\pi^6 D} \sum_{m=1}^{32} \sum_{n=1}^{32} \frac{\sin\left(\frac{m\pi x_0}{L_x}\right) \sin\left(\frac{n\pi y_0}{L_y}\right)}{mn\left\{\left(\frac{m}{L_x}\right)^2 + \left(\frac{n}{L_y}\right)^2\right\}^2} \\ &= \frac{2.2 \cdot 10^{-3} N/mm^2}{1.79 \cdot 10^{10} Nmm} \sum_{m=1}^{32} \sum_{n=1}^{32} \frac{\sin\left(\frac{m\pi}{2}\right) \sin\left(\frac{n\pi}{2}\right)}{mn\left\{\left(\frac{m}{746mm}\right)^2 + \left(\frac{n}{565mm}\right)^2\right\}^2} \\ &= 0.110mm \end{aligned} \tag{20}$$

The total maximum deformation is the sum of both types of deformation and is equal to 0.52mm at the centre of the table top.

C.4.3 Rolling of the table top

With the arm resting in the cart and the magnets pulling towards each other, there will be calculated if the ball of the ball transfer units will cause local deformation of the table top. The cart has four ball transfer units distributing the forces of the arm and the magnets. The mass of the arm supported by the cart is maximally around 5kg, the mass of the cart is 0.5kg and the magnets attract each other with approximately 20N. The total force acting on the table is 75N, $\sim 19N/ball$. Most seen ball material groups are carbon steel, stainless steel, glass, and plastic. The principle of table top rolling is shown for one ball transfer unit in figure 39.

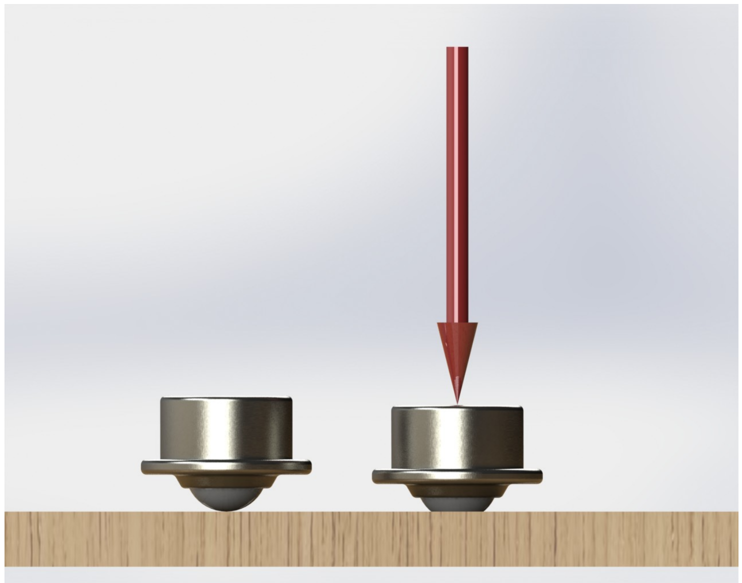

Figure 39: The left ball transfer unit represents the non-deformed situation. The right ball transfer unit the deformed state when a force (depicted by a red arrow) is applied. The deformation of the ball is exaggerated with respect to the real deformation to make the deformation visible. It can be seen that when a force is applied the contact point becomes a contact area.

To make the calculation easier it is assumed that the table top has a much higher Young's modulus than the ball material of the used ball transfer units, only the balls will deform the table top will not deform locally when the calculated stress stays below the yield stress.

The following balance should apply;

$$\sigma[N/mm^2] = \frac{F[N]}{A[mm^2]} = E[N/mm^2]\ \epsilon[1] \tag{21}$$

Because it is assumed that only the ball deforms, the contact area of the ball with the table is only dependent on the ball's radius and ϵ. Therefore the contact area can be expressed as a function of ϵ. Where ϵ is equal to;

$$\epsilon = \frac{L_0 - L}{L_0} \tag{22}$$

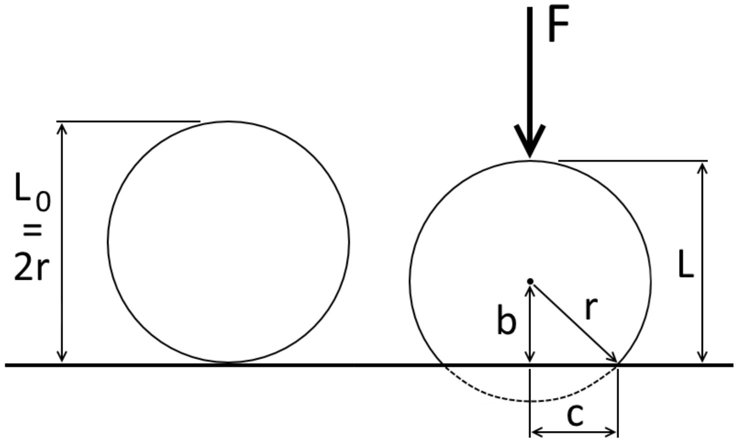

Figure 40: All the different parameters that are used in the derivation of the contact area formula.

The parameters used in equation 20 to derive the contact area as a function of the ball's radius and ϵ are shown in figure 40.

$$\begin{aligned} A &= \pi c^2 \\ &= \pi(r^2 - b^2) \\ &= \pi(r^2 - (r - [L_0 - L])^2) \\ &= \pi(r^2 - (r - \epsilon \cdot L_0)^2) \\ &= \pi(r^2 - (r - 2\epsilon \cdot r)^2) \\ &= 4\pi\epsilon(1-\epsilon)r^2 \end{aligned} \tag{23}$$

From equations 4 and 5 also the following should hold;

$$\begin{aligned} \frac{F}{E} &= \epsilon \cdot A \\ &= \epsilon(4\pi\epsilon(1-\epsilon)r^2) \\ &= 4\pi r^2(\epsilon^2 - \epsilon^3) \end{aligned} \tag{24}$$

Because ϵ is in the range of 0-0.02, the ϵ^3 can be discarted. This gives a lower calculated stress of around 0.2% for plastics ($E = 2500N/mm^2$) and a smaller devitation for stiffer materials like glass and steel. By discarting ϵ^3, ϵ will be equal to;

$$\epsilon = \sqrt{\frac{F}{4\pi r^2} \cdot \frac{1}{E}} \tag{25}$$

With Hooke's law the table top stress can be calculated as a function of the size of the ball, the force per ball applied to the table, and the Young's modulus of the ball material. The table top stress function is equal to;

$$\begin{aligned} \sigma_{TableTop} &= \epsilon E \\ &= \sqrt{\frac{F}{4\pi r^2}\frac{1}{E}} \cdot E \\ \sigma_{TableTop} &= \sqrt{\frac{FE}{4\pi r^2}} \end{aligned} \tag{26}$$

When this equation is plotted as table top stress against the Young's modulus of the ball transfer unit's ball material, the following relation can be seen.

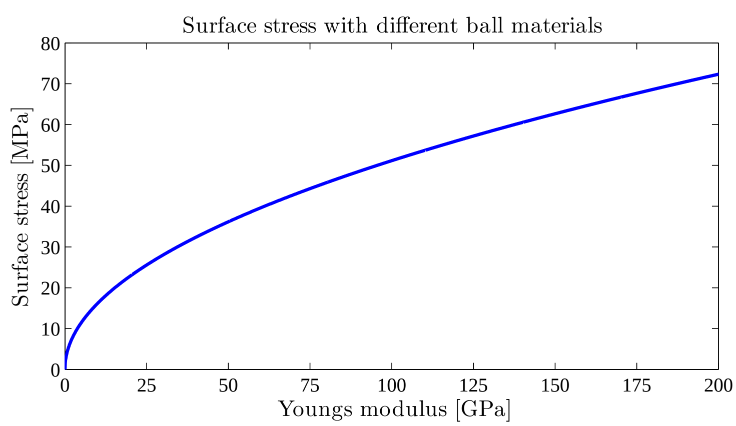

Figure 41: The stress at the table top surface for different materials

The table top stress should stay below the yield stress of HPL. Manufacturers only state the ultimate tensile strength of the material, which is $\geq 70N/mm^2$. When looked at other plastics it can be said that in general the yield stress of plastics is about 50% to 60% of their tensile strength. Applying this to HPL, the table top stress should stay below $35 - 40N/mm^2$. It can be seen that from the available ball material groups only plastic balls - Young's modulii between 0.1GPa and 6GPa - satisfy with the stress requirement.

C.5 Controller

C.5.1 Model of the plant

To be able to design a basic P(I)D controller, a simple model of the plant needs to be made. This P(I)D controller can be tuned later on with the real prototype. With this model the frequency response function is determined and therefore the eigenfrequency and the rigid body mode are roughly known. The model is undamped and uses ideal components (figure 42). The transfer function is from the motor torque to the position of the X-manipulator.

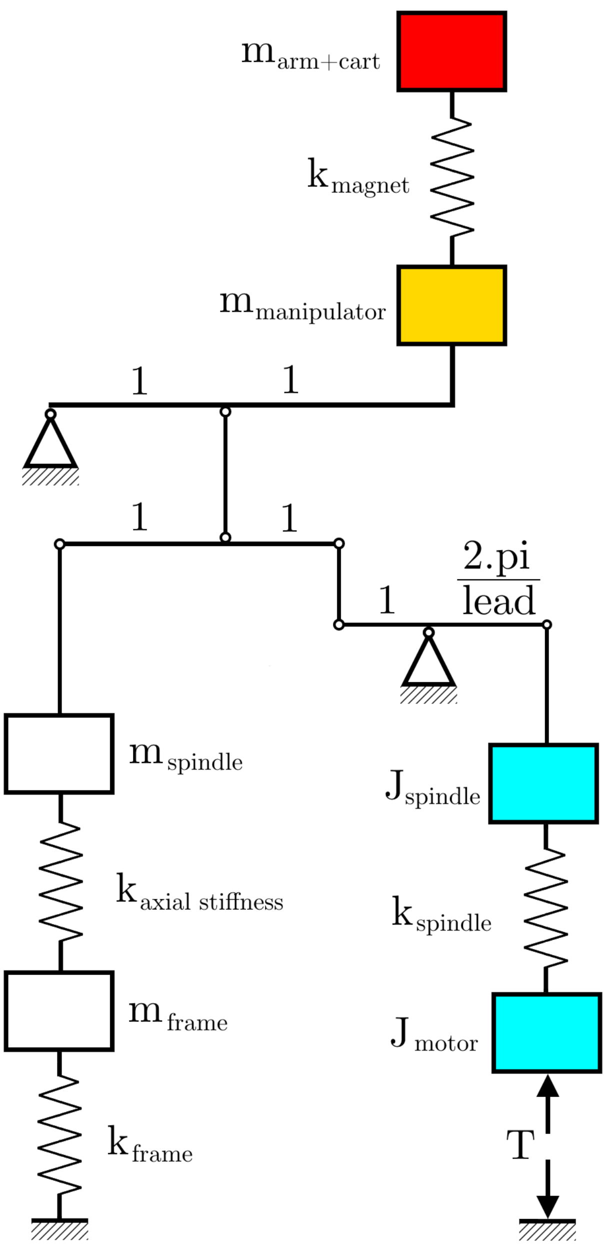

Figure 42: An ideal model of the plant

This model can be simplified to a 2DOF model. With such a model reduction only the lowest mode of vibration of the plant remains. When a stiffness is 10 times stiffer than the lowest stiffness, it can be considered rigid. When a mass is 10 times less than the next lowest mass, it can be considered as zero mass. The transmission can be omitted by multiplying the inertia and stiffness with the inverse ratio squared, and the torque with the inverse ratio. With the known parameters (table 3) this results in one of the standard classes, i.e. the flexible transmission (figure 43).

Table 3: The parameters and values of the modelled plant

Parameter	Formula	Value
$m_{arm+cart}$	-	4 kg
$m_{manipulator}$	-	1.5 kg
k_{magnet}	-	1000 N/m
$J_{spindle}$	-	$1.5 \cdot 10^{-5} kg \cdot m^2$
$k_{spindle}$	$\frac{G \cdot I_{spindle}}{l}$	138.1 Nm/rad
$m_{spindle}$	-	0.55 kg
$k_{axial\ stiffness}$	$2\frac{EA}{l}$	$50.6 \cdot 10^6$ N/m
J_{motor}	-	$9 \cdot 10^{-7} kg \cdot m^2$
m_{frame}	-	20 kg
i	$\frac{2 \cdot pi}{lead}$	2094.4

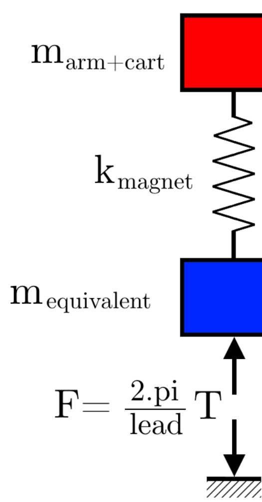

Figure 43: A simplified ideal model of the plant. The final model complies with the 'flexible transmission' model.

Where $m_{equivalent}$ is equal to;

$$\begin{aligned} m_{equivalent} &= m_{manipulator} + \frac{J_{spindle}}{(\frac{2\pi}{lead})^2} + \frac{J_{motor}}{(\frac{2\pi}{lead})^2} \\ &= 1.5kg + \frac{9 \cdot 10^{-7}}{(\frac{2\pi}{3 \cdot 10^{-3}})^2} + \frac{1.5 \cdot 10^{-5}}{(\frac{2\pi}{3 \cdot 10^{-3}})^2} \\ &= 1.5kg \end{aligned} \tag{27}$$

Now the reduced model is known the frequency response function can be determined. In this case we have two modes, i.e. one rigid body mode and one mode of vibration.

The plant's frequency response function is equal to;

$$\left| \frac{x_{X-manipulator}}{F_{motor}} \right| (s) = P(s) = \frac{\omega_e^2}{\omega_a^2 (m_{arm+cart} + m_{equivalent})} \; \frac{s^2 + \omega_a^2}{s^2 (s^2 + \omega_e^2)} \tag{28}$$

Where;

$$\omega_e = \sqrt{\frac{k_{magnet}}{m_{arm+cart}} + \frac{k_{magnet}}{m_{equivalent}}}$$

$$\omega_a = \sqrt{\frac{k_{magnet}}{m_{arm+cart}}}$$

This results in the following Bode diagram;

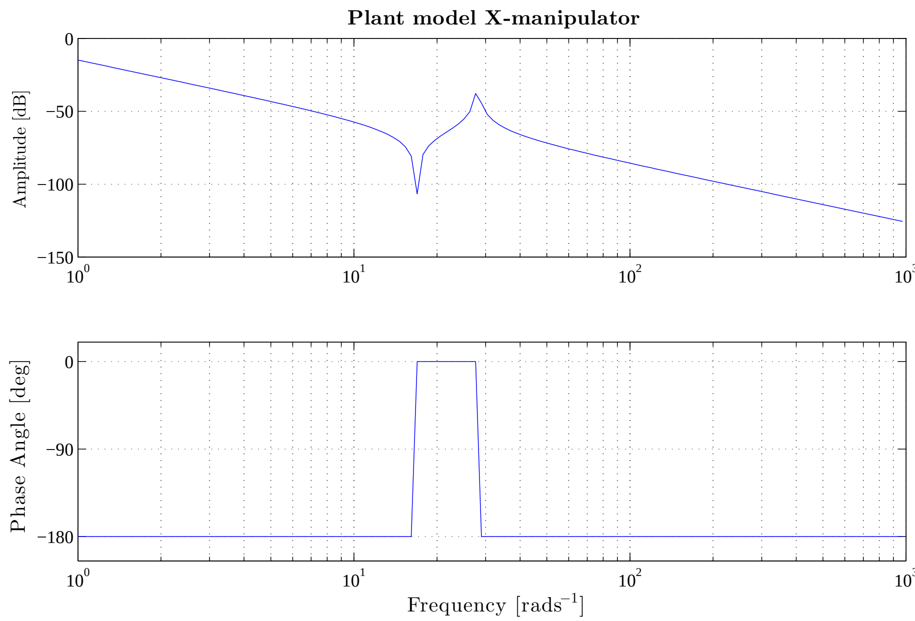

Figure 44: The Bode diagram of the reduced plant model of the XY-table. Both the rigid body mode and the mode of vibration can be seen clearly. In the magnitude plot the rigid body mode is the downward peak at 16.9 rad/s, the vibration mode the upward peak at 28 rad/s.

C.5.2 Controller

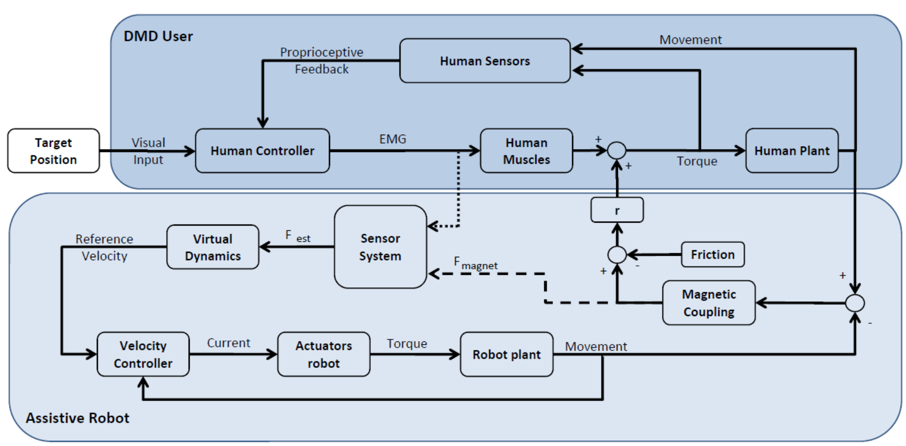

Figure 45: The control schematic of the final controller used for the XY-table.

C.5.3 Filtering the input

The EMG input signal is a noisy signal and is not usable as a raw input for the controller. Therefore filtering needs to be done to get a useful steering signal for the controller. The mains will cause some noise at 50Hz or 60Hz (depending on mains frequency). This will be filtered by a notch filter at the frequency of the mains. After the notch filter the right envelope needs to be taken. This is done by highpass filtering at 20Hz to remove the static offset, rectifying that signal, and lowpass filtering at 3Hz to get a smoother signal (46). The filters are implemented digitally.

An 2^{nd} order Notch filter in the discrete form looks like:

$$H_{notch}(z) = \frac{Y(z)}{X(z)} = \frac{b_0 + b_1 \cdot z^{-1} + b_2 \cdot z^{-2}}{1 - a_1 \cdot z^{-1} - a_2 \cdot z^{-2}} \tag{29}$$

In the usefull form (timestep) for the controller this results in;

$$\begin{aligned} y(n) = a_1 \cdot y(n-1) + a_2 \cdot y(n-2) \\ + b_0 \cdot x(n) + b_1 \cdot x(n-1) + b_2 \cdot x(n-2) \end{aligned} \tag{30}$$

Where:
$x(m)$ is the input at timestep m
$y(m)$ is the output at timestep m
$a_1 = 2r \cdot cos(2\pi \frac{f_n}{f_s})$
$a_2 = r^2$
$b_0 = 1$
$b_1 = -2 \cdot cos(2\pi \frac{f_n}{f_s})$
$b_2 = 1$
f_n is the frequency to be filtered in Hz
f_s is the sampling frequency in Hz
r usually $.95 < r < .99$ to ensure stability of the filter, defines the width of the notch.

The frequency that needs to be filtered is 50Hz and the sampling frequency used is 250Hz. For r a value of 0.95 is chosen.

$$y(n) = 0.5871 \cdot y(n-1) + 0.9025 \cdot y(n-2) + x(n) - 0.6180 \cdot x(n-1) + x(n-2) \tag{31}$$

A general form of a 2^{nd} order highpass Butterworth filter in the Laplace domain is:

$$H_{Highpass}(s) = \frac{Y(s)}{X(s)} = \frac{s^2}{s^2 + \sqrt{2}\omega_c s + \omega_c^2} \tag{32}$$

To use this in the controller, which is in the discrete time domain, the filter needs to be discretized. Discretization will be done into the Infinite Integral Response

(IIR) shape (i.e. $s = \frac{T}{2}\frac{1-z^{-1}}{1+z^{-1}}$, where T is the sampling time). For this bilinear transformation the crossover frequency in the analogue domain also needs to be converted into the discrete cossover frequency. The used sampling frequency is 250Hz, resulting in a sampling time of 4 milliseconds. The crossover frequency (ω_c) is 20Hz converted into the shape of $\omega_c = \frac{2}{T}\alpha$. This results in the following filter;

$$
\begin{aligned}
H_{Highpass}(z) = \frac{Y(z)}{X(z)} &= \frac{\frac{2}{T}^2 \frac{1-z^{-1}}{1+z^{-1}}^2}{\frac{2}{T}^2 \frac{1-z^{-1}}{1+z^{-1}}^2 + \frac{2}{T}^2 \sqrt{2}\alpha \frac{1-z^{-1}}{1+z^{-1}} + \frac{2}{T}^2 \alpha^2} \\
&= 0.705 \frac{1 - 2z^{-1} + z^{-2}}{1 - 1.321z^{-1} + 0.499z^{-2}}
\end{aligned}
\tag{33}
$$

This results in the IIR equation;
$y(n) = 0.705 \cdot x(n) - 1.410 \cdot x(n-1) + 0.705 \cdot x(n-2) + 1.321 \cdot y(n-1) - 0.499 \cdot y(n-2)$

The same will be done for the 2^{nd} order lowpass Butterworth filter. The crossover frequency for the lowpass filter is 3Hz.

$$
\begin{aligned}
H_{Lowpass}(s) = \frac{Y(s)}{X(s)} &= \frac{\omega_c^2}{s^2 + \sqrt{2}\omega_c s + \omega_c^2} \\
H_{Lowpass}(z) = \frac{Y(z)}{X(z)} &= \frac{\frac{2}{T}^2 \alpha^2}{\frac{2}{T}^2 \frac{1-z^{-1}}{1+z^{-1}}^2 + \frac{2}{T}^2 \sqrt{2}\alpha \frac{1-z^{-1}}{1+z^{-1}} + \frac{2}{T}^2 \alpha^2} \\
&= 1.347e{-3} \ \frac{1 - 2z^{-1} + z^{-2}}{1 - 1.894z^{-1} + 0.899z^{-2}}
\end{aligned}
\tag{34}
$$

This results in the IIR equation;
$y(n) = 1.347e{-3} \ \cdot x(n) + 2.695e{-3} \ \cdot x(n-1) + 1.347e{-3} \ \cdot x(n-2) + 1.894 \cdot y(n-1) - 0.899 \cdot y(n-2)$

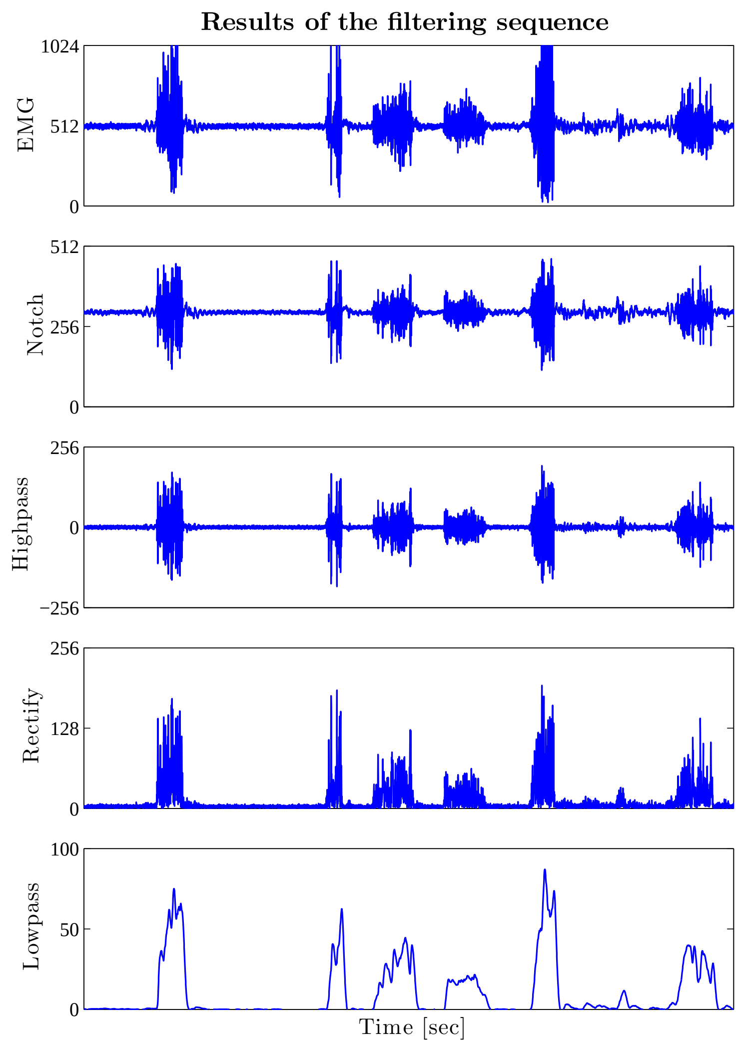

Figure 46: A typical result of EMG filtering. The peaks in the EMG graph are caused by muscle contractions.

C.5.4 Admittance model

The admittance model is there to smoothen the signal coming from the force sensor. It consists of a virtual mass and a virtual damper. Depending on the desired control signal, e.g. a velocity signal or a position signal, it has one or two integration actions. Values for the virtual mass and damper are chosen arbitrary to get a smooth signal. The virtual mass has chosen to be $2kg$, the virtual damping to be $10Ns/m$. To control the stepper motor a desired prosition is needed. Therefore an admittance model with two integration actions is needed. The transfer function of the admittance model in the Laplace domain is;

$$H_{adm}(s) = \frac{X(s)}{F(s)} = \frac{1}{ms^2 + bs} \tag{35}$$

To use this in the digital controller, the admittance model needs to be discretized in the same way as is done with the EMG input. Velocity is the desired output of the admittance model.

$$\begin{aligned} H_{adm}(s) &= \frac{\dot{X}(s)}{F(s)} = \frac{s}{ms^2 + bs} = \frac{1}{ms + b} \\ H_{adm}(z) &= \frac{\dot{X}(z)}{F(z)} = \frac{1}{m\frac{2}{T}\frac{1-z^{-1}}{1+z^{-1}} + b} \\ &= \frac{1}{2m + Tb}\frac{T(1 + z^{-}1)}{1 + \frac{Tb-2m}{2m+Tb}z^{-}1} \end{aligned} \tag{36}$$

In the IIR form this is:

$$v(n) = \frac{T}{2m + Tb}F(n) + \frac{T}{2m + Tb}F(n-1) + \frac{2m - Tb}{2m + Tb}v(n-1) \tag{37}$$

Where;
$F(m)$ is the estimated force at timestep m
$v(m)$ is the output at timestep m
T is the sample time
m is the virtual mass
b is the virtual damping

C.5.5 Additional control actions

Limiting the maximum velocity
In the admittance controller the velocity can be limited. This can be done by dividing the X- and Y-velocity with the norm of the resulting velocity vector above certain speeds.

Also there is a possiblity to set a maximum velocity of the motor in the controller. This is just a limit without taking a norm or similar. It can be seen as a second safety feature for limiting the velocity. Limiting the velocity by dividing wih the norm of the velocity vector is the first velocity safety.

Limiting the maximum motor torque
The pulse width modulation(PWM) signal, i.e. the output signal from the controller to the stepper motors, controls the power of the signal and therefore the voltage and the current.

Also by hardware the current can be lowered. This can be done by changing the resistance by the potentiometer on the stepper driver board. The lowered current obviously results in a lowered output torque by stepper motor.

Limiting the position
The position of the cart will be limited by software near the ends of the spindles. To be sure that the sofware endstop is not acting like a stiff environment which could case instability issues more damping will be added when the cart is near a software boundary. The mechanical endstops are an extra safety feature to completely stop movement. This only come into action when the software endstop failes to work.

D Validation

D.1 EMG Filtering

EMG signals are filtered at 50Hz with a Notch filter to remove the noise introduced by the mains. After that it is filtered at 20Hz with a digital 2^{nd} order high pass Butterworth filter and rectified. Last the signal is filtered with a 2^{nd} order low pass Butterworth filter at 3Hz (Fig. 47).

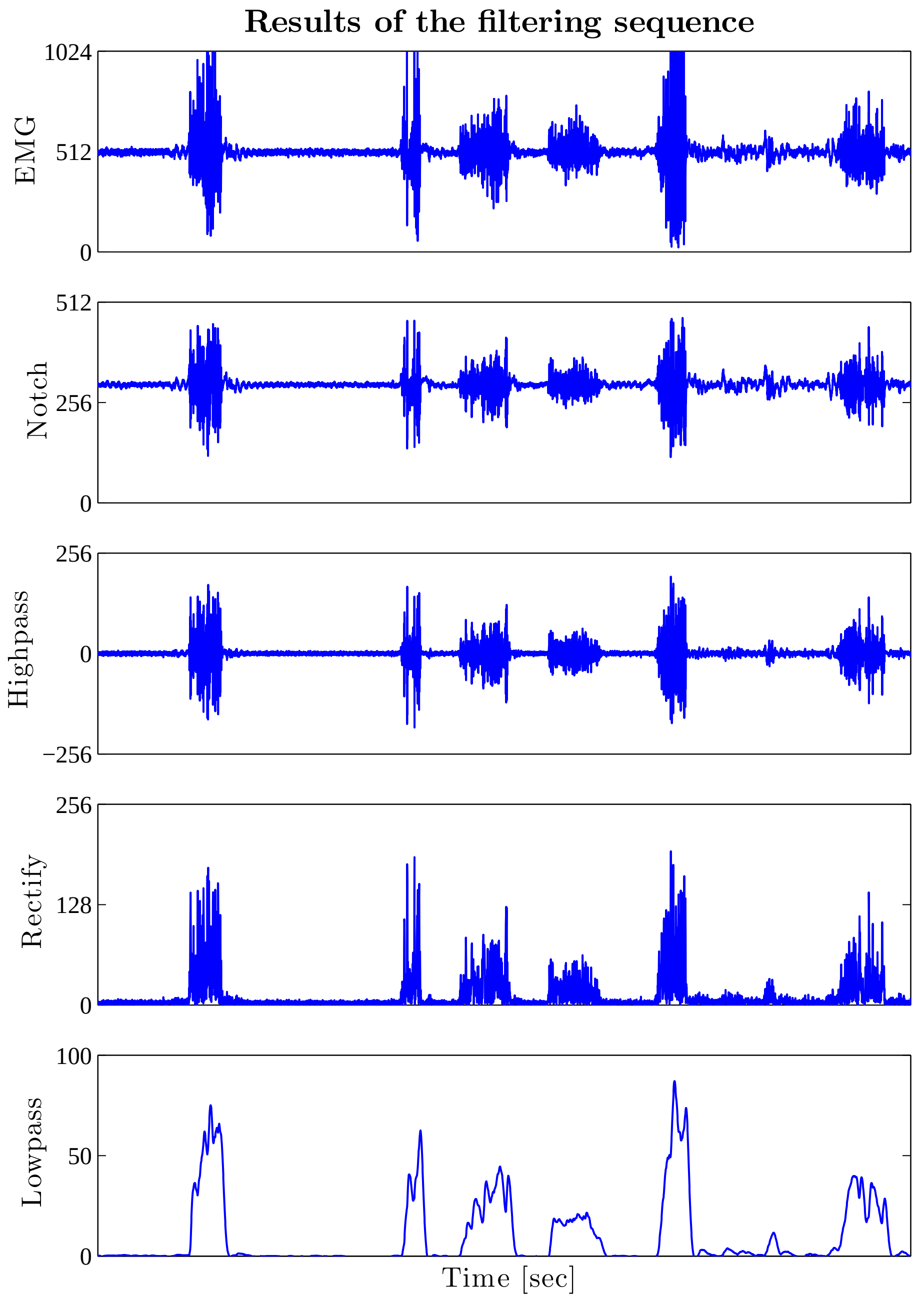

Figure 47: The filtered EMG signal from the raw input to the smoothed control signal.

The design is validated by measuring how much EMG signal is needed to move the arm of the user (Fig. 48). This validation was done with a healthy subject, and setting the proportional gain very high to simulate the volutairy force of a person with DMD. The normalized EMG signals of the subject wes measured. Targets were set at positions 250mm and 400mm. Normalized EMG signals below 0.3 are easy to perform. It can be seen that the normalized EMG signals stay below 0.1 most of the time. A maximum speed was set at 15mm/s.

D.2 Haptic performance parameters

To validate the working of the designed assistive device the performance needs to be determined. This can be done by measuring the relevant performance parameters stated by Hayward and Astley [62]. To measure the haptic performance of the designed device to following indicators are measured: Workspace, play at the arm cuff, stiffness, maximal force, maximum velocity, maximum acceleration and deceleration, frequency response, and static friction of the arm cart. Next to these performance measures also the software set workspace boundaries, velocity limits, and changing damping near the boundaries are checked.

D.2.1 Workspace

The workspace is the 2dimensional space the centre of the cart can reach. It will be measured in a way that it is independant of orientation. The maximum workspace of the device is 409mm x 260mm (Fig. 49). The workspace can be limited in software.

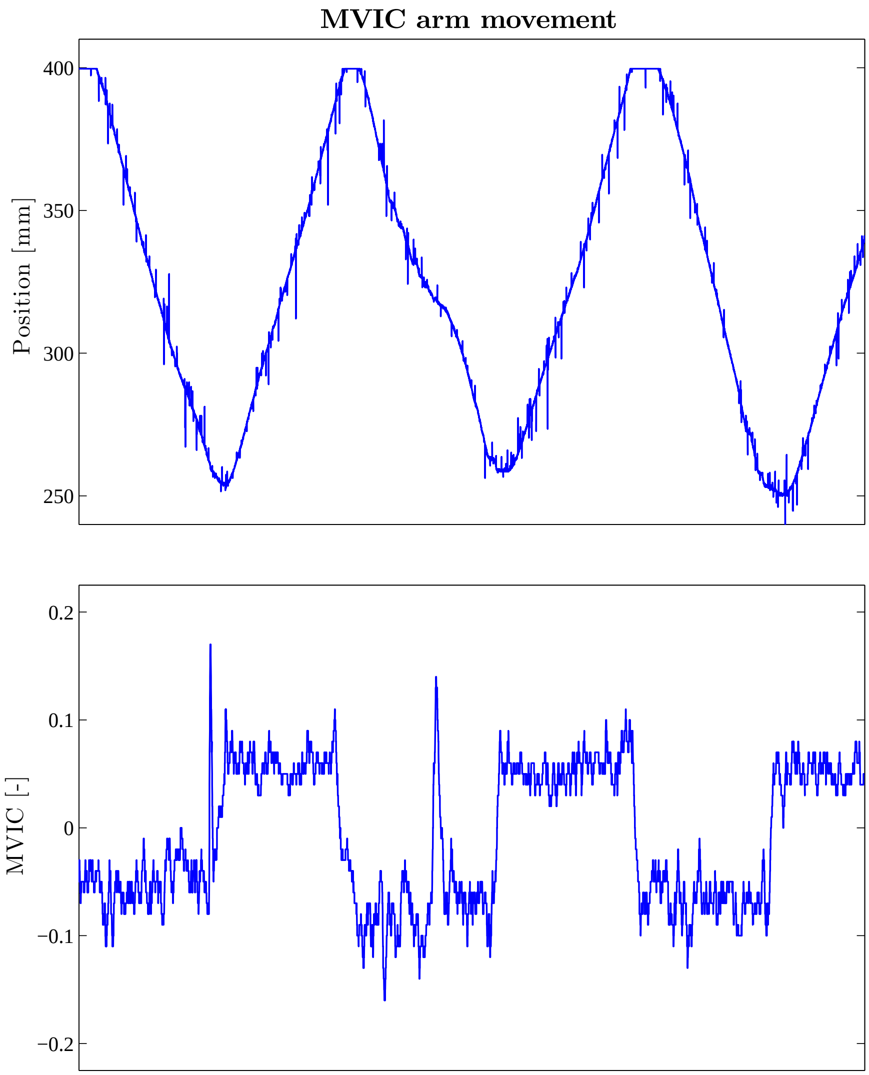

Figure 48: The result of the validation. Plotted are the position of the end effector (top) and the normalized EMG signal, MVIC (bottom). Targets were at 250mm and 400mm.

D.2.2 Stiffness

The stiffness will be measured at the cart side of the device and at 5 different positions on the table in different direction (see Fig. 50).

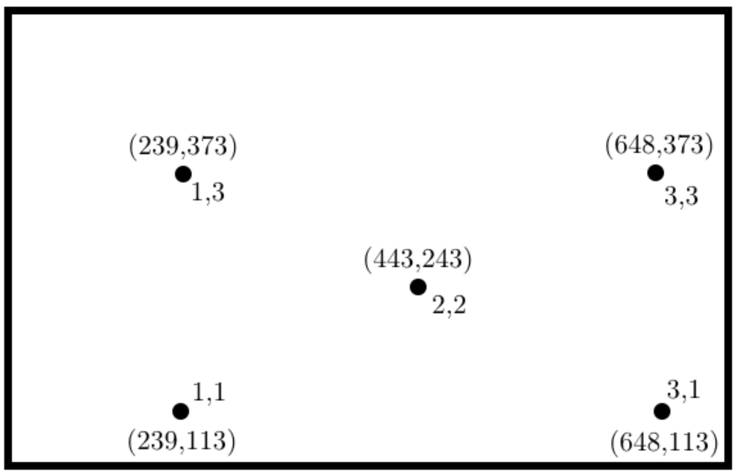

Figure 50: Positions of the measurement named '1,1','1,3','2,2','3,1','3,3' with the representing position in mm, i.e. (x[mm],y[mm]). Left bottom is the origin (0,0) and the top right (800,610).

It will be measured in the x-direction (i.e. from left to right) and the y-direction (i.e. forward and backward). This is done to be sure because the manipulator underneath the table surface has different stiffnesses at different position due to the asymmetric suspension of the Y-table. In case the stiffness of the magnetic interface is lowest, stiffness will be approximately the same of the entire table surface.

Results of the stiffness measurement are given in Table4 & 5 and Fig.51.

Table 4: The measured stiffnesses of the XY-table prototype

Position	Direction	Distance [mm]	Force [N]	Stiffness [N/mm]
1.1	X	0.6	0	-
		6.7	4.9	0.73
		11.1	7.5	0.58
		14	8.2	0.27
	Y	0.6	0	-
		3.7	4.9	1.33
		8.1	6.9	0.45
		9.9	7.3	0.22
		12.6	7.7	0.15
1.3	X	0.6	0	-
		5.7	4.9	0.86
		8.0	5.9	0.43
		10.5	6.9	0.39
		14.3	7.1	0.05
	Y	0.6	0	-
		5.4	4.9	0.91
		7.5	5.9	0.47
		11.2	6.9	0.27
2.2	X	0.6	0	-
		4.2	3.9	0.93
		5.9	4.9	0.58
		7.6	5.9	0.58
		9.9	6.9	0.43
		12.8	7.2	0.17
	Y	0.6	0	-
		4.1	3.9	0.96
		5.8	4.9	0.58
		7.4	5.9	0.61
		10.1	6.9	0.36
		12.3	7.4	0.13
3.1	X	0.6	0	-
		5.2	4.9	0.94
		8.8	6.9	0.55
		12.6	7.3	0.10
	Y	0.6	0	-
		5.0	4.9	0.98
		9.1	6.9	0.48
		12.0	7.3	0.14
3.3	X	0.6	0	-
		5.7	3.9	0.69
		7.7	4.9	0.49
		9.9	5.9	0.45
		14.8	6.3	0.08
	Y	0.6	0	-
		5.4	3.9	0.70
		7.5	4.9	0.49
		7.5	5.9	0.49
		11.2	6.3	0.15

Table 5: The control measurements of the stiffnesses of the XY-table prototype. This is done in a random direction in the planar surface

Position	Distance [mm]	Force [N]	Stiffness [N/mm]
Control w\ load (near 2.2)	0.6	0	-
	1.5	1.0	0.67
	2.2	2.0	1.40
	3.2	2.9	1.46
	4.0	3.9	1.23
	5.1	4.9	0.93
	6.6	5.9	0.65
	9.2	6.9	0.37
	13.7	7.7	0.17
Control with load (near 2.2)	0.3	0	-
	1.4	2.0	1.40
	2.4	3.9	1.96
	3.3	4.9	1.15
	7.0	6.9	0.55
	7.9	7.4	0.46
	9.4	7.8	0.33
	12.3	8.3	0.17

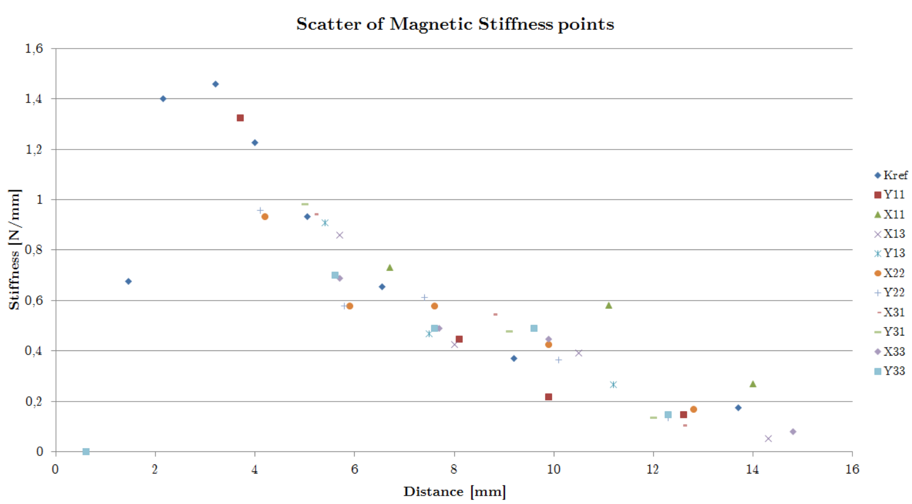

Figure 51: Scatter plot of all the stiffness at the different positions in the X and Y direction. Measured without a load in the cart

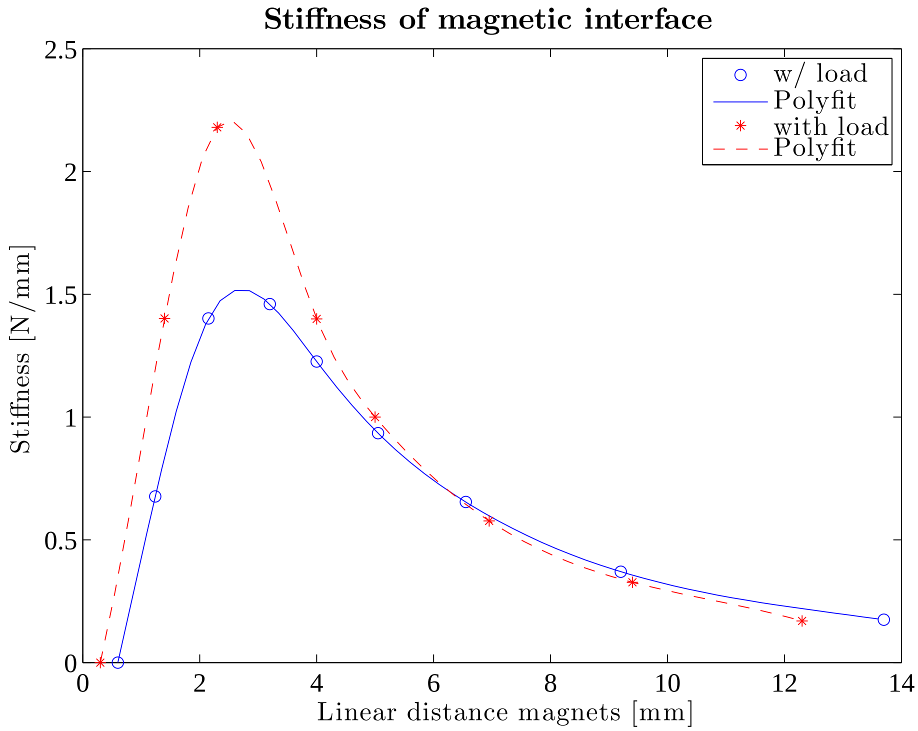

Figure 52: Lines of the stiffness with and without a load in the cart

D.2.3 Maximum force

Maximum force is an important measure for this device because this will determine if the supported arm will move and this will also determine what the maximum acceleration and velocity are. The maximum force Should be measured at the cart side with a long term and a short term test. This will be done because in the short term test heat losses will not have affected the maximum force that can be delivered. At the long term test a thermal equilibrium will be reached and a lower peak force is expected because the higher thermal losses.

Because of the issues with the stepper motor driver, which gets hot after 20sec - 30sec, only a short term test is done. This is done by hooking a spring balance to the cart and a fixed point. Then the end effector will move at a slow speed (i.e. ¿1cm/s) up to the point where the arm cart gets disconnected. At this point the maximum force is reached. The maximum force is measured multiple with and without a weight of 2kg in the arm cart. The maximum force of the unloaded cart was measured to be 7.4 ± 1N, and with a load at 7.8 ± 0.8N (Table 6).

Table 6: Maximum force measured at the arm cart

No.	Force[N] w\ load	Force[N] with load
1	8.2	8.0
2	7.7	7.8
3	7.1	7.0
4	6.9	7.6
5	7.2	8.3
6	7.4	7.4
7	7.3	7.9
8	7.3	8.6
9	6.3	7.9
10	6.3	8.3
11	7.7	7.7
Avg.	7.2	7.8

Next to the maximum force the static friction of the arm cart with the table surface also has been determined. The static friction without a load in the cart is determened to be approximately 0.1N. The static friction with a load of 2kg in the cart is determened to be approximately 0.8N

D.2.4 Maximum acceleration

If the inertia and the maximum force are known a maximum acceleration could theoretically be determined. Maximum acceleration is important to make sure that the reference set by the user is reached quickly and does feel natural. Maximum acceleration can be measured with accelerometers. Only the position sensors were available for measurements. This data was collected through the microcontroller and processed afterwards. The position during acceleration of the cart was fitted and a second order derivative was taken from that to determine the acceleration. The maximum measured acceleration in the X-direction was $72.2mm/s^2$ (Fig. 53). The maximum measured acceleration in the Y-direction was $76.4mm/s^2$ (Fig. 54). These accelerations were taken without a load in the arm cart. With a load of 2kg in the arm cart only the measurement in the Y-direction gave a reliable result, which was an acceleration of $50mm/s^2$ (Fig. 55).

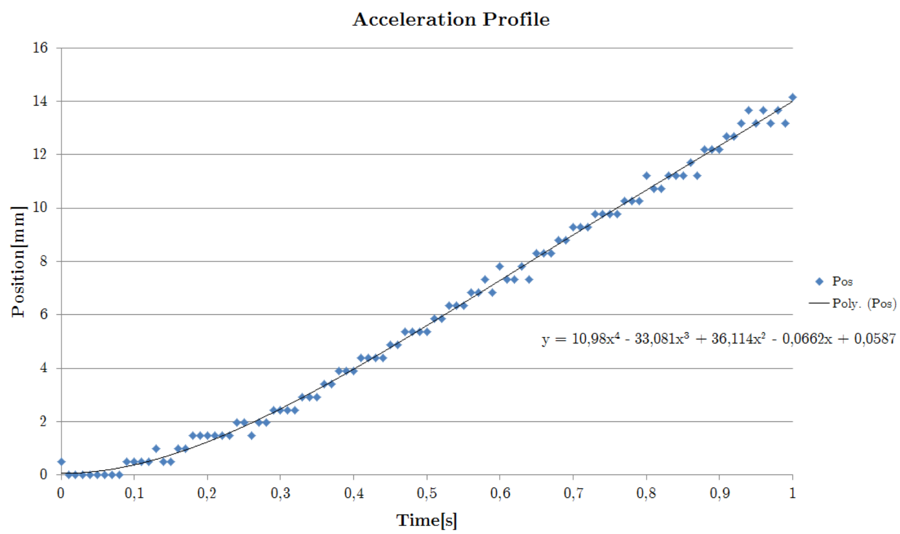

Figure 53: Maximum acceleration data of the X-direction. The polynomial fit line is for the position. This fit line needs to be integrated twice to get the acceleration. Measurement without load in the cart.

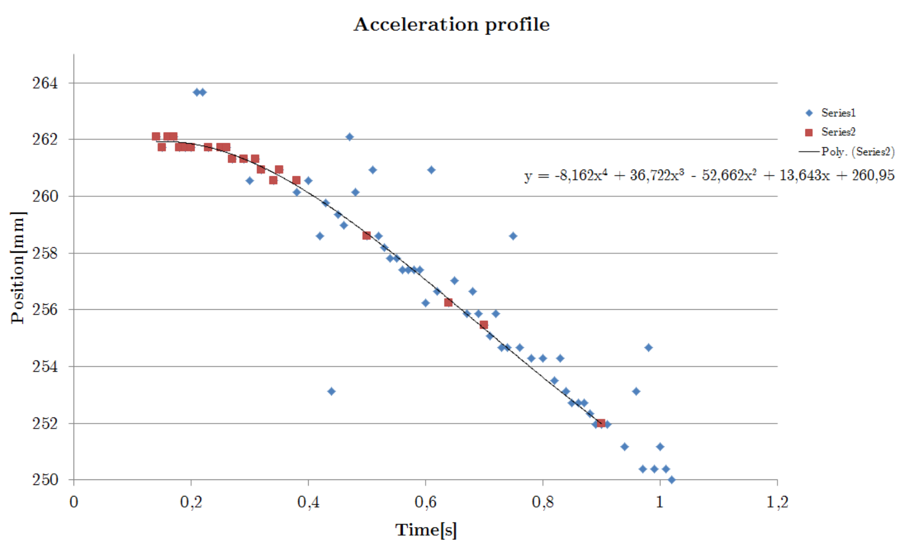

Figure 54: Maximum acceleration data of the Y-direction. The polynomial fit line is for the position. This fit line needs to be integrated twice to get the acceleration. Measurement without load in the cart.

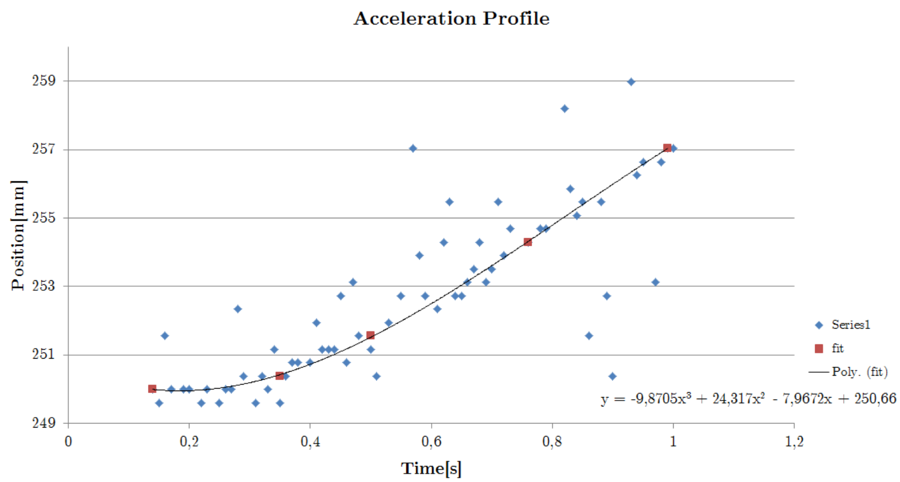

Figure 55: Maximum acceleration data of the Y-direction. The polynomial fit line is for the position. This fit line needs to be integrated twice to get the acceleration. Measurement with a load of 2kg in the cart.

D.2.5 Maximum deceleration

As with acceleration, the maximum deceleration is also important. An example where deceleration is important are the software set boundaries, that are simulated to be stiff walls. The maximum deceleration is measured in the same way as with the maximum acceleration. Three situations were measured, namely stopping by setting the force to 0, stopping by using the “stepper.stop()” command of the Accelstepper library, and deceleration by reversing the force. The last of the situation gave the quickest deceleration during normal useage. This deceleration was equal to $90mm/s^2$ in the X-direction (Fig. 56) and $93.5mm/s^2$ in the Y-direction (Fig. 57). These decelerations were measured without a load in the arm cart. With a load of 2kg in the arm cart only the measurement in the Y-direction gave a reliable result, which was an acceleration of $83.4mm/s^2$ (Fig. 58).

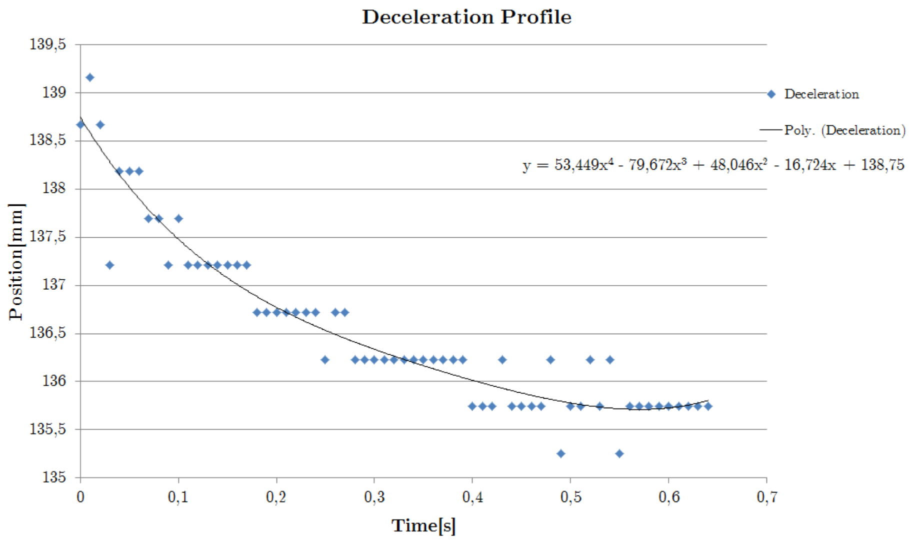

Figure 56: Maximum deceleration data of the X-direction. The polynomial fit line is for the position. This fit line needs to be integrated twice to get the deceleration. Measurement without load in the cart.

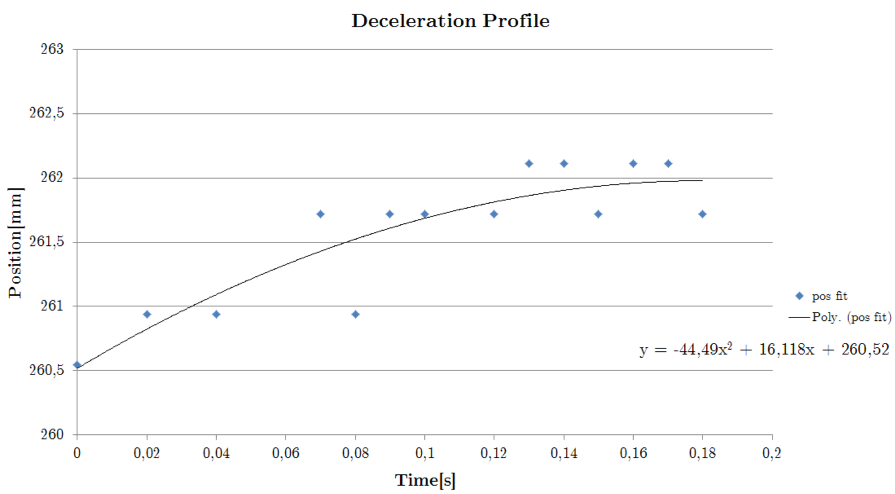

Figure 57: Maximum deceleration data of the Y-direction. The polynomial fit line is for the position. This fit line needs to be integrated twice to get the deceleration. Measurement without load in the cart.

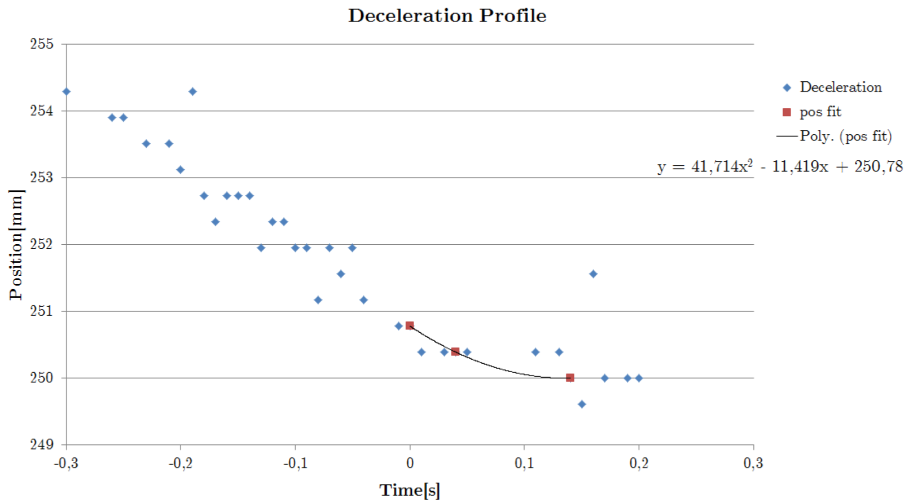

Figure 58: Maximum deceleration data of the Y-direction. The polynomial fit line is for the position. This fit line needs to be integrated twice to get the deceleration. Measurement with a load of 2kg in the cart.

D.2.6 Maximum velocity

Maximum velocity is tested in both the X- and Y-direction. This is done by setting the gain of the speed to the point where the motors cannot follow the steps properly and start to have jerky motion. The position data aqcuired through the position sensors is line fitted. From this line the derivative is taken to determine the velocity. The stepper motors were operated in half step mode because operation in full step mode (which is potentially twice as fast) did not work well. In full step mode jerky motion of the stepper motor was present at lower speeds than at operation in half step mode. The maximum measured velocity in the X-direction is $17mm/s$. This was without a load in the arm cart. With a load of 2kg in the arm cart results were incosistant. The maximum measured velocity in the Y-direction without a load in the arm cart was equal to $28.8mm/s$. With a load of 2kg in the arm cart consistant results were at half of that velocity, i.e. $14.4mm/s$.

D.2.7 Frequncy Response Function

The frequency response functions (FRF) will be determined in both the directions of the manipulator. The frequency response function will be the open loop function from the estimated force input to the output velocity/position.

$$H_i(\omega) = \left\| \frac{U_{EMG,i}(\omega)}{v_i(\omega)} \right\| \tag{38}$$

Where i represents the direction of the movement, $U_{EMG,i}(\omega)$ is the estimated force input comming from the EMG signals from the muscle pair, $v_i(\omega)$ is the measured velocity, and ω is the frequency of the input.

The force input will be set in software as an oscillation starting at 0.1Hz and ending at 10Hz. The amplitude of the oscillating force is chosen to be constant over the entire frequency range and has a value of 5. The output velocity is measured by differentiation of the measured position that are measured with the position sensors. This is done for both the X- and Y-direction without a load in the arm cart. With a load in the arm cart results were very inconsistent. Bandwith of the velocity controller is around 3Hz for both directions (Fig. 59).

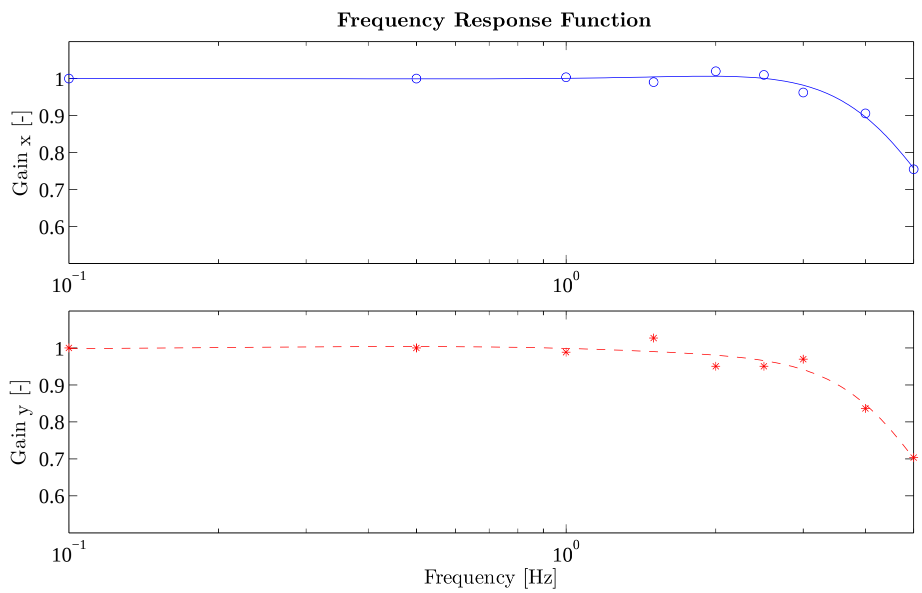

Figure 59: The frequency responses of the manipulator in the X- and Y-direction

E Technical Drawings

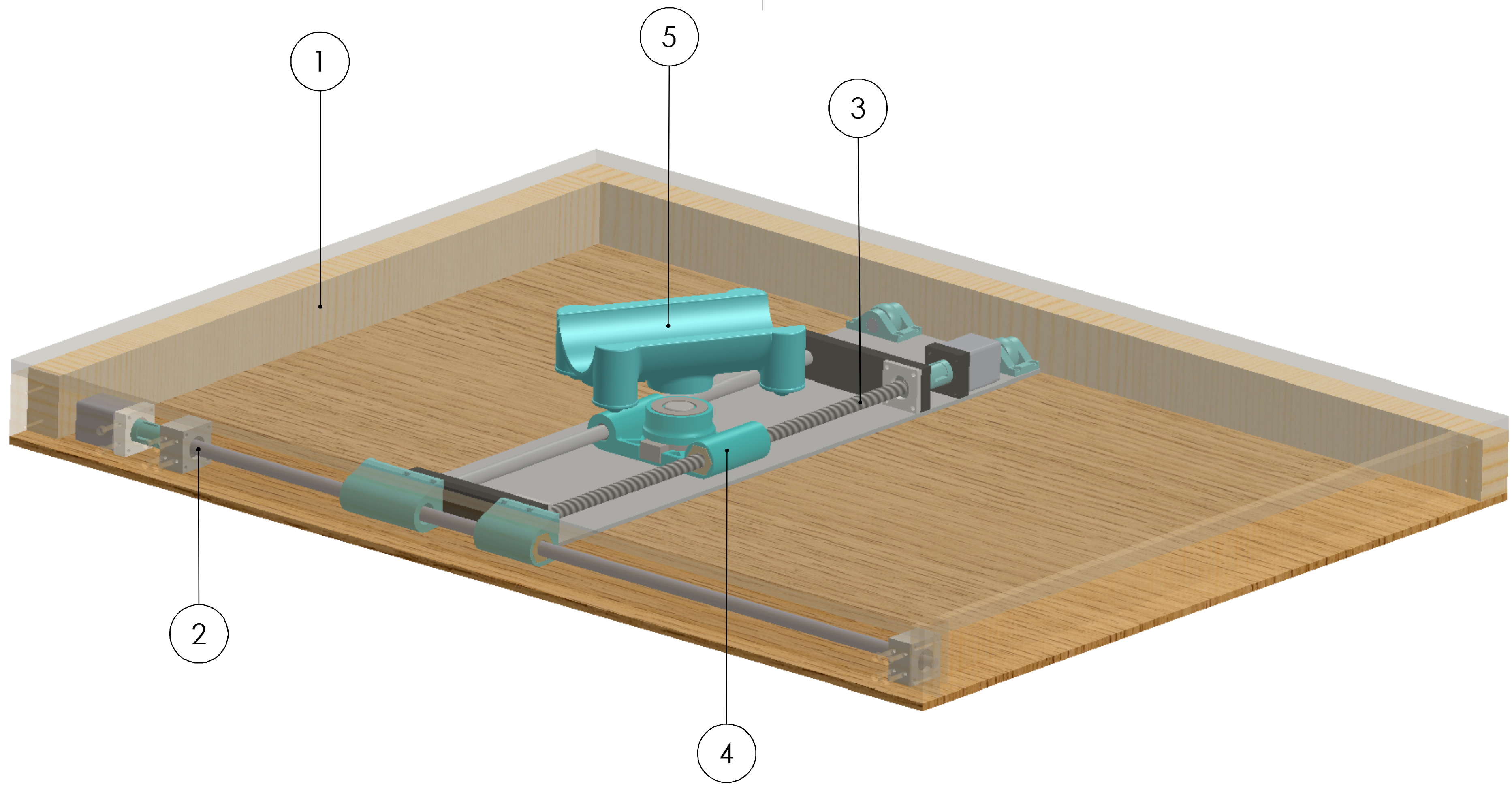

UNLESS OTHERWISE SPECIFIED: DIMENSIONS ARE IN MILLIMETERS SURFACE FINISH: TOLERANCES: LINEAR: ANGULAR:	FINISH:	DEBUR AND BREAK SHARP EDGES	DO NOT SCALE DRAWING	REVISION	
	NAME	SIGNATURE	DATE	TITLE:	
DRAWN					
CHK'D					
APPV'D					
MFG					
Q.A			MATERIAL:	DWG NO. XY_Table	A4
			WEIGHT:	SCALE:1:4	SHEET 1 OF 1

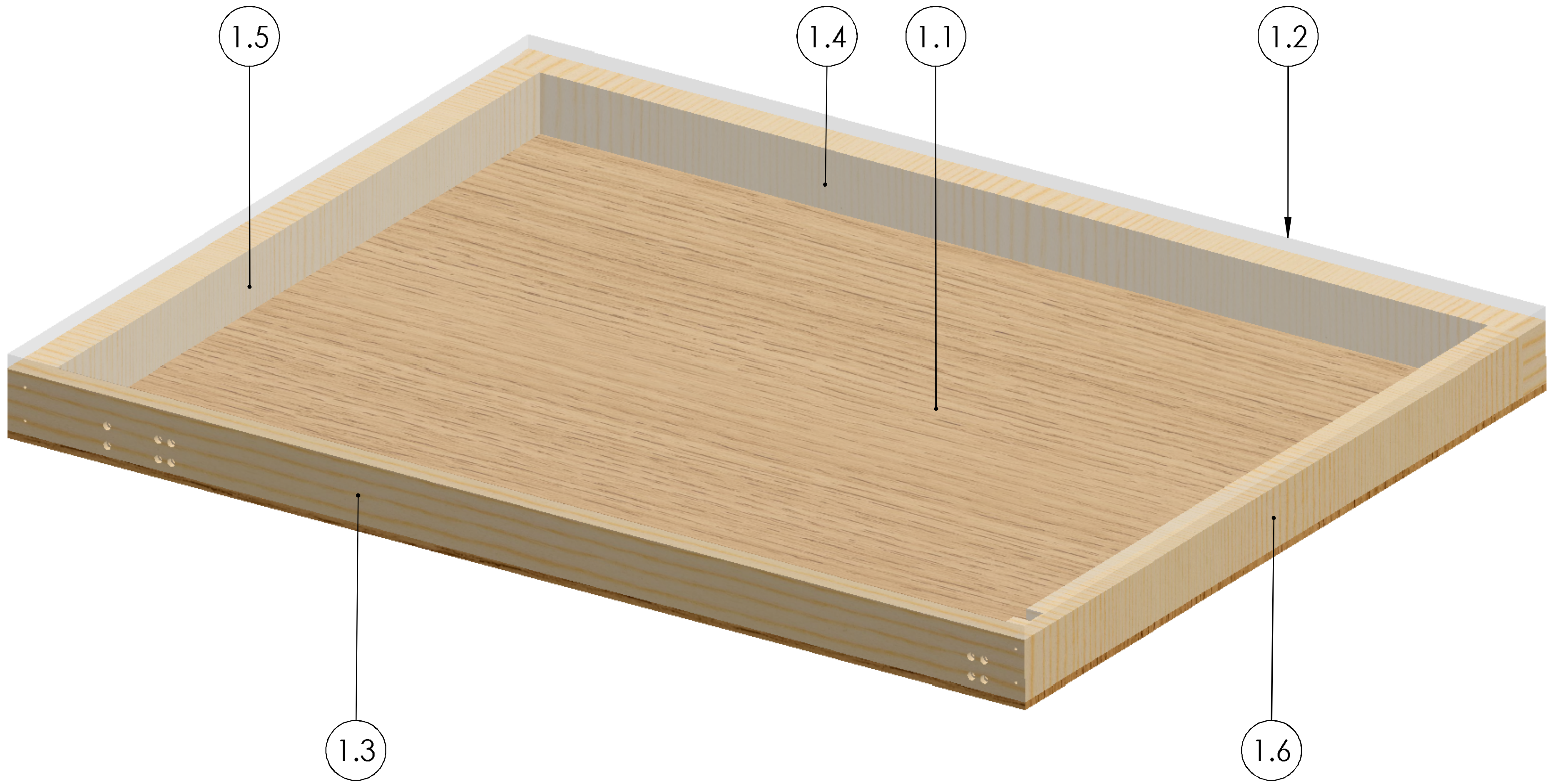

UNLESS OTHERWISE SPECIFIED: DIMENSIONS ARE IN MILLIMETERS SURFACE FINISH: TOLERANCES: LINEAR: ANGULAR:	FINISH:	DEBUR AND BREAK SHARP EDGES	DO NOT SCALE DRAWING	REVISION	
	NAME	SIGNATURE	DATE	TITLE:	
DRAWN					
CHK'D					
APPV'D					
MFG					
Q.A			MATERIAL:	DWG NO. 1_Table	A4
			WEIGHT:	SCALE:1:4	SHEET 1 OF 1

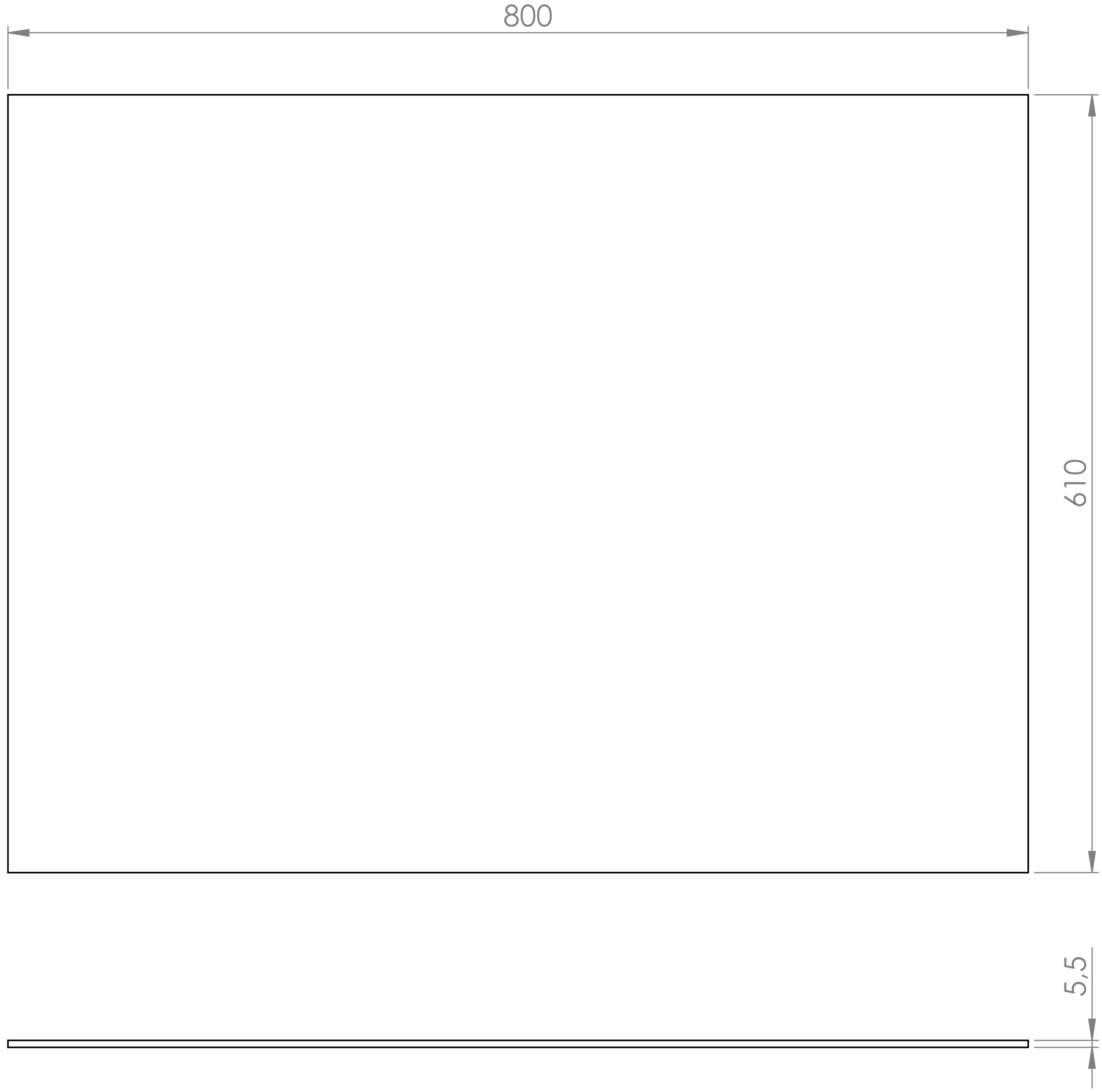

UNLESS OTHERWISE SPECIFIED:
DIMENSIONS ARE IN MILLIMETERS
SURFACE FINISH:
TOLERANCES:
LINEAR:
ANGULAR:

FINISH:

DEBUR AND BREAK SHARP EDGES

DO NOT SCALE DRAWING

REVISION

	NAME	SIGNATURE	DATE		
DRAWN					
CHK'D					
APPV'D					
MFG					
Q.A					

TITLE:

MATERIAL:
Oak

DWG NO.
1.1_Table_Bottom

A4

WEIGHT:

SCALE:1:5

SHEET 1 OF 1

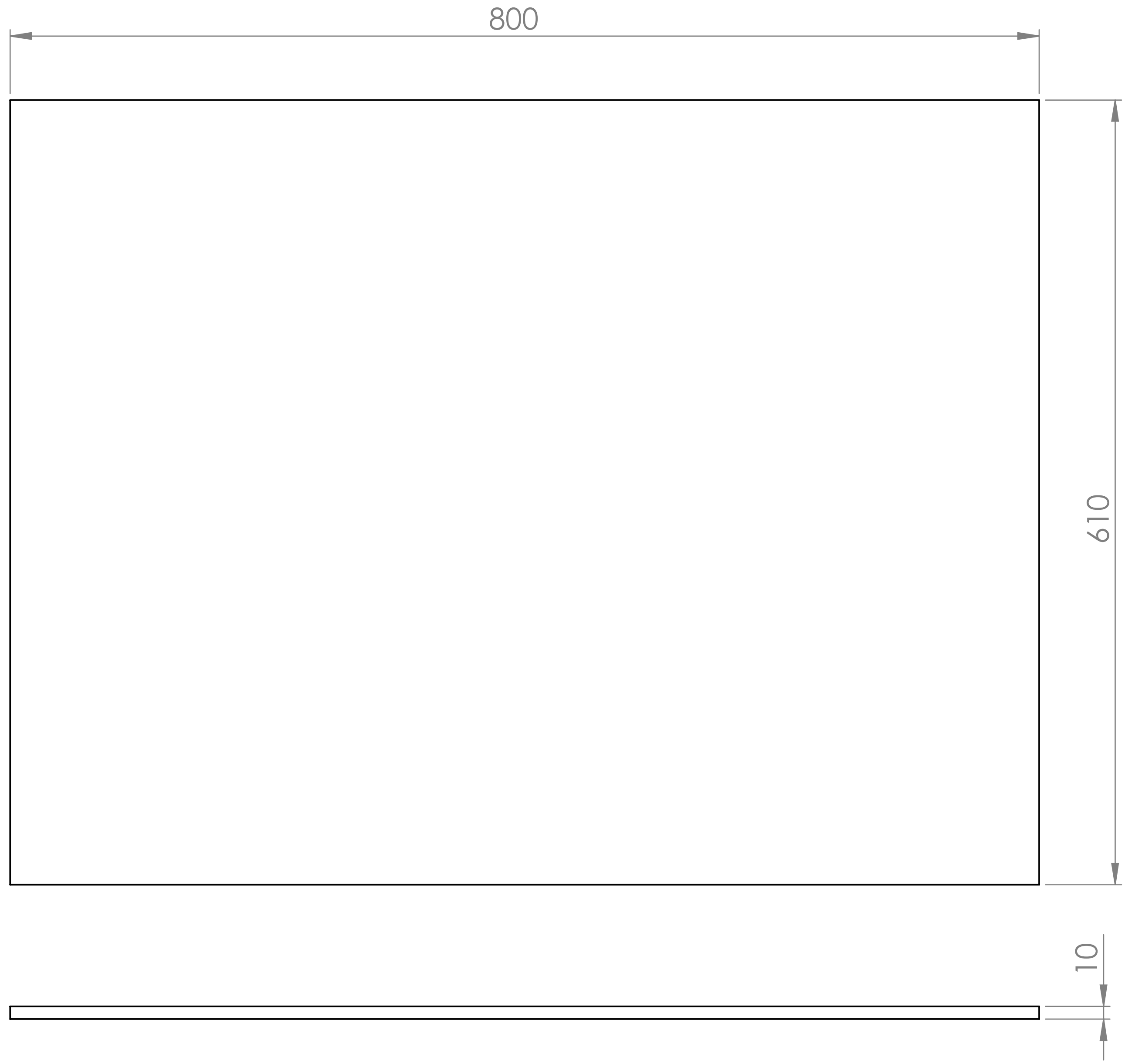

UNLESS OTHERWISE SPECIFIED:
DIMENSIONS ARE IN MILLIMETERS
SURFACE FINISH:
TOLERANCES:
LINEAR:
ANGULAR:

FINISH:

DEBUR AND BREAK SHARP EDGES

DO NOT SCALE DRAWING

REVISION

	NAME	SIGNATURE	DATE
DRAWN			
CHK'D			
APPV'D			
MFG			
Q.A			

TITLE:

MATERIAL:
HPL / Trespa

DWG NO.
1.2_Table_Top

A4

WEIGHT:

SCALE:1:5

SHEET 1 OF 1

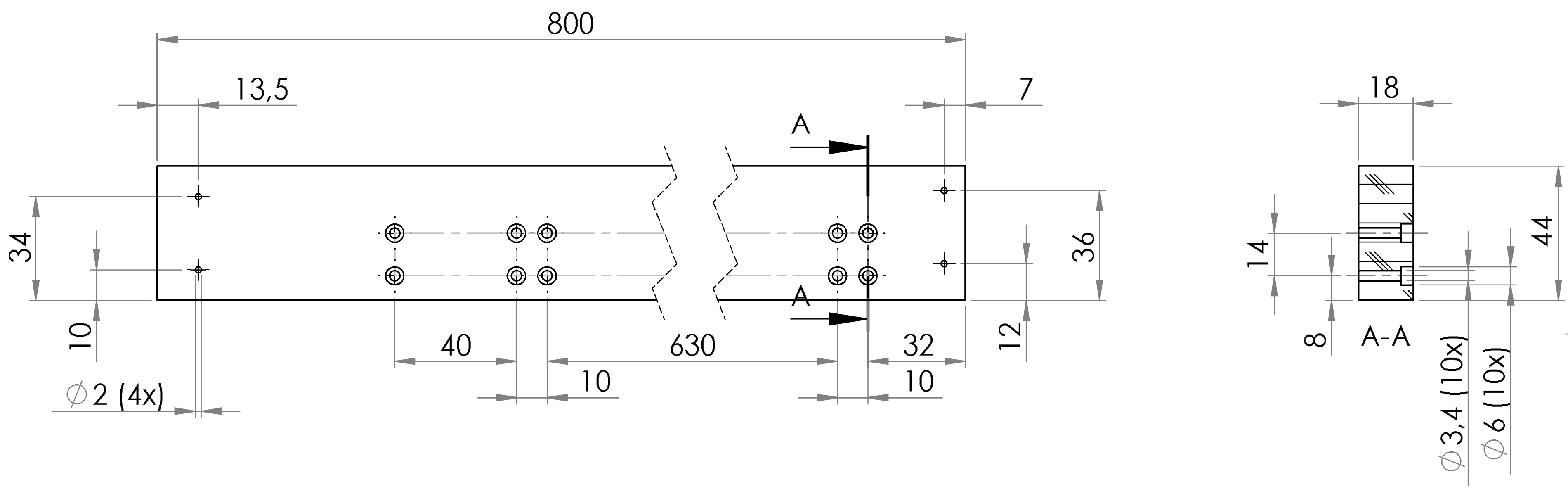

UNLESS OTHERWISE SPECIFIED: DIMENSIONS ARE IN MILLIMETERS SURFACE FINISH: TOLERANCES: LINEAR: ANGULAR:	FINISH:		DEBUR AND BREAK SHARP EDGES	DO NOT SCALE DRAWING	REVISION	
	NAME	SIGNATURE	DATE	TITLE:		
DRAWN						
CHK'D						
APPV'D						
MFG						
Q.A			MATERIAL: Spruce	DWG NO. 1.3_Table_Front		A4
			WEIGHT:	SCALE:1:2	SHEET 1 OF 1	

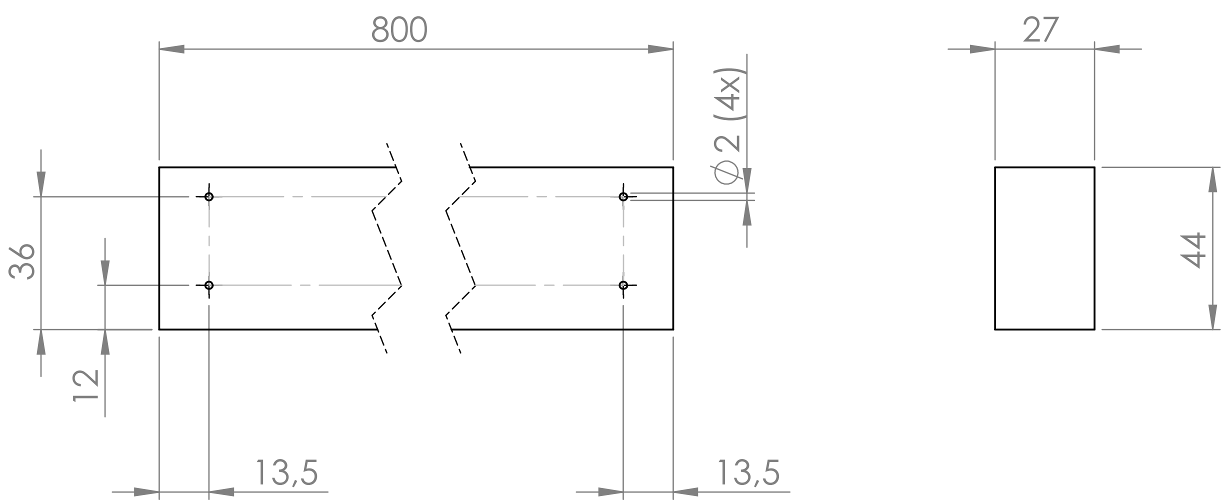

UNLESS OTHERWISE SPECIFIED: DIMENSIONS ARE IN MILLIMETERS SURFACE FINISH: TOLERANCES: LINEAR: ANGULAR:	FINISH:	DEBUR AND BREAK SHARP EDGES	DO NOT SCALE DRAWING	REVISION	
	NAME	SIGNATURE	DATE		TITLE:
DRAWN					
CHK'D					
APPV'D					
MFG					
Q.A				MATERIAL: Spruce	DWG NO. 1.4_Table_Back A4
				WEIGHT:	SCALE:1:2 SHEET 1 OF 1

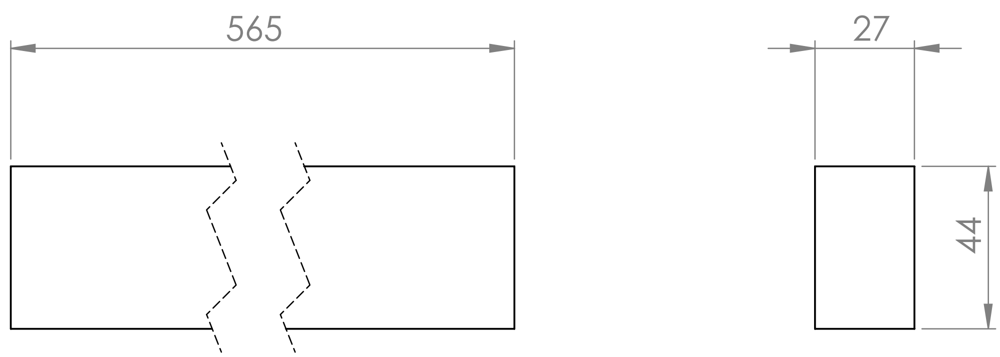

UNLESS OTHERWISE SPECIFIED: DIMENSIONS ARE IN MILLIMETERS SURFACE FINISH: TOLERANCES: LINEAR: ANGULAR:	FINISH:			DEBUR AND BREAK SHARP EDGES	DO NOT SCALE DRAWING	REVISION
	NAME	SIGNATURE	DATE		TITLE:	
DRAWN						
CHK'D						
APPV'D						
MFG						
Q.A				MATERIAL: Spuce	DWG NO. 1.5_Table_Left	A4
				WEIGHT:	SCALE:1:2	SHEET 1 OF 1

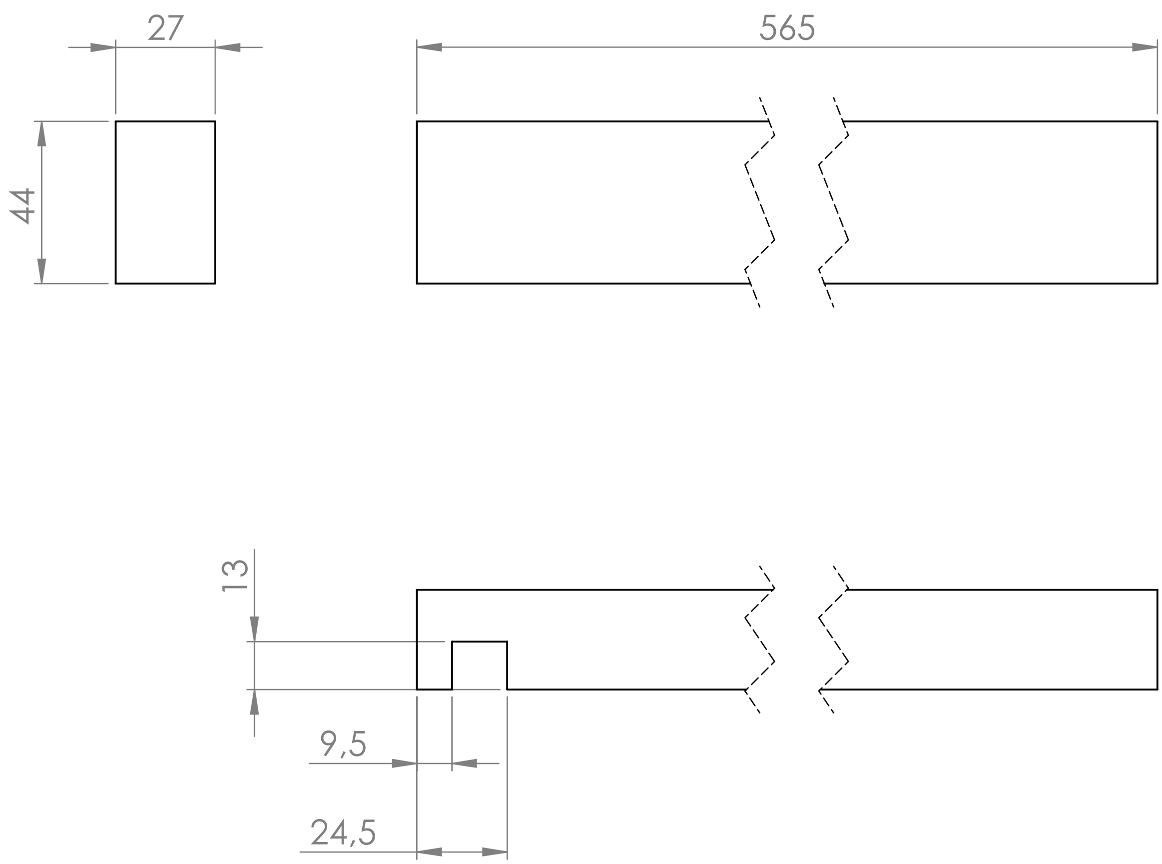

UNLESS OTHERWISE SPECIFIED:
DIMENSIONS ARE IN MILLIMETERS
SURFACE FINISH:
TOLERANCES:
LINEAR:
ANGULAR:

FINISH:

DEBUR AND BREAK SHARP EDGES

DO NOT SCALE DRAWING

REVISION

	NAME	SIGNATURE	DATE
DRAWN			
CHK'D			
APPV'D			
MFG			
Q.A			

TITLE:

MATERIAL:
Spruce

DWG NO. 1.6_Table_Right

A4

WEIGHT:

SCALE:1:2

SHEET 1 OF 1

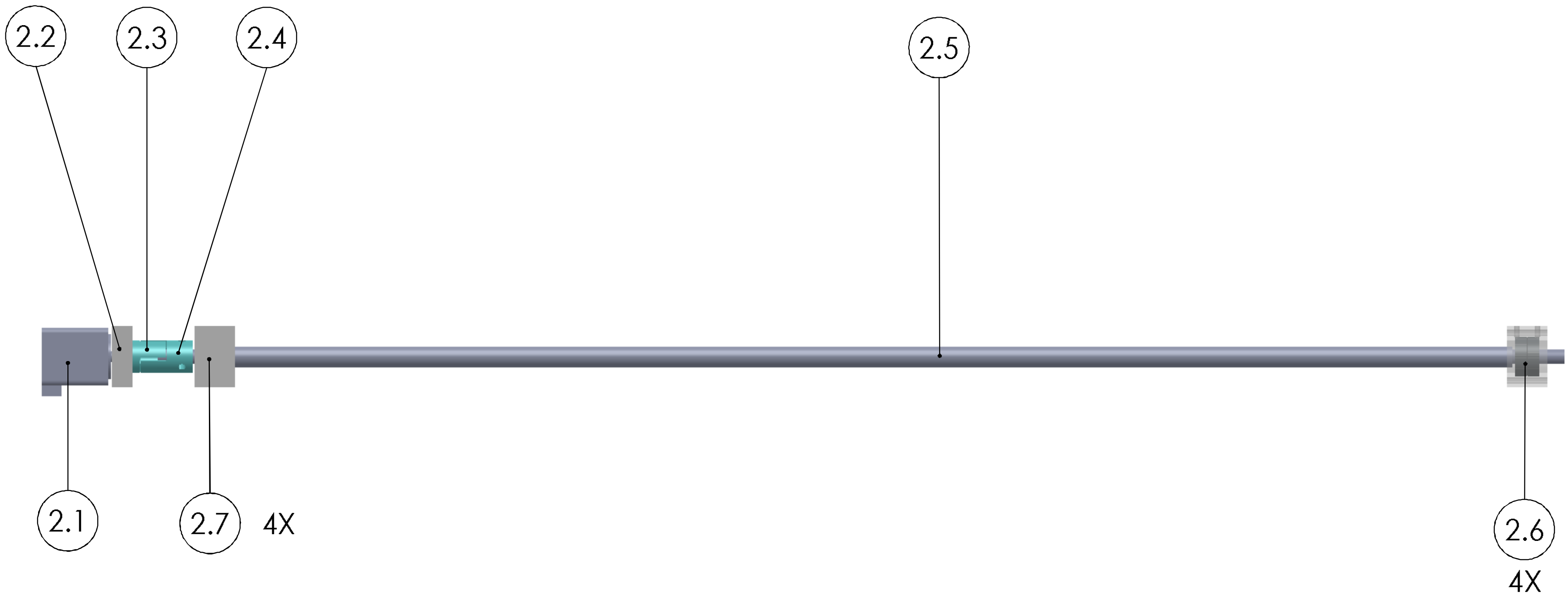

UNLESS OTHERWISE SPECIFIED: DIMENSIONS ARE IN MILLIMETERS SURFACE FINISH: TOLERANCES: LINEAR: ANGULAR:	FINISH:	DEBUR AND BREAK SHARP EDGES	DO NOT SCALE DRAWING	REVISION

	NAME	SIGNATURE	DATE
DRAWN			
CHK'D			
APPV'D			
MFG			
Q.A			

TITLE:

MATERIAL:

DWG NO. 2_X_manipulator

A4

WEIGHT:

SCALE:1:3

SHEET 1 OF 1

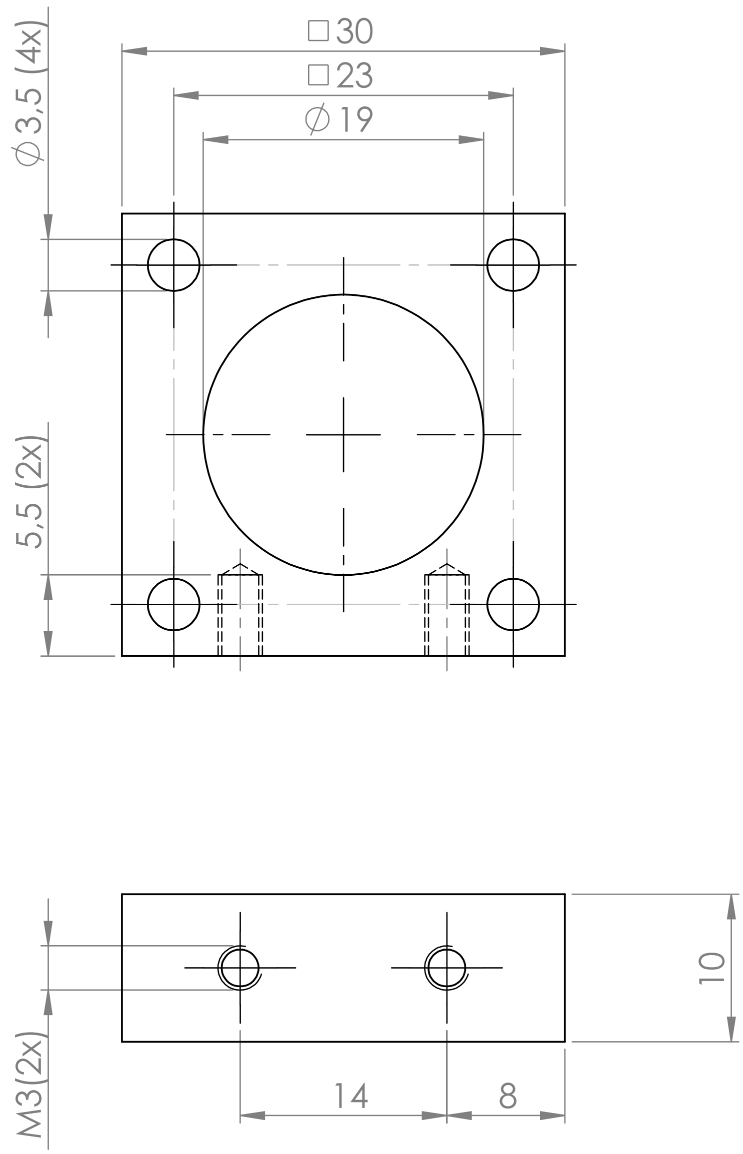

UNLESS OTHERWISE SPECIFIED: DIMENSIONS ARE IN MILLIMETERS SURFACE FINISH: TOLERANCES: LINEAR: ANGULAR:	FINISH:	DEBUR AND BREAK SHARP EDGES	DO NOT SCALE DRAWING	REVISION

	NAME	SIGNATURE	DATE			TITLE:
DRAWN						
CHK'D						
APPV'D						
MFG						
Q.A				MATERIAL: PVC		DWG NO. 2.2_Motor_Mount A4
				WEIGHT:		SCALE:2:1 SHEET 1 OF 1

3D printed part

Part interlocks with
2.4_Motor_coupling_d7

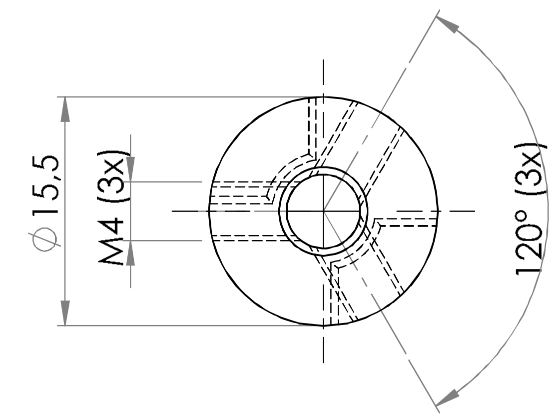

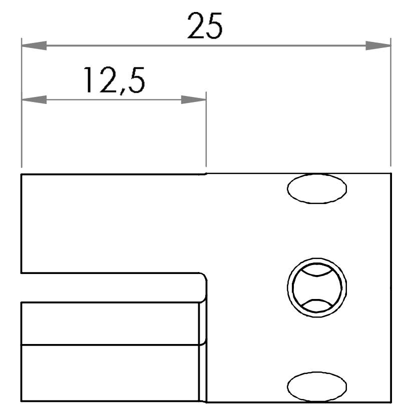

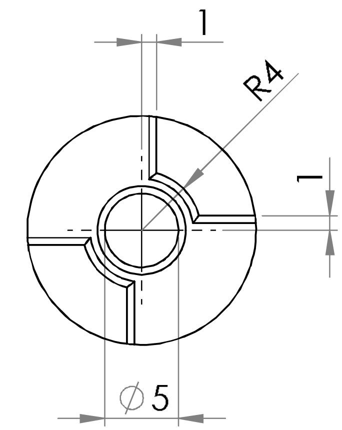

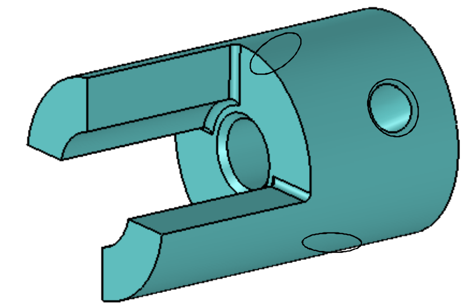

UNLESS OTHERWISE SPECIFIED: DIMENSIONS ARE IN MILLIMETERS SURFACE FINISH: TOLERANCES: LINEAR: ANGULAR:	FINISH:	DEBUR AND BREAK SHARP EDGES	DO NOT SCALE DRAWING
			REVISION

	NAME	SIGNATURE	DATE
DRAWN			
CHK'D			
APPV'D			
MFG			
Q.A			

TITLE:

MATERIAL: PLA

DWG NO. 2.3_Motor_coupling_d5

A4

WEIGHT:

SCALE:2:1

SHEET 1 OF 1

3D printed part

Place 3mm thick foam on contact surfaces with part 2.3_Motor_coupling_d5

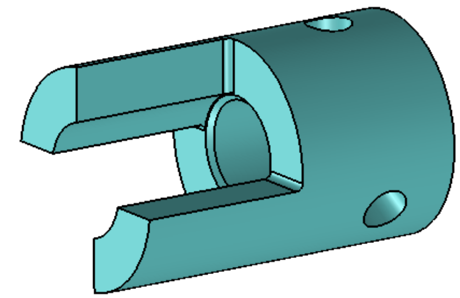

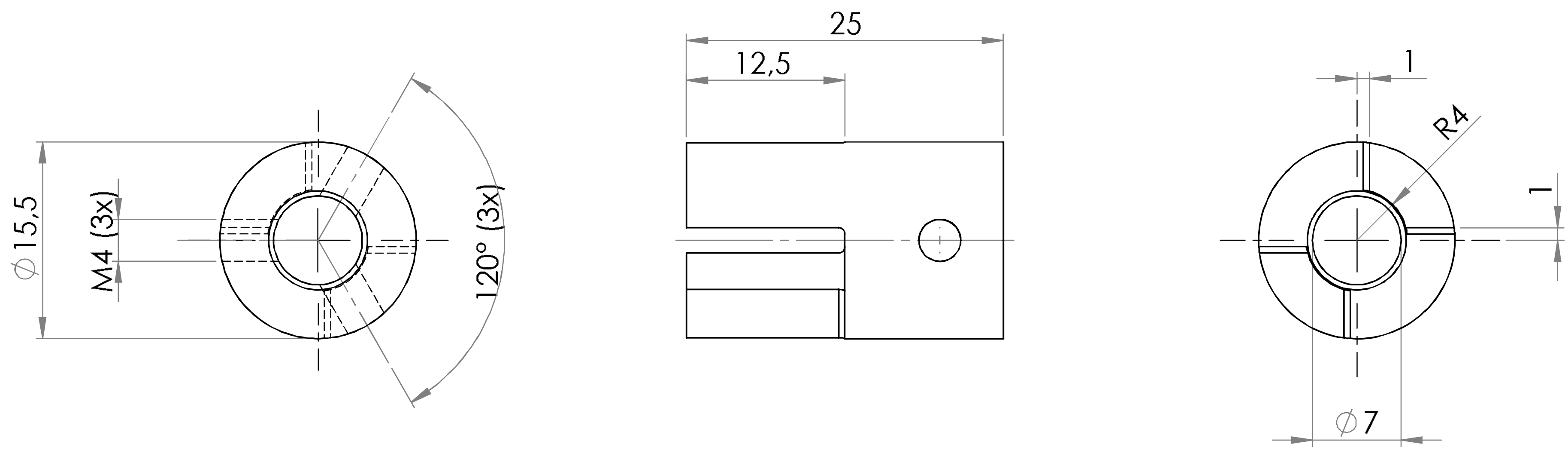

UNLESS OTHERWISE SPECIFIED: DIMENSIONS ARE IN MILLIMETERS SURFACE FINISH: TOLERANCES: LINEAR: ANGULAR:	FINISH:			DEBUR AND BREAK SHARP EDGES	DO NOT SCALE DRAWING	REVISION
	NAME	SIGNATURE	DATE		TITLE:	
DRAWN						
CHK'D						
APPV'D						
MFG						
Q.A			MATERIAL: PLA		DWG NO. 2.4_Motor_coupling_d7	A4
			WEIGHT:		SCALE:2:1	SHEET 1 OF 1

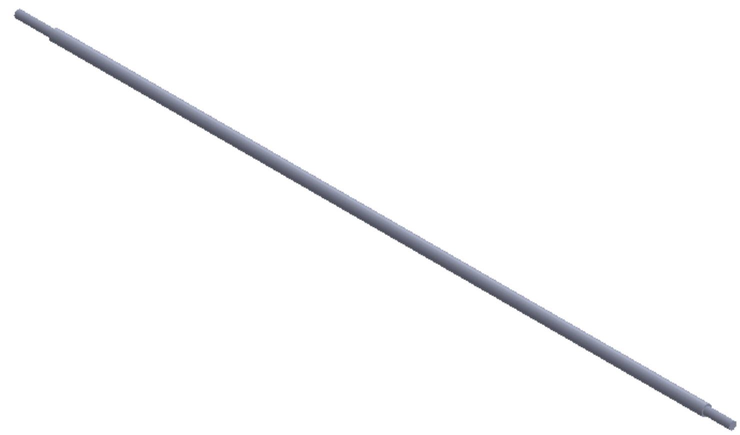

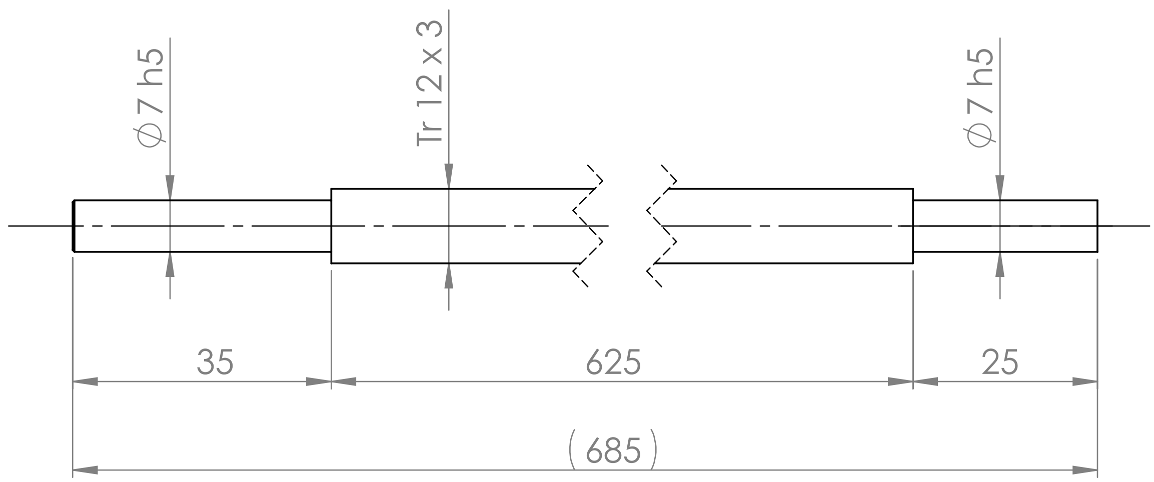

A
B
C
D
E
F

UNLESS OTHERWISE SPECIFIED:
DIMENSIONS ARE IN MILLIMETERS
SURFACE FINISH:
TOLERANCES:
LINEAR:
ANGULAR:

FINISH:

DEBUR AND BREAK SHARP EDGES

DO NOT SCALE DRAWING

REVISION

	NAME	SIGNATURE	DATE
DRAWN			
CHK'D			
APPV'D			
MFG			
Q.A			

TITLE:

MATERIAL:

C35 / C45

DWG NO.

2.5_Lead_Spindle_X

A4

WEIGHT:

SCALE:1:5

SHEET 1 OF 1

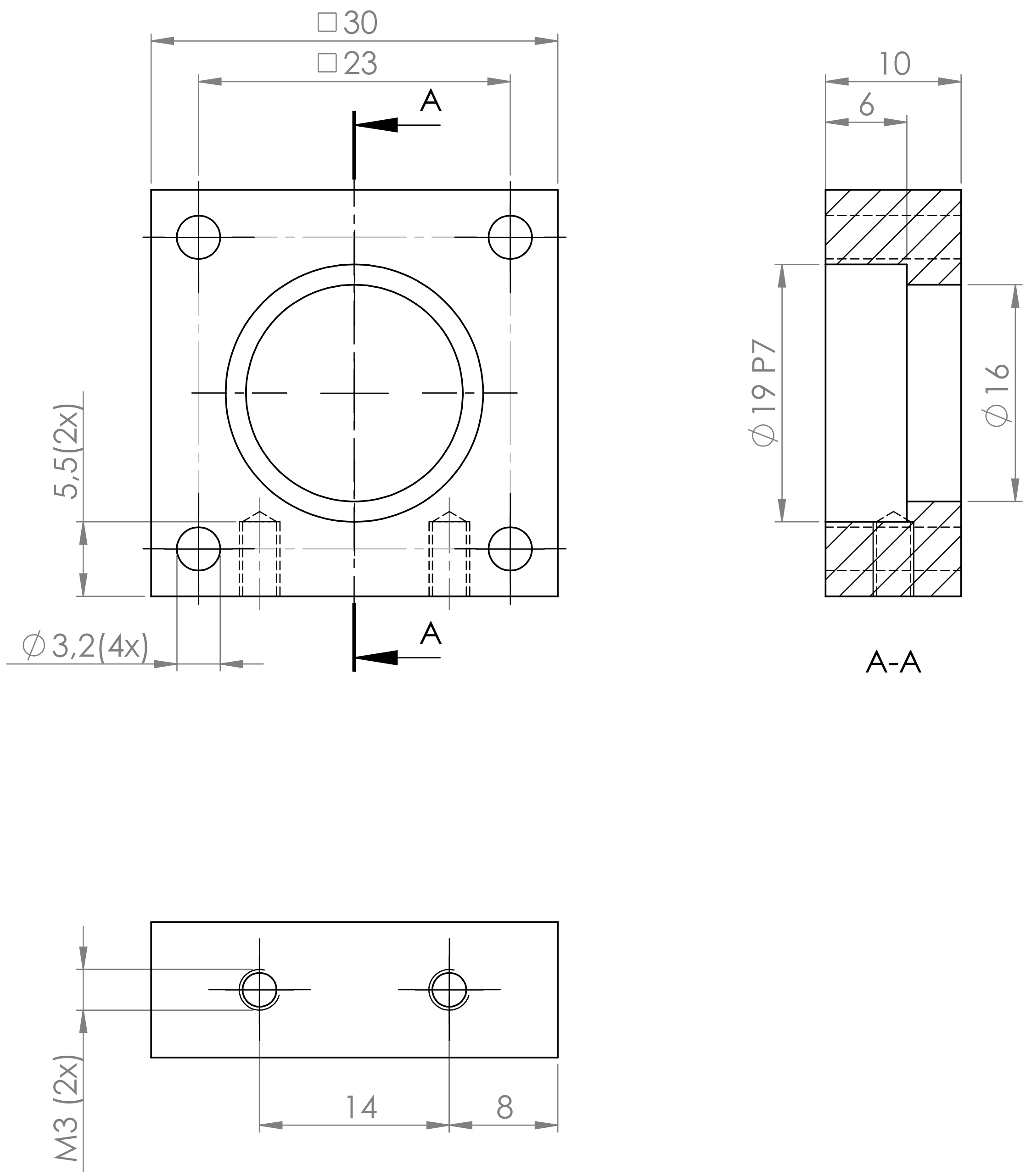

UNLESS OTHERWISE SPECIFIED:
DIMENSIONS ARE IN MILLIMETERS
SURFACE FINISH:
TOLERANCES:
LINEAR:
ANGULAR:

FINISH:

DEBUR AND BREAK SHARP EDGES

DO NOT SCALE DRAWING

REVISION

	NAME	SIGNATURE	DATE		
DRAWN					
CHK'D					
APPV'D					
MFG					
Q.A					

TITLE:

MATERIAL:
PVC

DWG NO.
2.7_Bearing_Mount

A4

WEIGHT:

SCALE:2:1

SHEET 1 OF 1

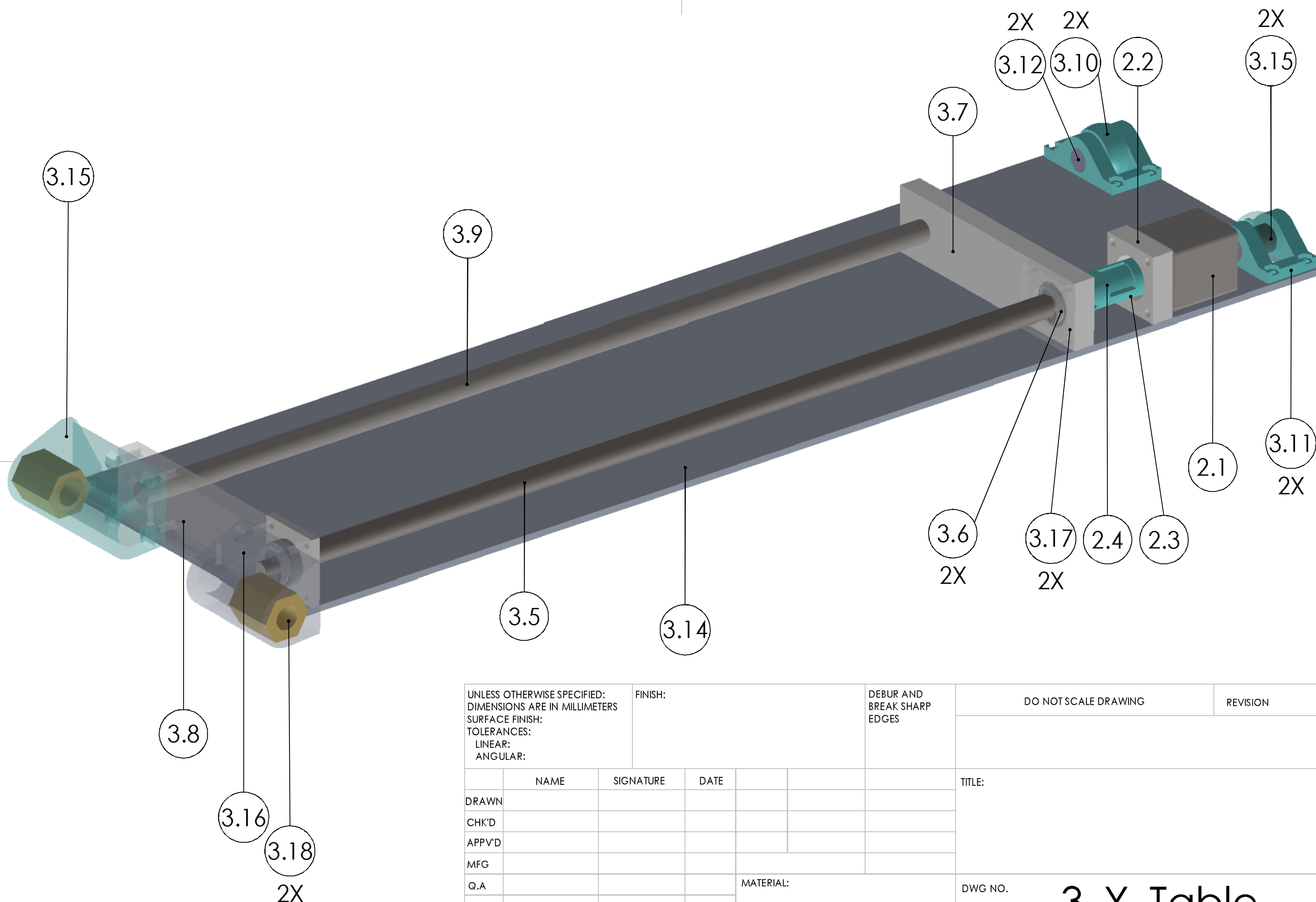

UNLESS OTHERWISE SPECIFIED:
DIMENSIONS ARE IN MILLIMETERS
SURFACE FINISH:
TOLERANCES:
LINEAR:
ANGULAR:

FINISH:

DEBUR AND BREAK SHARP EDGES

DO NOT SCALE DRAWING

REVISION

	NAME	SIGNATURE	DATE
DRAWN			
CHK'D			
APPV'D			
MFG			
Q.A			

TITLE:

MATERIAL:

DWG NO. 3_Y_Table

A4

WEIGHT:

SCALE:1:2

SHEET 1 OF 1

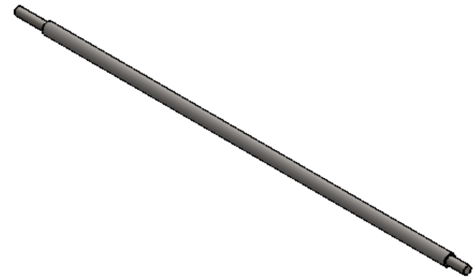

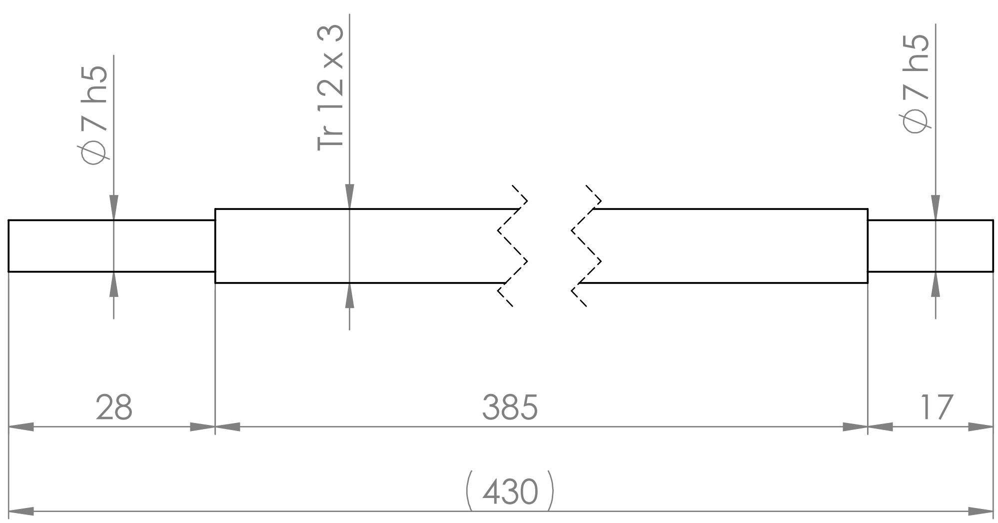

UNLESS OTHERWISE SPECIFIED:
DIMENSIONS ARE IN MILLIMETERS
SURFACE FINISH:
TOLERANCES:
LINEAR:
ANGULAR:

FINISH:

DEBUR AND BREAK SHARP EDGES

DO NOT SCALE DRAWING

REVISION

	NAME	SIGNATURE	DATE
DRAWN			
CHK'D			
APPV'D			
MFG			
Q.A			

TITLE:

MATERIAL: C35 / C45

WEIGHT:

DWG NO. 3.5_Lead_Spindle_Y

A4

SCALE:1:5

SHEET 1 OF 1

Bearing mount for the driven side

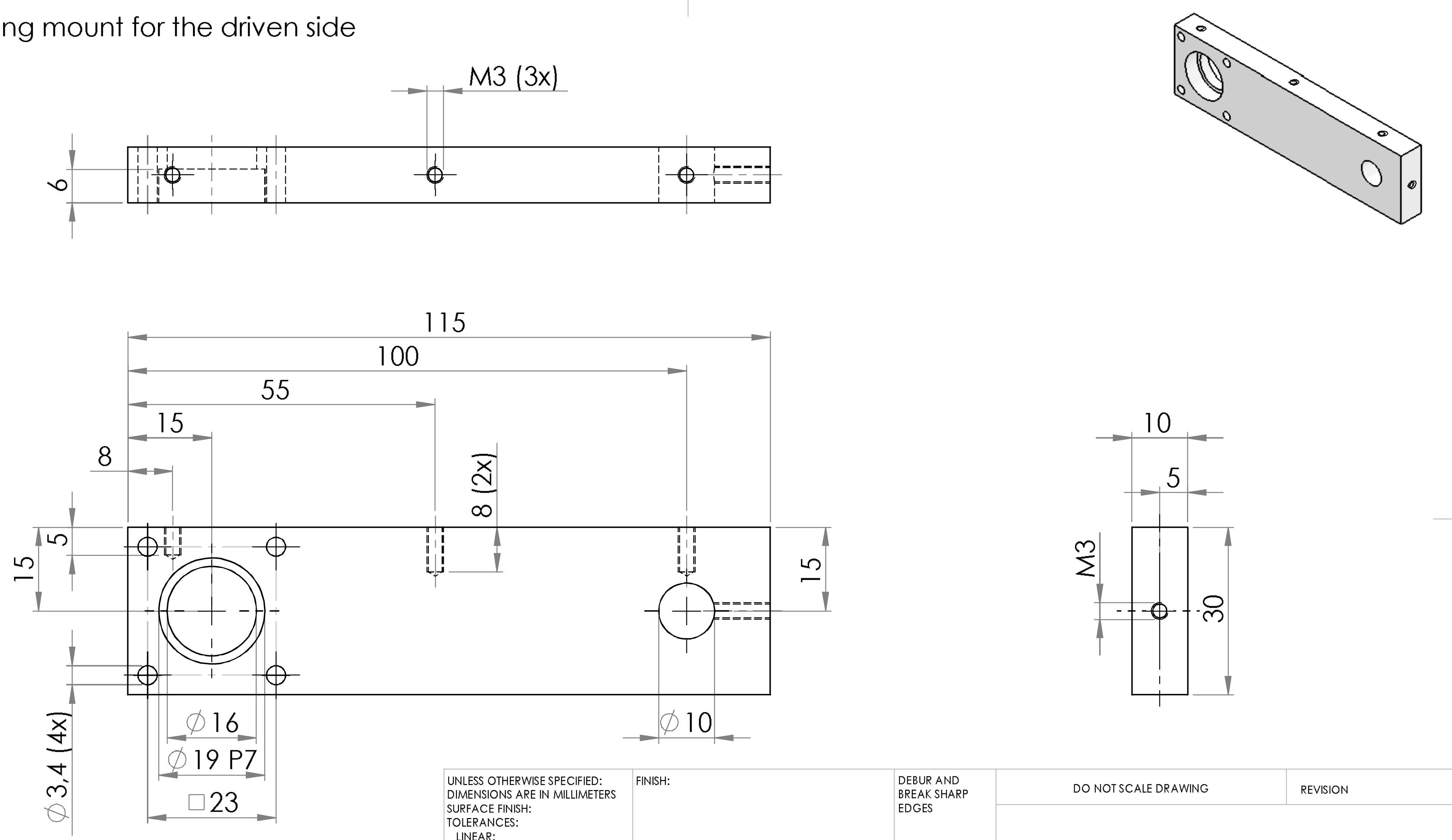

UNLESS OTHERWISE SPECIFIED: DIMENSIONS ARE IN MILLIMETERS SURFACE FINISH: TOLERANCES: LINEAR: ANGULAR:	FINISH:	DEBUR AND BREAK SHARP EDGES	DO NOT SCALE DRAWING	REVISION

	NAME	SIGNATURE	DATE
DRAWN			
CHK'D			
APPV'D			
MFG			
Q.A			

TITLE:

MATERIAL: PVC

DWG NO. 3.7_Bearing_Mount_D

A4

WEIGHT:

SCALE:1:1

SHEET 1 OF 1

Bearing mount for the non-driven side

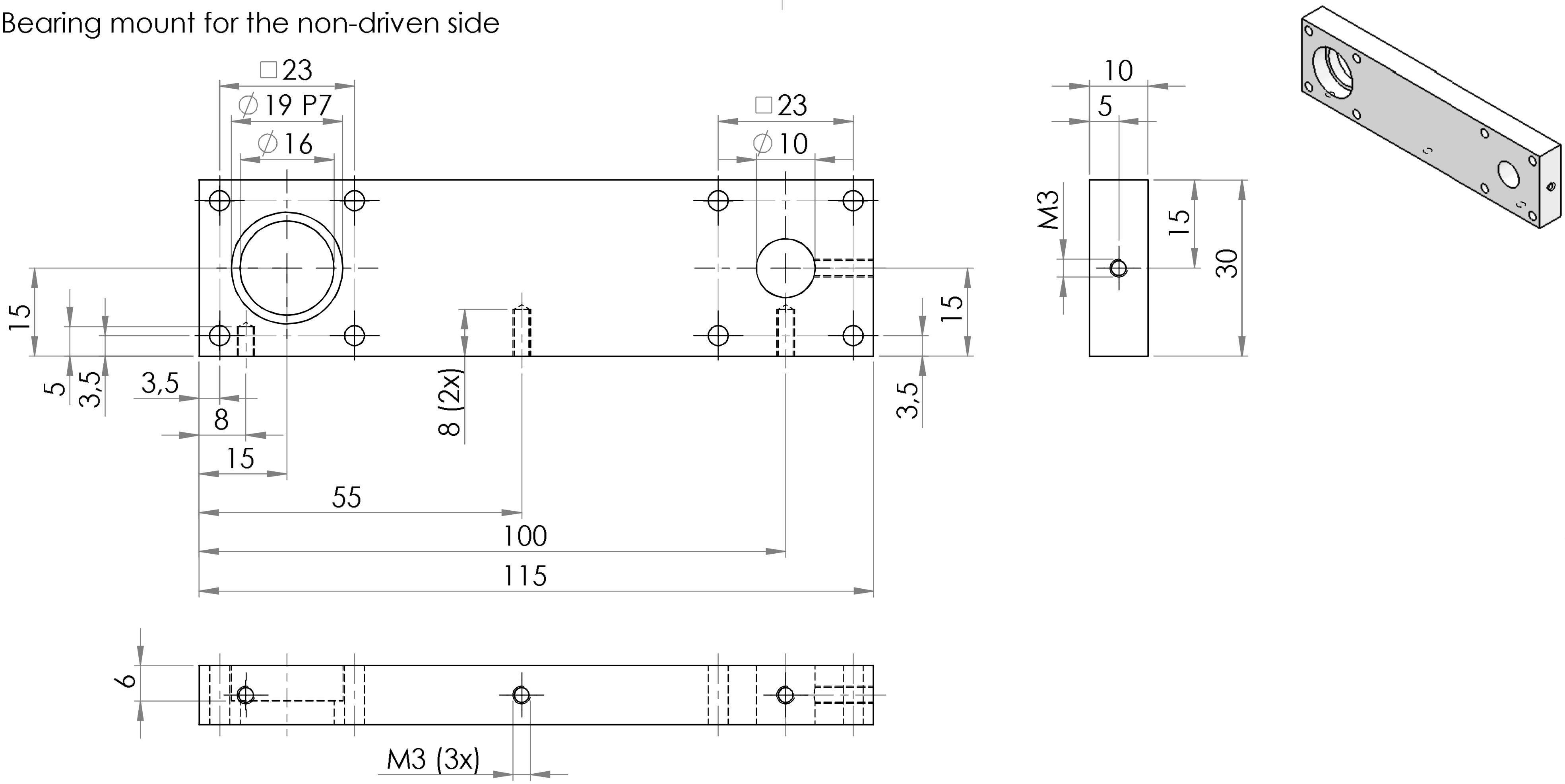

UNLESS OTHERWISE SPECIFIED: DIMENSIONS ARE IN MILLIMETERS SURFACE FINISH: TOLERANCES: LINEAR: ANGULAR:	FINISH:	DEBUR AND BREAK SHARP EDGES	DO NOT SCALE DRAWING	REVISION	
	NAME	SIGNATURE	DATE	TITLE:	
DRAWN					
CHK'D					
APPV'D					
MFG					
Q.A			MATERIAL: PVC	DWG NO. 3.8_Bearing_Mount_ND	A4
			WEIGHT:	SCALE:1:1	SHEET 1 OF 1

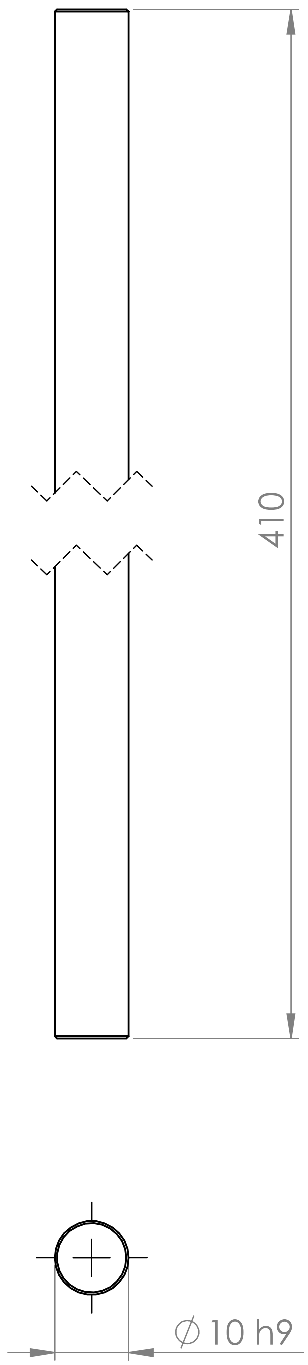

UNLESS OTHERWISE SPECIFIED:
DIMENSIONS ARE IN MILLIMETERS
SURFACE FINISH:
TOLERANCES:
LINEAR:
ANGULAR:

FINISH:

DEBUR AND BREAK SHARP EDGES

DO NOT SCALE DRAWING

REVISION

	NAME	SIGNATURE	DATE
DRAWN			
CHK'D			
APPV'D			
MFG			
Q.A			

TITLE:

MATERIAL:
AISI 316

DWG NO. 3.9_Lin_guiding

A4

WEIGHT:

SCALE:1:1

SHEET 1 OF 1

3d printed part

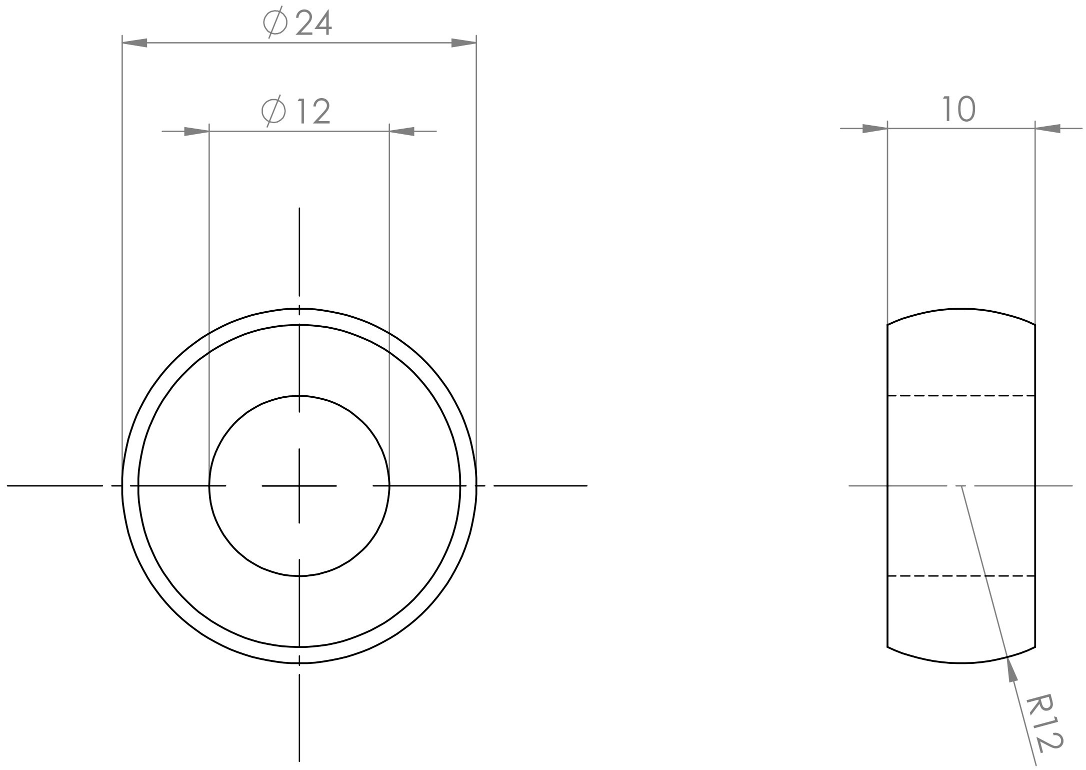

UNLESS OTHERWISE SPECIFIED: DIMENSIONS ARE IN MILLIMETERS SURFACE FINISH: TOLERANCES: LINEAR: ANGULAR:		FINISH:			DEBUR AND BREAK SHARP EDGES	DO NOT SCALE DRAWING	REVISION
	NAME	SIGNATURE	DATE			TITLE:	
DRAWN							
CHK'D							
APPV'D							
MFG							
Q.A				MATERIAL: PLA		DWG NO. 3.10_Wheel_d24	A4
				WEIGHT:		SCALE:2:1	SHEET 1 OF 1

3d printed part

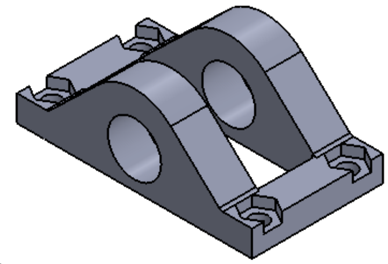

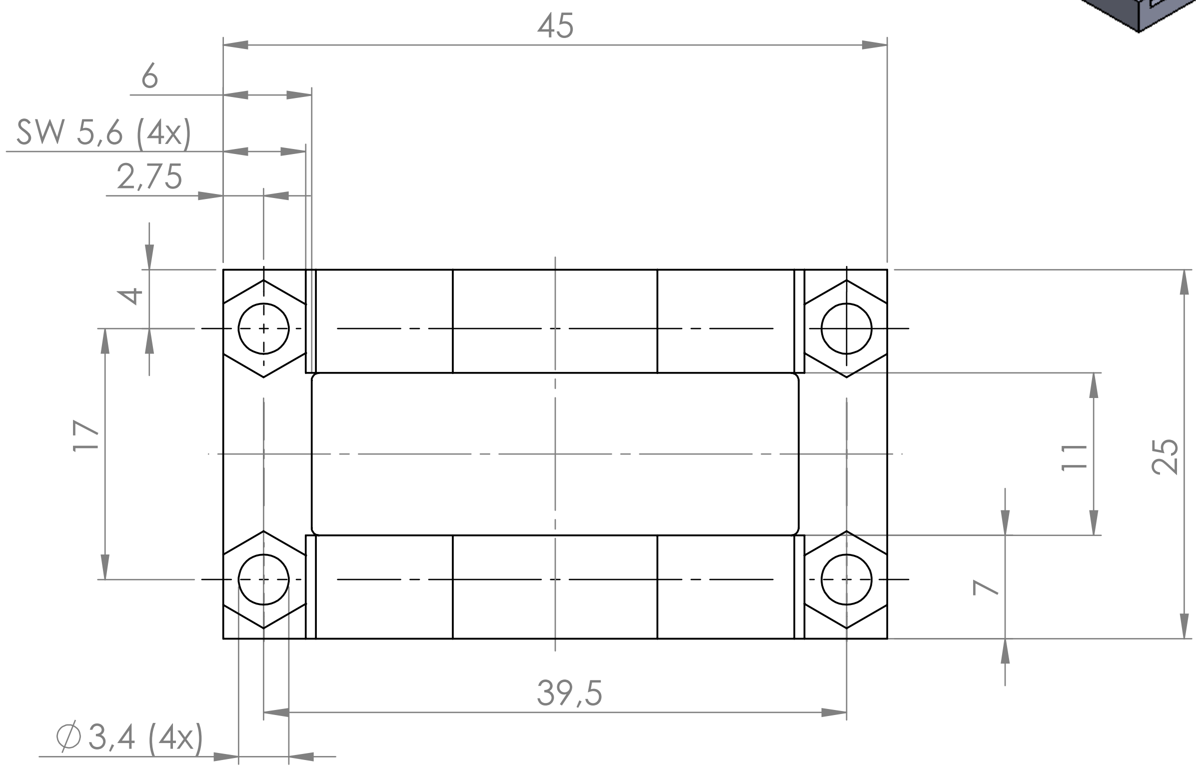

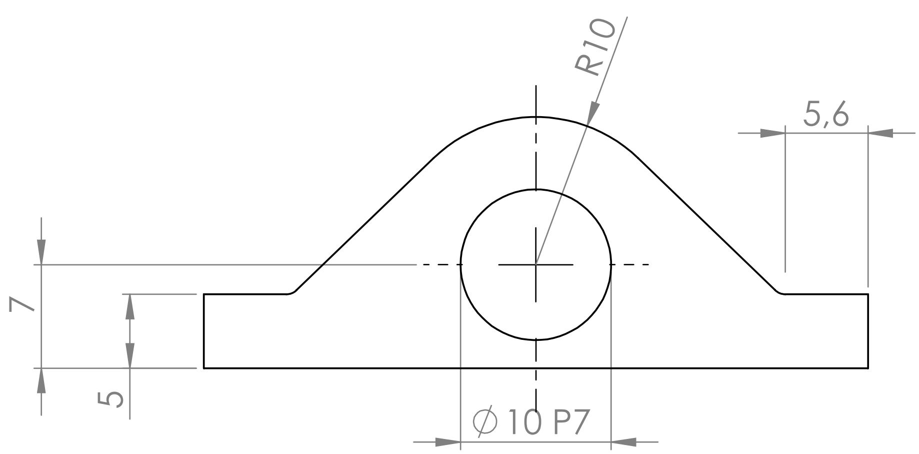

UNLESS OTHERWISE SPECIFIED:
DIMENSIONS ARE IN MILLIMETERS
SURFACE FINISH:
TOLERANCES:
LINEAR:
ANGULAR:

FINISH:

DEBUR AND BREAK SHARP EDGES

DO NOT SCALE DRAWING

REVISION

	NAME	SIGNATURE	DATE
DRAWN			
CHK'D			
APPV'D			
MFG			
Q.A			

TITLE:

MATERIAL:
PLA

DWG NO. 3.11_Wheel_Hub

A4

WEIGHT:

SCALE:2:1

SHEET 1 OF 1

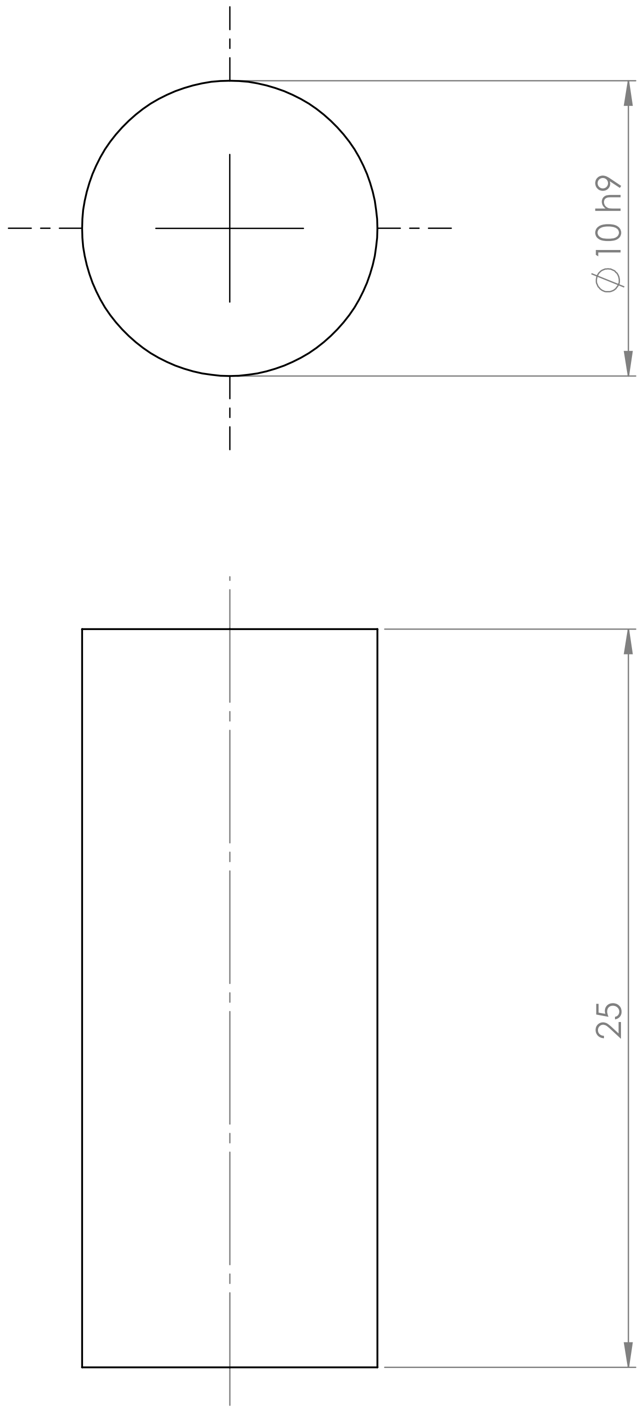

UNLESS OTHERWISE SPECIFIED:
DIMENSIONS ARE IN MILLIMETERS
SURFACE FINISH:
TOLERANCES:
LINEAR:
ANGULAR:

FINISH:

DEBUR AND BREAK SHARP EDGES

DO NOT SCALE DRAWING

REVISION

	NAME	SIGNATURE	DATE
DRAWN			
CHK'D			
APPV'D			
MFG			
Q.A			

TITLE:

MATERIAL:
AISI 316

DWG NO.
3.12_Wheel_Shaft

A4

WEIGHT:

SCALE:4:1

SHEET 1 OF 1

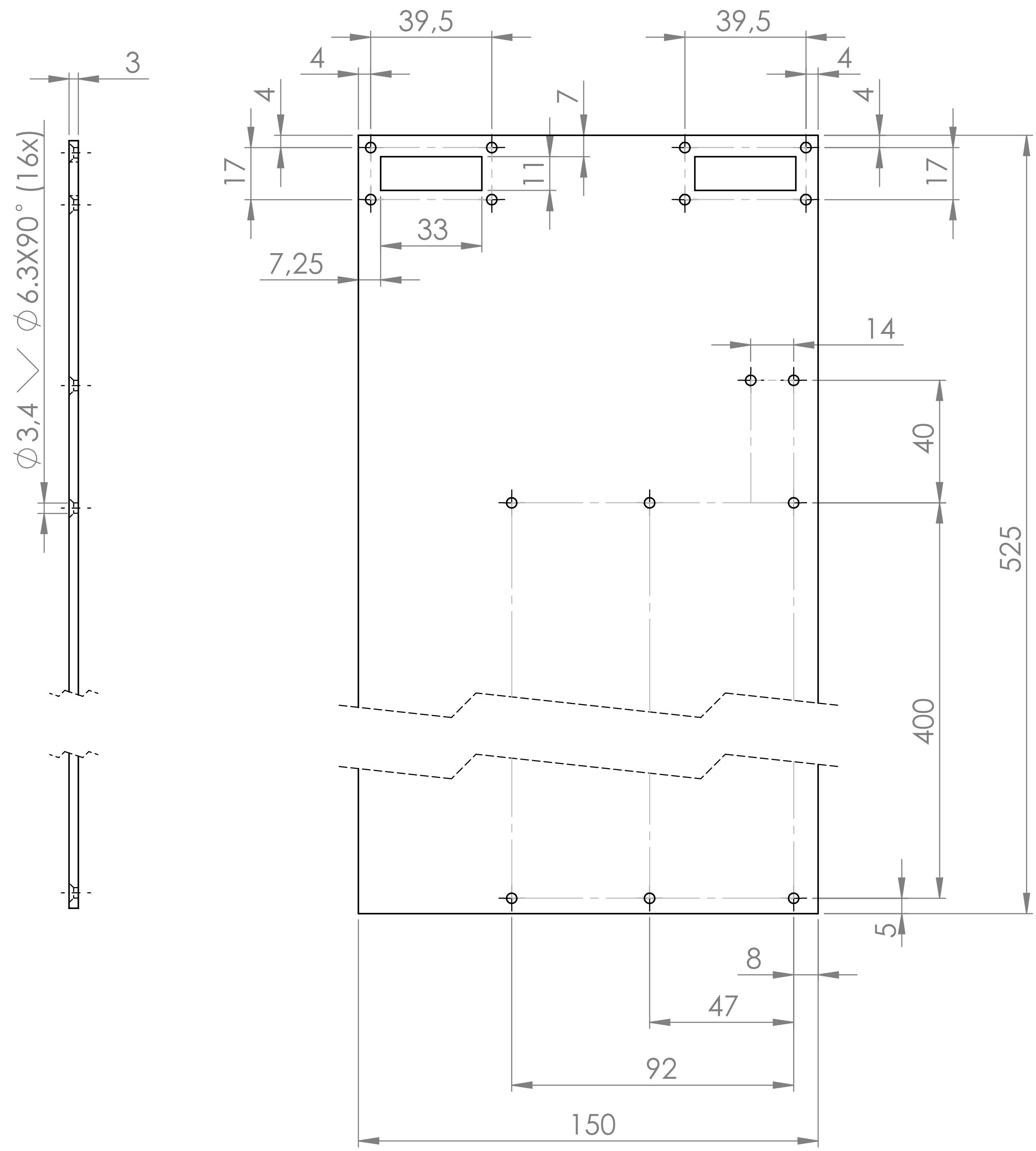

UNLESS OTHERWISE SPECIFIED:
DIMENSIONS ARE IN MILLIMETERS
SURFACE FINISH:
TOLERANCES:
LINEAR:
ANGULAR:

FINISH:

DEBUR AND BREAK SHARP EDGES

DO NOT SCALE DRAWING

REVISION

	NAME	SIGNATURE	DATE
DRAWN			
CHK'D			
APPV'D			
MFG			
Q.A			

TITLE:

MATERIAL:
Aluminium 6010

DWG NO.
3.14_Mounting_sheet

A4

WEIGHT:

SCALE:1:2

SHEET 1 OF 1

3d printed part

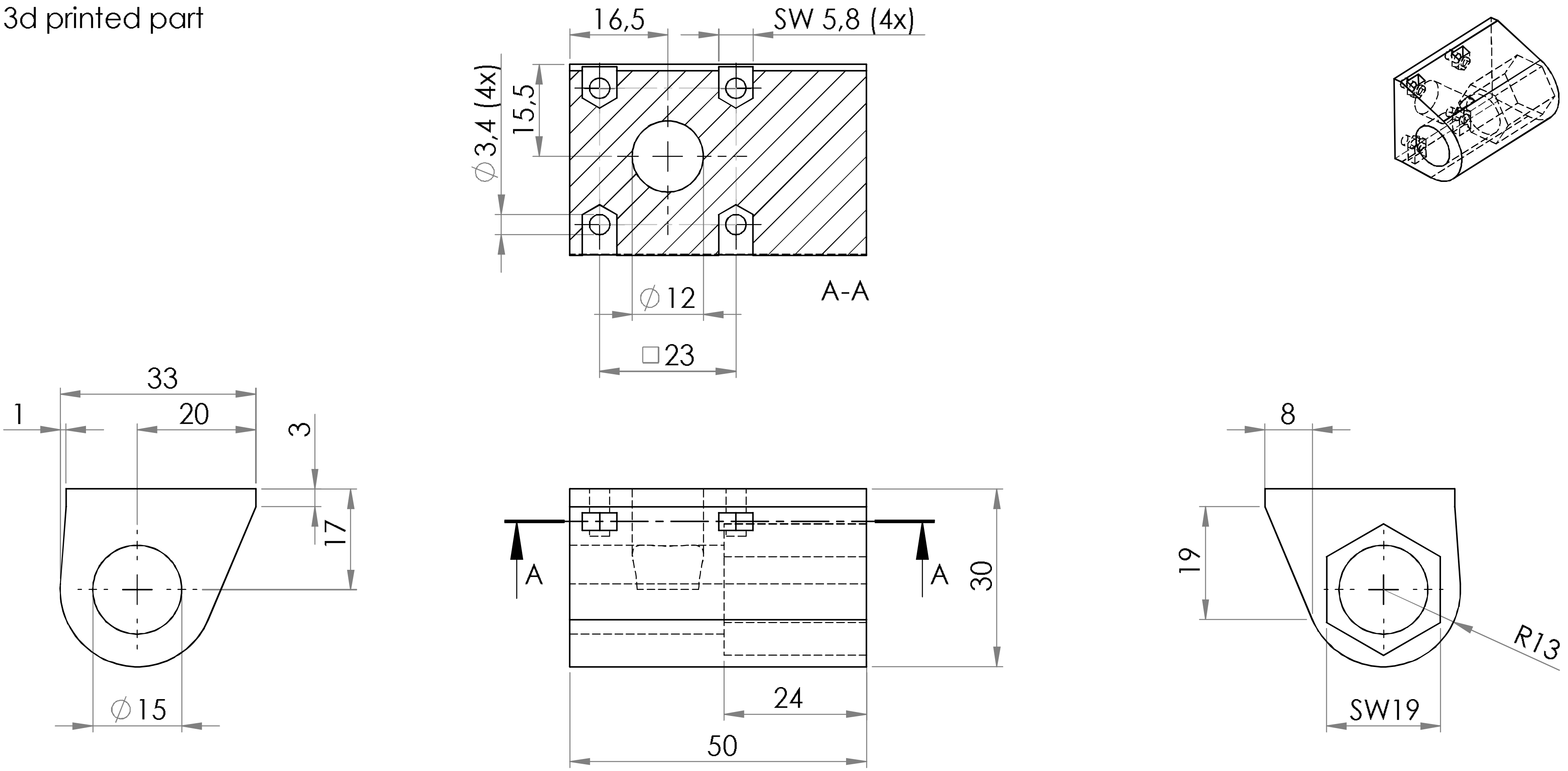

UNLESS OTHERWISE SPECIFIED: DIMENSIONS ARE IN MILLIMETERS SURFACE FINISH: TOLERANCES: LINEAR: ANGULAR:	FINISH:		DEBUR AND BREAK SHARP EDGES	DO NOT SCALE DRAWING	REVISION
	NAME	SIGNATURE	DATE	TITLE:	
DRAWN					
CHK'D					
APPV'D					
MFG					
Q.A			MATERIAL: PLA	DWG NO. 3.15_Nut_mount_R	A4
			WEIGHT:	SCALE:1:1	SHEET 1 OF 1

3d printed part

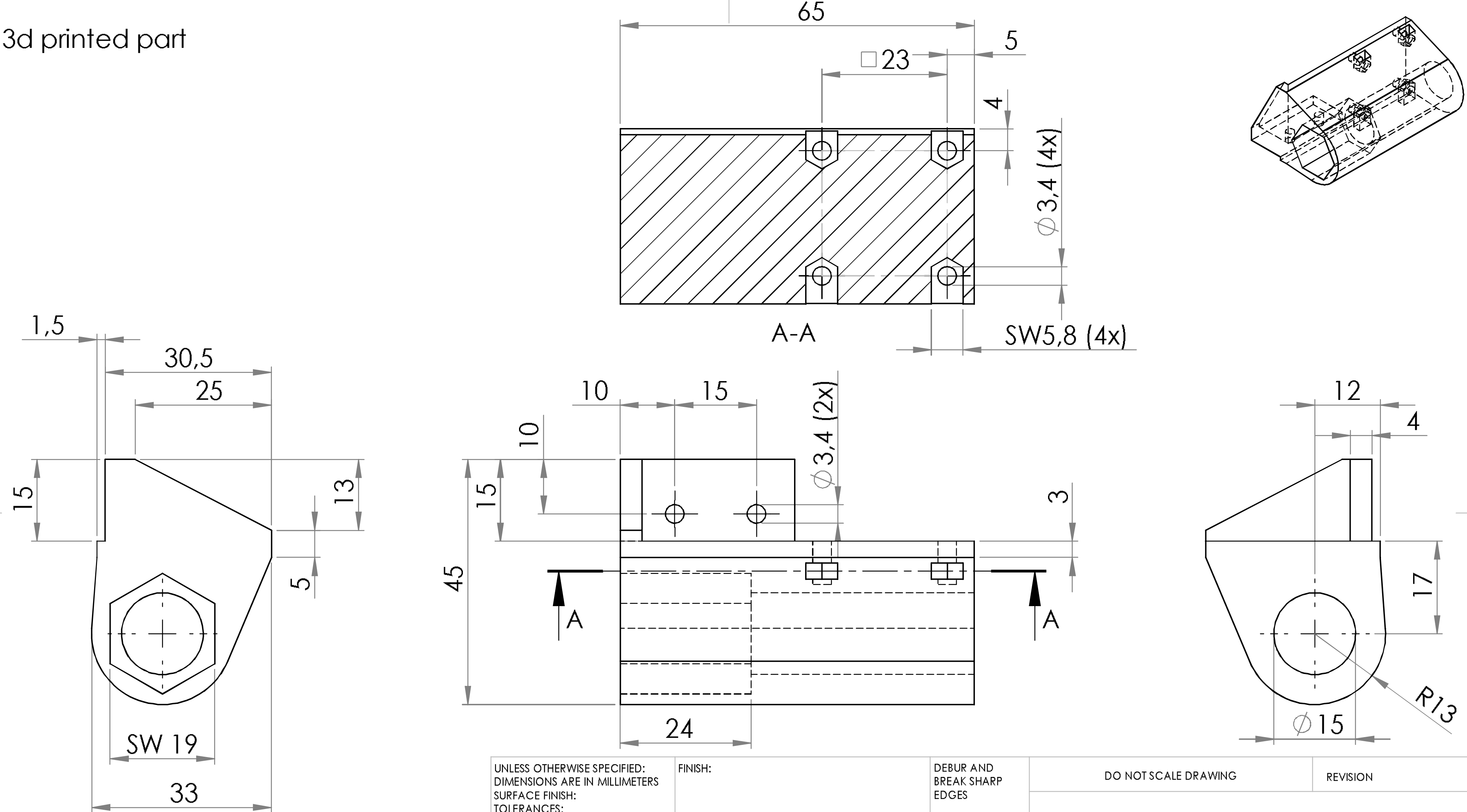

UNLESS OTHERWISE SPECIFIED: DIMENSIONS ARE IN MILLIMETERS SURFACE FINISH: TOLERANCES: LINEAR: ANGULAR:	FINISH:	DEBUR AND BREAK SHARP EDGES	DO NOT SCALE DRAWING	REVISION

	NAME	SIGNATURE	DATE	TITLE:
DRAWN				
CHK'D				
APPV'D				
MFG				
Q.A				

MATERIAL: PLA

DWG NO. 3.16_Nut_mount_L

A4

WEIGHT:

SCALE:1:1

SHEET 1 OF 1

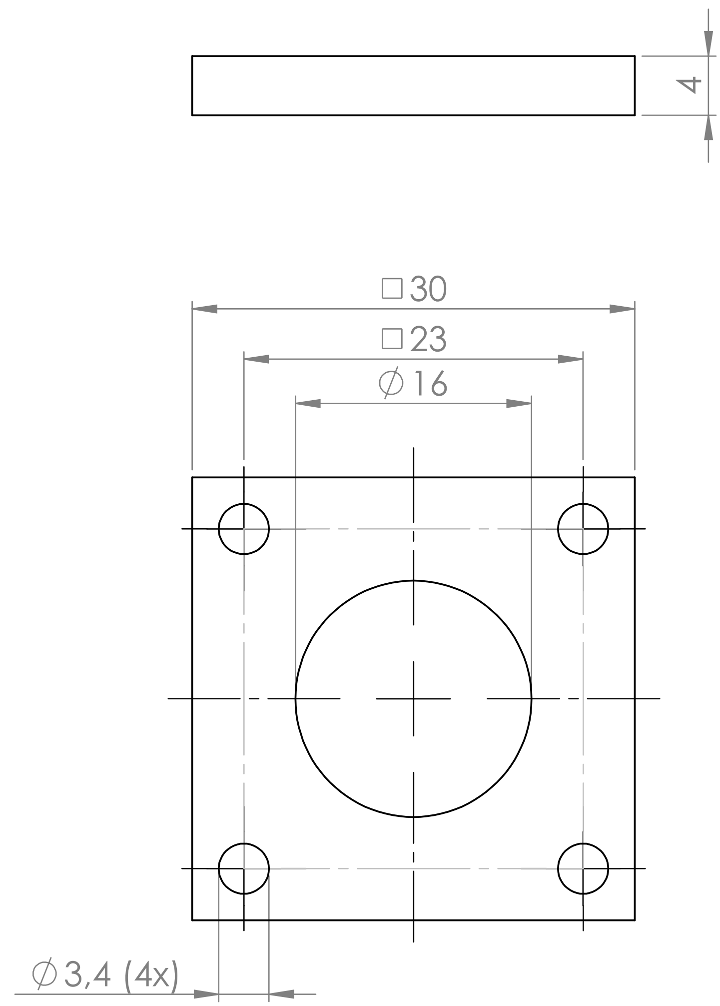

A B C D E F

UNLESS OTHERWISE SPECIFIED:
DIMENSIONS ARE IN MILLIMETERS
SURFACE FINISH:
TOLERANCES:
LINEAR:
ANGULAR:

FINISH:

DEBUR AND BREAK SHARP EDGES

DO NOT SCALE DRAWING

REVISION

	NAME	SIGNATURE	DATE
DRAWN			
CHK'D			
APPV'D			
MFG			
Q.A			

TITLE:

MATERIAL: PVC

DWG NO. 3.17_Bearing_Fix

A4

WEIGHT:

SCALE:2:1

SHEET 1 OF 1

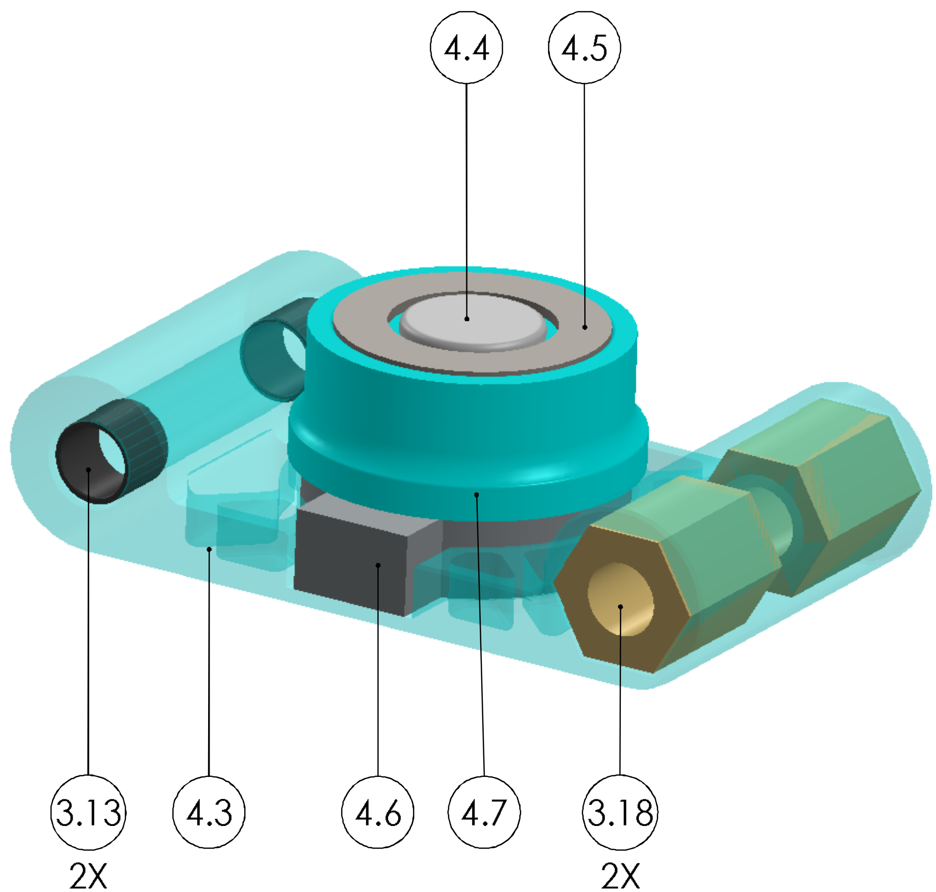

UNLESS OTHERWISE SPECIFIED: DIMENSIONS ARE IN MILLIMETERS SURFACE FINISH: TOLERANCES: LINEAR: ANGULAR:	FINISH:			DEBUR AND BREAK SHARP EDGES	DO NOT SCALE DRAWING	REVISION
	NAME	SIGNATURE	DATE		TITLE:	
DRAWN						
CHK'D						
APPV'D						
MFG						
Q.A				MATERIAL:	DWG NO. 4_Magnet_assembly	A4
				WEIGHT:	SCALE:1:1	SHEET 1 OF 1

3d printed part

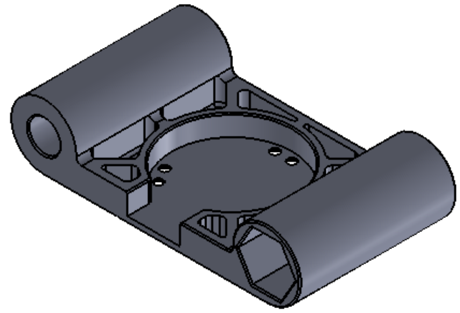

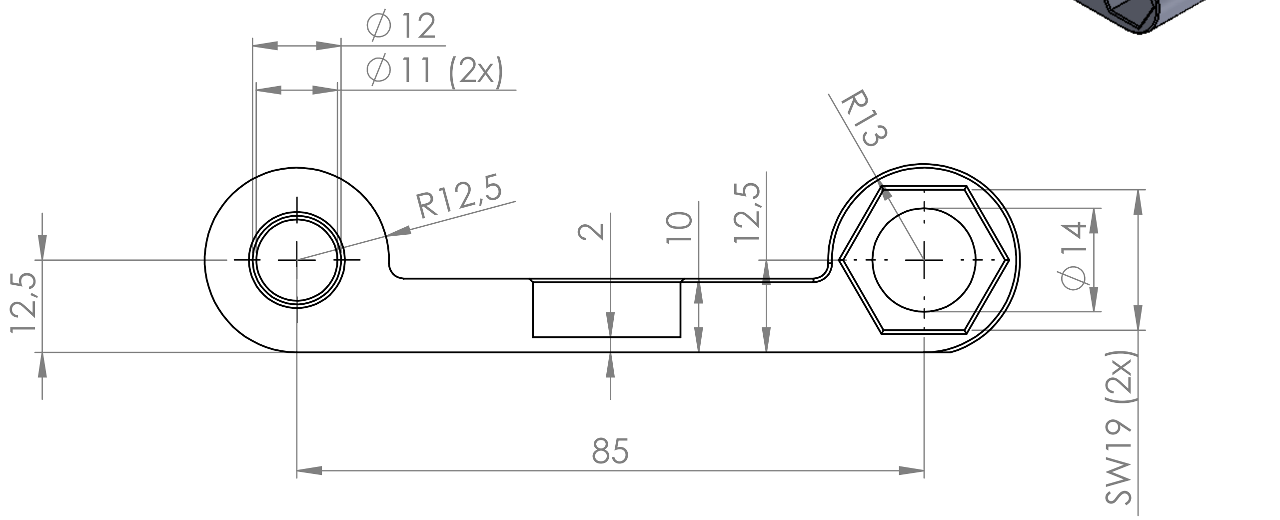

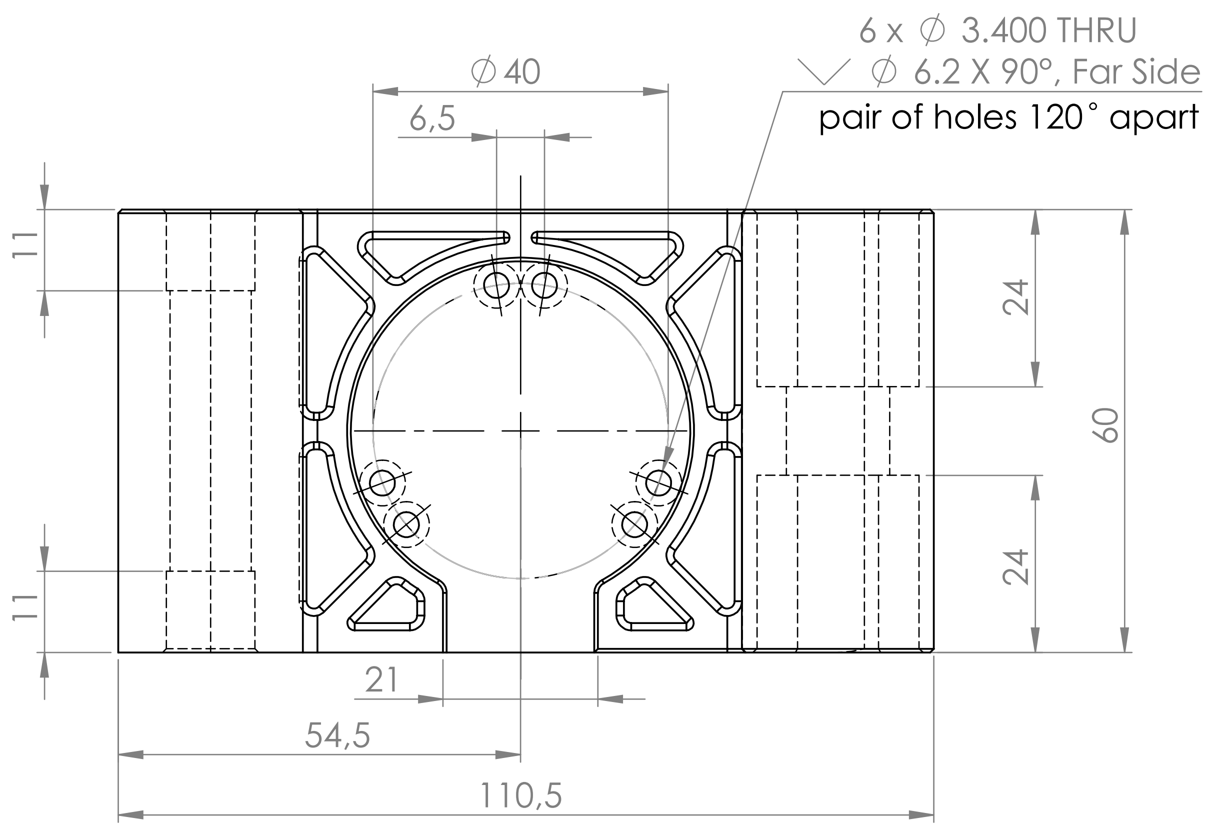

UNLESS OTHERWISE SPECIFIED:
DIMENSIONS ARE IN MILLIMETERS
SURFACE FINISH:
TOLERANCES:
LINEAR:
ANGULAR:

FINISH:

DEBUR AND BREAK SHARP EDGES

DO NOT SCALE DRAWING

REVISION

	NAME	SIGNATURE	DATE
DRAWN			
CHK'D			
APPV'D			
MFG			
Q.A			

TITLE:

MATERIAL:
PLA

DWG NO. 4.3_End_effector

A4

WEIGHT:

SCALE:1:1

SHEET 1 OF 1

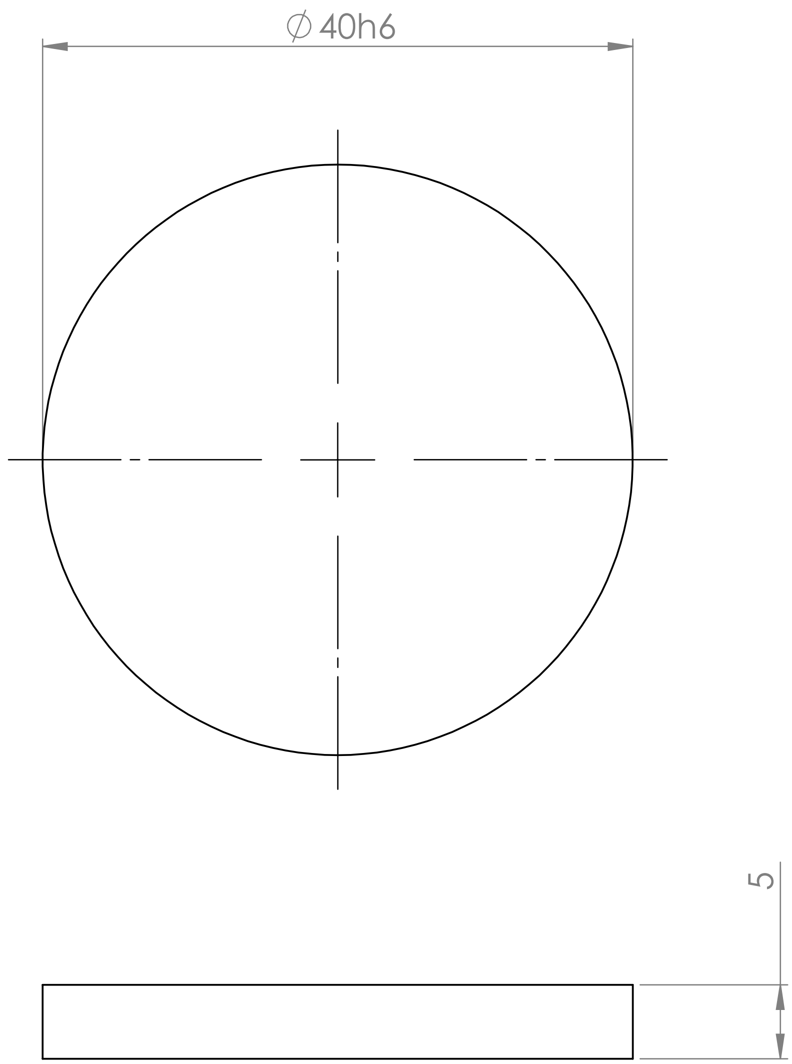

UNLESS OTHERWISE SPECIFIED: DIMENSIONS ARE IN MILLIMETERS SURFACE FINISH: TOLERANCES: LINEAR: ANGULAR:	FINISH:		DEBUR AND BREAK SHARP EDGES		DO NOT SCALE DRAWING	REVISION
	NAME	SIGNATURE	DATE		TITLE:	
DRAWN						
CHK'D						
APPV'D						
MFG						
Q.A				MATERIAL: C35 / C45	DWG NO. 4.5_Magnet_shield	A4
				WEIGHT:	SCALE:2:1	SHEET 1 OF 1

A
B
C
D
E
F

3d printed part

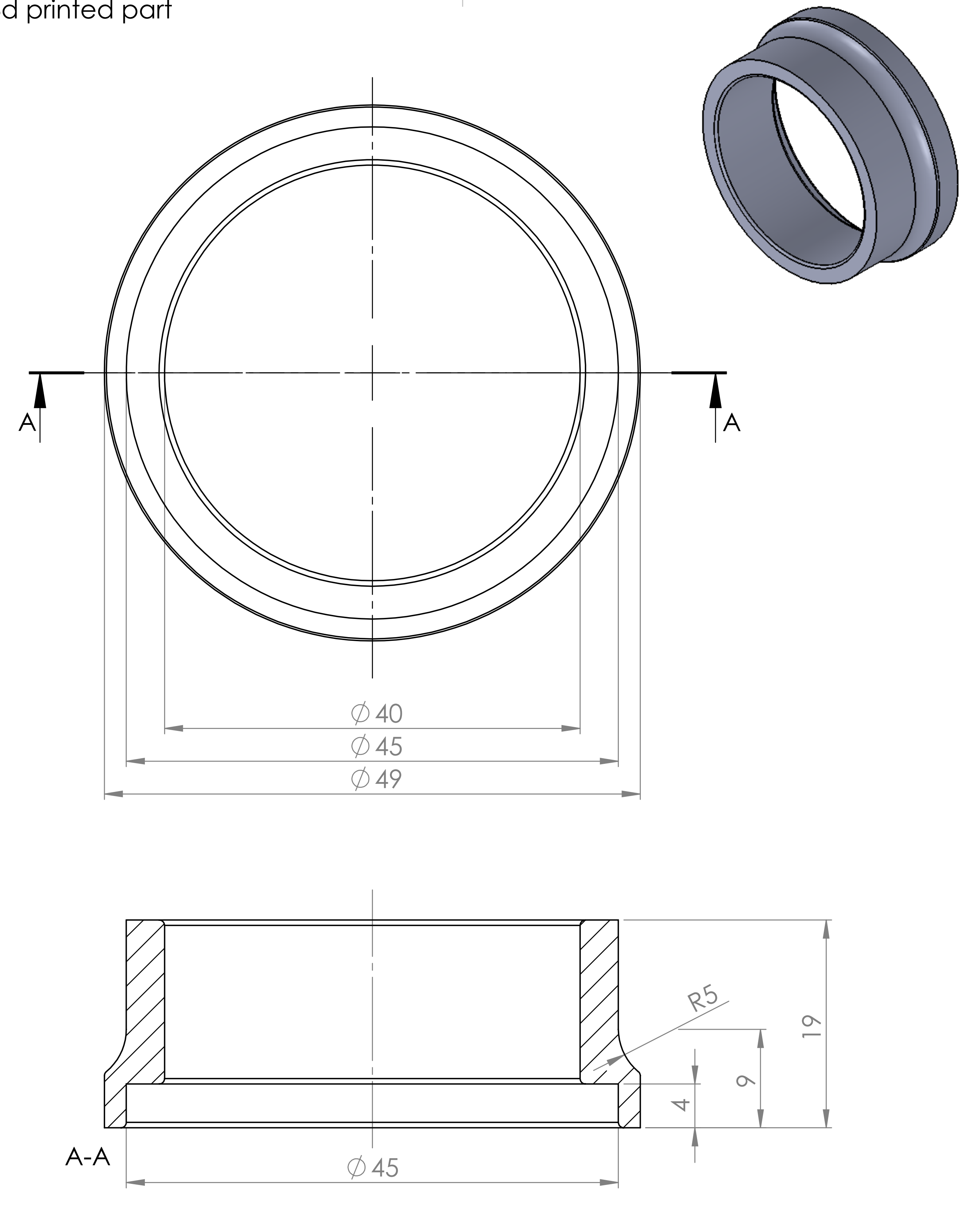

UNLESS OTHERWISE SPECIFIED:
DIMENSIONS ARE IN MILLIMETERS
SURFACE FINISH:
TOLERANCES:
LINEAR:
ANGULAR:

FINISH:

DEBUR AND BREAK SHARP EDGES

DO NOT SCALE DRAWING

REVISION

	NAME	SIGNATURE	DATE
DRAWN			
CHK'D			
APPV'D			
MFG			
Q.A			

TITLE:

MATERIAL:
PLA

DWG NO.
4.7_Magnet_holder

A4

WEIGHT:

SCALE:2:1

SHEET 1 OF 1

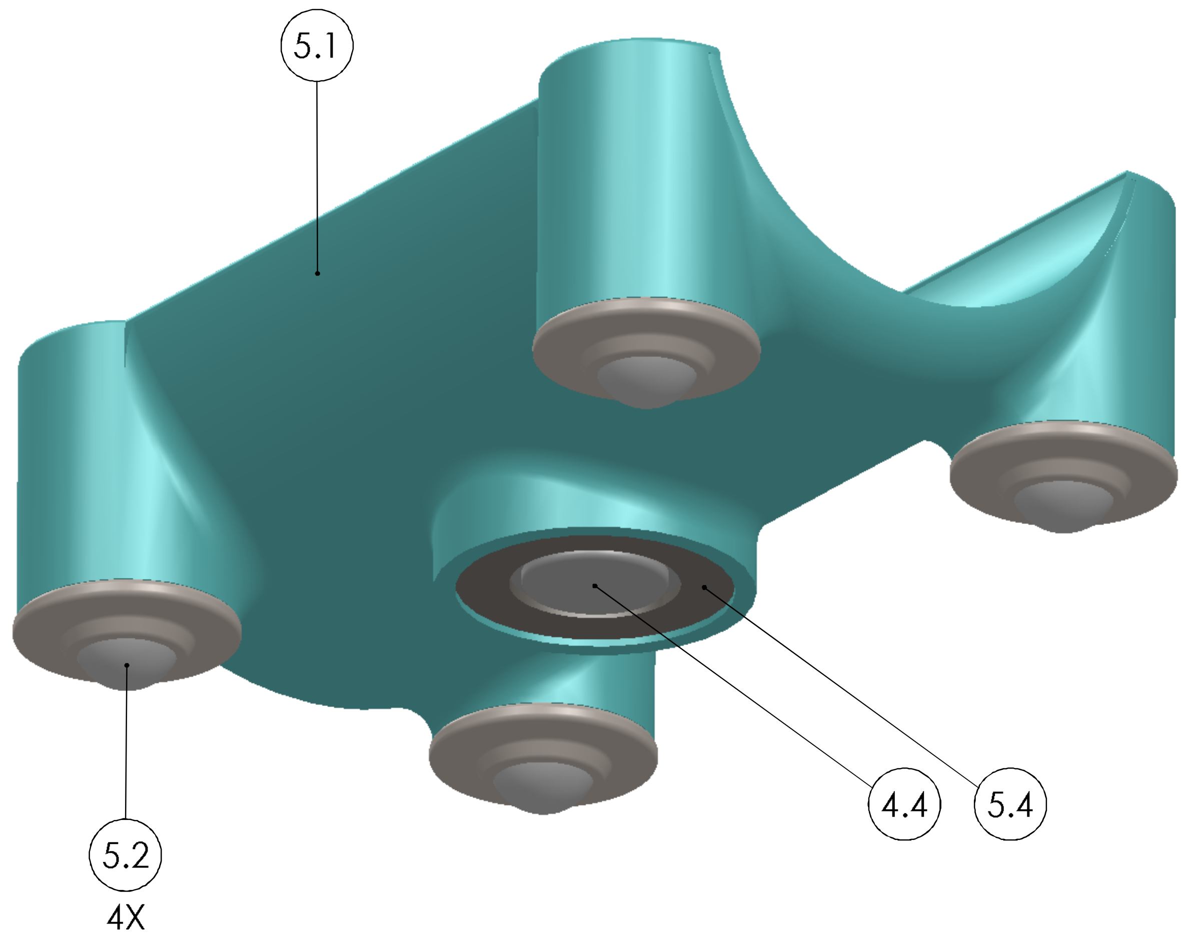

UNLESS OTHERWISE SPECIFIED: DIMENSIONS ARE IN MILLIMETERS SURFACE FINISH: TOLERANCES: LINEAR: ANGULAR:	FINISH:		DEBUR AND BREAK SHARP EDGES	DO NOT SCALE DRAWING	REVISION
	NAME	SIGNATURE	DATE	TITLE:	
DRAWN					
CHK'D					
APPV'D					
MFG					
Q.A			MATERIAL:	DWG NO. 5_Arm_cart	A4
			WEIGHT:	SCALE:1:1	SHEET 1 OF 1

3d printed part
Wall thickness 3mm
Rounded edges, r=1mm

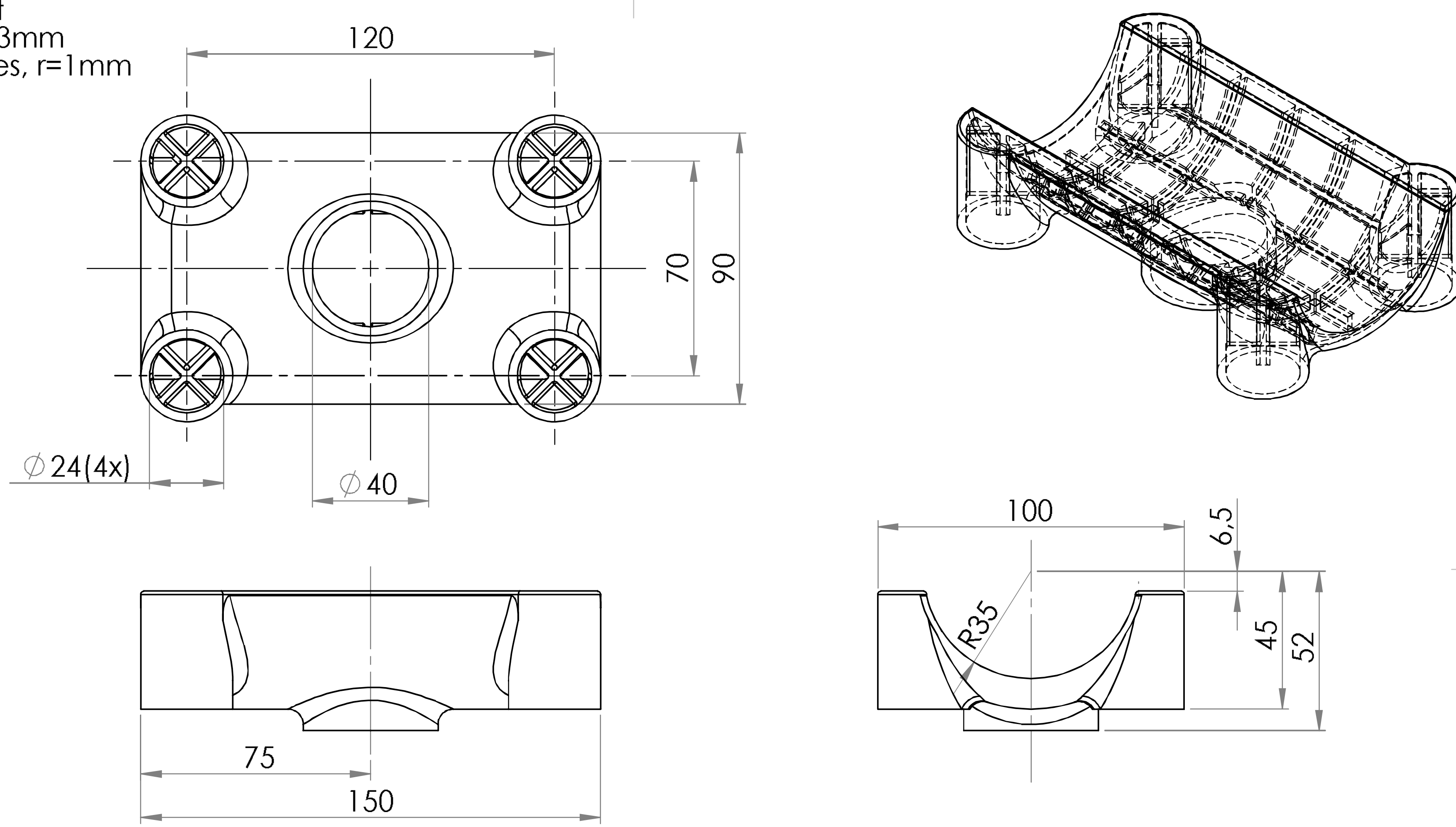

UNLESS OTHERWISE SPECIFIED: DIMENSIONS ARE IN MILLIMETERS SURFACE FINISH: TOLERANCES: LINEAR: ANGULAR:	FINISH:	DEBUR AND BREAK SHARP EDGES	DO NOT SCALE DRAWING	REVISION
	NAME	SIGNATURE	DATE	TITLE:
DRAWN				
CHK'D				
APPV'D				
MFG				
Q.A			MATERIAL: PLA	DWG NO. 5.1_Arm_cart — A4
			WEIGHT:	SCALE:1:2 — SHEET 1 OF 1

F Bill of Materials

Table 7: BOM list for the XY-Table prototype

Material	Dimensions	Amount
Oak sheet	800x610x5.5mm	1
HPL sheet	800x610x10mm	1
Spruce beam	44x18x800mm	1
Spruce beam	44x27x800mm	1
Spruce beam	44x27x565mm	2
Stepper motor	Oriental motor PKP223D15A-L	2
NMB Radial ball bearing	DDR-1970ZZRA1P25LY121	6
Ball transfer unit	Alwayse Engineering 515-0-14	4
Closed plain linear bearing	IGUS GSM-1012-10	4
Lead spindle	Tr12x3, l=685mm	1
Lead spindle	Tr12x3, l=430mm	1
Bronze lead nut	Tr12x3, SLW19, l=24mm	4
Potentiometer	Spectra Symbol SP-L-0400-103-3%-ST	1
Potentiometer	Spectra Symbol SP-L-0500-103-3%-ST	1
Wiper	Spectra Symbol WP-M6-01-03-014-DI	2
NdFeB disc magnet	Supermagnete S-20-10-N	2
PVC	30x30x10mm	6
PVC	30x30x4mm	2
PVC	110x30x10mm	2
Aluminium sheet	525x150x3mm	1
Stainless steel shaft	∅10mm, l=410mm	1
Stainless steel shaft	∅10mm, l=25mm	2
Steel C45 round bar	∅40mm, l=5mm	2
Woodscrews	PK3.5x50mm	8
Nail	PK1x16mm	40
Screw	M2.5x20mm	8
Screw	M3x6mm	16
Screw	M3x20mm	22
Screw	M3x25mm	8
Nut	M3	28
Stepper motor driver	Big Easy Driver v1.2	2
Microcontroller	Arduino Mega2560	1
EMG Shield	Olimex shield-EKG-EMG	2
EMG Shield cables	Olimex shield-EKG-EMG-PRO	2
sEMG electrodes	Disposable push button gel electrodes	6/time
Electric wires	l=1000mm	9
Electric wires	l=250mm	9
DC-DC converter	24V-10V	1
AC-DC adapter	230VAC-24VDC	1

G Arduino Code

Preamble

In the preamble used libraries are included, fixed parameter values are set, and type and begin values of the variables are set.

```
//Define high and low bits for the ADC clock

      #ifndef cbi
      #define cbi(sfr, bit) (_SFR_BYTE(sfr) &= ~_BV(bit))
      #endif
      #ifndef sbi
      #define sbi(sfr, bit) (_SFR_BYTE(sfr) |= _BV(bit))
      #endif

//include libraries and other files
      #include <AccelStepper.h>
      #include "MilliTimer.h"
      #include "parameters.h"

//set variables
      …

//set frequency of loop
      MilliTimer Hz100;

//tell Accelstepper library we are using a stepper motor driver and
to which pins it is connected
      AccelStepper stepper(1, motorStepPin, motorDirPin);
```

Void setup()

The void setup() runs one time at the beginning. ADC clock speed is set, microstep resolution is set, maximum step speed is set (extra safety limit), and the initialisation of the EMG filter and Position sensors are run.

```
void setup(){
/*set ADC clock speed with prescaler, standard = 128
single conversion takes 13 ADC clock cycles
This results in a sampling rate of 9600Hz (=125kHz/13)
taking one sample takes 1s/9600Hz = 104us

for 10bit resolution clock speed needs to be in range 50kHz-200kHz
to have optimal performance
only prescale factor of 128 can be used
Resolution is 5V/1023 = 4.9mV

but Atmel datasheet says that up to 1MHz clock speed, accuracy will
not degrade much
so we can give it a try (http://www.atmel.com/Images/doc2559.pdf
p.10 $$2.8)
```

```
ADPS2    ADPS1    ADPS0    devision factor    clock speed
-----------------------------------------------------------
  0        0        0        2                16 MHz / 2 = 8 MHz
  0        0        1        2                -
  0        1        0        4                16 MHz / 4 = 4 MHz
  0        1        1        8                16 MHz / 8 = 2 MHz
  1        0        0        16               16 MHz / 16 = 1 MHz
  1        0        1        32               16 MHz / 32 = 500 kHz
  1        1        0        64               16 MHz / 64 = 250 kHz
  1        1        1        128              16 MHz / 128 = 125 kHz
*/


  sbi(ADCSRA,ADPS2); //sbi is high(1), cbi is low(0)
  sbi(ADCSRA,ADPS1);
  cbi(ADCSRA,ADPS0);

//set extra limit on stepper speed of stepper motor
  stepper.setMaxSpeed(6000);

//stepper motors, see below for microstepping resolution
  pinMode(MS1, OUTPUT);   //set MS1 as output
  pinMode(MS2, OUTPUT);   //set MS2 as output
  pinMode(MS3, OUTPUT);   //set MS3 as output
  digitalWrite(MS1, HIGH); //set value to high(1, 5V) or low(0, 0V)
  digitalWrite(MS2, LOW);  //set value to high(1, 5V) or low(0, 0V)
  digitalWrite(MS3, LOW);  //set value to high(1, 5V) or low(0, 0V)

  // For microstepping MS pins need to be set high or low
  // Microsteps            MS1      MS2      MS3
  //-----------------------------------------------------------
  // Full Step(200st/rev) low      low      low
  // 1/2 Step             high     low      low
  // 1/4 Step             low      high     low
  // 1/8 Step             high     high     low
  // 1/16 Step (Default)  high     high     high

  emg_init();
  pos_init();
}

\\emg_init()
  pinMode(emgPin_bic, INPUT); //set as input
  pinMode(emgPin_tri, INPUT);
  pinMode(emgPin_pec, INPUT);
  pinMode(emgPin_tra, INPUT);

\\pos_init()
  pinMode(PosPinX,INPUT); //set as input
  pinMode(PosPinX,INPUT);
  digitalWrite(PosPinY, HIGH); //enable pullup resistor
  digitalWrite(PosPinY, HIGH);
```

Void loop()

To keep it simple only one direction will be given. Within the loop another loop is called every 0.01s. This loop gets the filtered EMG steering signal and sends it through the admittance model. It also gets the position and checks this with the set position boundaries.

```
void loop(){
  if(Hz100.poll(10)){
    getEMG_bic();
    getEMG_tri();

    EMGy = EMG_bic-EMG_tri;
  //Admittance model
  speedY = 0.0024*EMGy + 0.0024*EMGy_old + 0.95*speedY_old;
  //set stepper speed
  stepper.setSpeed(4000*speedY);
  //Read Position (0-1023)
  PosY = analogRead(PosPinY);

  //Check boundaries
  if(posY <= boundY_up && EMGy < 0){
    EMGy = 0;
    }
  else if(posY >= boundY_low && EMGy > 0){
    EMGy = 0;
    }
  else{
    EMGy = EMGy;
    }

  //hold old speed & force
  speedy_old=speedY;
  EMGy_old = EMGy;

} //end 100Hz loop

  //Call as much as possible to ensure smooth running
  //Every call is one step
  //Is fixed speed mode with no accelerations
  //Start with slow speed when using this
  stepper.runSpeed();

} //end of void loop()
```

EMG Filter loop for one muscle

```
void loop(){
  //read EMG signal from Olimex EMG shield
  EMG = analogRead(emgPin);

  //notch filter input @ 50Hz to eliminate noise from mains
  EMG2= EMG;  //input n
  NF2= (EMG2 - 2*EMG1 + EMG0 + 2*NF1 + NF0)/3.821598301; //output n

  EMG0= EMG1;           //input n-2
  EMG1= CA*EMG2;        //input n-1
  NF0= ALPHA2*NF1;      //output n-2
  NF1= ALPHA*CA*NF2;    //output n- 1

  //get envelope of EMG signal
  //high pass filter(2nd order Butterworth) @ 20Hz to eliminate
//static offset/drift
  HP2 =  ((0.6997743165180 * NF2) + (-0.4918122372 * HP0) +
(1.3072850288 * HP1));//1.515247108; //250Hz filter
  HP3 = (HP0 + HP2 - 2*HP1);

  HP0 = HP1;
  HP1 = HP2;

  //rectify signal
  HP3 = abs(HP3);

  //low pass filter(2st order Butterworth) @ 3Hz
  LP2 =  ((0.001348711948 * HP3) + (1.8934641464 * LP1) + (-
0.8988589942 * LP0));
  EMG = (LP0 + LP2 + 2*LP1)-OFFSET_BI;

  LP0 = LP1;
  LP1 = LP2;

  }
}
```

References

[1] A. Dunning and J. Herder, “A review of assistive devices for arm balancing,” in *Rehabilitation Robotics (ICORR), 2013 IEEE International Conference on.* IEEE, 2013, Conference Proceedings, pp. 1–6. [Online]. Available: http://ieeexplore.ieee.org/xpls/abs_all.jsp?arnumber=6650485&tag=1

[2] Y. Boyd, V. Buckle, S. Holt, E. Munro, D. Hunter, and I. Craig, “Muscular dystrophy in girls with x; autosome translocations,” *Journal of medical genetics*, vol. 23, no. 6, pp. 484–490, 1986. [Online]. Available: http://jmg.bmj.com/content/23/6/484.full.pdf

[3] J. Hendriksen, R. Hendriksen, J. Kuijer, and E. Vroom, *The psychology of Duchenne Muscular Dystrophy.* Parent Project Production, 2011. [Online]. Available: http://www.parentprojectmd.org/site/DocServer/Internet_pdf.pdf?docID=12183

[4] L. A. Van der Heide, B. van Ninhuijs, A. Bergsma, G. J. Gelderblom, D. J. van der Pijl, and L. P. de Witte, “An overview and categorization of dynamic arm supports for people with decreased arm function,” *Prosthetics and orthotics international*, pp. 1–16, 2013. [Online]. Available: http://poi.sagepub.com/content/early/2013/08/14/0309364613498538.abstract

[5] I. TeacherWeb, “Muscle contractions.” [Online]. Available: http://teacherweb.com/CA/NogalesHighSchool/mespinoza/fig60muscleanatomy.JPG

[6] J. Stoeberl, “The mysteries of muscular dystrophy.” [Online]. Available: http://2.bp.blogspot.com/-GfLBf2PD7jM/T48Y0FPjp2I/AAAAAAAAAB0/YuIcasS1WzU/s1600/10406903.jpg

[7] A. Burke, “Gowers sign.” [Online]. Available: http://www.alison-burke.com/works-medicine.html

[8] C. Rhodes, “Scott sands: 1966 - 2014,” 2014. [Online]. Available: http://dmdpioneers.org/blog/in-memoriam/scott-sands-1966-2014.html

[9] ——, “Tom mecke: 1960 - 2014,” 2014. [Online]. Available: http://dmdpioneers.org/blog/in-memoriam/tom-mecke-1960-2014.html

[10] Prosensa, “Overview clinical symptons dmd.” [Online]. Available: http://prosensa.eu/img/timeline-DMD-patient.png

[11] S. Pheasant and C. M. Haslegrave, *Bodyspace: Anthropometry, ergonomics*

and the design of work. CRC Press, 2005.

[12] T. Delft, "Dined anthropometric database." [Online]. Available: http://dined.io.tudelft.nl/dined/

[13] A. Kumar and M. F. Phillips, "Use of powered mobile arm supports by people with neuromuscular conditions," *Journal of rehabilitation research and development*, vol. 50, no. 1, pp. 61–70, 2013.

[14] T. Rahman, R. Ramanathan, S. Stroud, W. Sample, R. Seliktar, W. Harwin, M. Alexander, and M. Scavina, "Towards the control of a powered orthosis for people with muscular dystrophy," *Proceedings of the Institution of Mechanical Engineers, Part H: Journal of Engineering in Medicine*, vol. 215, no. 3, pp. 267–274, 2001.

[15] F. Meditech, "Sling." [Online]. Available: http://www.focalmeditech.nl/nl/content/sling

[16] ——, "Sling elektrisch." [Online]. Available: http://www.focalmeditech.nl/nl/content/sling-elektrisch

[17] Nitzbon, "Nitzbon mobility arm." [Online]. Available: http://www.nitzbon.de/products.html

[18] A. Forever, "Swedish help arm." [Online]. Available: http://www.activeforever.com/swedish-help-arm

[19] J. Orthopedic, "Standard mas." [Online]. Available: http://jaecoorthopedic.com/products/products/Standard-MAS-w%7B47%7D-Adjustable-Mount.html

[20] F. Meditech, "Top/help." [Online]. Available: http://www.focalmeditech.nl/nl/content/tophelp

[21] G. Kramer, G. Romer, and H. J. Stuyt, "Design of a dynamic arm support (das) for gravity compensation," in *Rehabilitation Robotics, 2007. ICORR 2007. IEEE 10th International Conference on*. IEEE, 2007, Conference Proceedings, pp. 1042–1048.

[22] N. Solutions, "Neater arm support." [Online]. Available: http://www.neater.co.uk/neater-arm-support

[23] ErgoGuys, "Eg - ergoarm." [Online]. Available: http://store.ergoguys.com/eg-armrest.html

[24] Flextension, "A-gear project." [Online]. Available: http://www.flextension.

nl/en/projects/a-gear-project/

[25] J. Orthopedic, "Wrex: Wilmington robotic exoskeleton arm." [Online]. Available: http://jaecoorthopedic.com/products/products/WREX%3A-Wilmington-Robotic-EXoskeleton-Arm.html#

[26] Y. Mao and S. K. Agrawal, "Wearable cable-driven upper arm exoskeleton-motion with transmitted joint force and moment minimization," in *Robotics and Automation (ICRA), 2010 IEEE International Conference on.* IEEE, 2010, Conference Proceedings, pp. 4334–4339.

[27] A. H. A. Stienen, *Development of novel devices for upper-extremity rehabilitation.* University of Twente, 2009.

[28] J. C. Perry and J. Rosen, "Design of a 7 degree-of-freedom upper-limb powered exoskeleton," in *Biomedical Robotics and Biomechatronics, 2006. BioRob 2006. The First IEEE/RAS-EMBS International Conference on.* IEEE, 2006, Conference Proceedings, pp. 805–810.

[29] J. C. Perry, H. Zabaleta, A. Belloso, C. Rodrguez-de Pablo, F. I. Cavallaro, and T. Keller, "Armassist: development of a functional prototype for at-home telerehabilitation of post-stroke arm impairment," in *Biomedical Robotics and Biomechatronics (BioRob), 2012 4th IEEE RAS EMBS International Conference on.* IEEE, 2012, Conference Proceedings, pp. 1561–1566.

[30] N. Hogan, H. I. Krebs, J. Charnnarong, P. Srikrishna, and A. Sharon, "Mit-manus: a workstation for manual therapy and training. i," in *Robot and Human Communication, 1992. Proceedings., IEEE International Workshop on.* IEEE, 1992, Conference Proceedings, pp. 161–165.

[31] J. Lobo-Prat, P. N. Kooren, A. Q. Keemink, M. I. Paalman, E. E. Hekman, P. H. Veltink, A. H. Stienen, and B. F. Koopman, "Design and control of an experimental active elbow support for adult duchenne muscular dystrophy patients," in *Biomedical Robotics and Biomechatronics (2014 5th IEEE RAS EMBS International Conference on.* IEEE, 2014, Conference Proceedings, pp. 187–192.

[32] J. Rosen, M. Brand, M. B. Fuchs, and M. Arcan, "A myosignal-based powered exoskeleton system," *Systems, Man and Cybernetics, Part A: Systems and Humans, IEEE Transactions on*, vol. 31, no. 3, pp. 210–222, 2001.

[33] J. Rosen, M. B. Fuchs, and M. Arcan, "Performances of hill-type and neural network muscle modelstoward a myosignal-based exoskeleton," *Computers and Biomedical Research*, vol. 32, no. 5, pp. 415–439, 1999.

[34] K. Kiguchi, T. Tanaka, and T. Fukuda, "Neuro-fuzzy control of a robotic exoskeleton with emg signals," *Fuzzy Systems, IEEE Transactions on*, vol. 12, no. 4, pp. 481–490, 2004.

[35] T. Lenzi, S. M. M. De Rossi, N. Vitiello, and M. C. Carrozza, "Intention-based emg control for powered exoskeletons," *Biomedical Engineering, IEEE Transactions on*, vol. 59, no. 8, pp. 2180–2190, 2012.

[36] F. Daerden and D. Lefeber, "Pneumatic artificial muscles: actuators for robotics and automation," *European journal of mechanical and environmental engineering*, vol. 47, no. 1, pp. 11–21, 2002.

[37] H. J. Hermens, B. Freriks, R. Merletti, D. Stegeman, J. Blok, G. Rau, C. Disselhorst-Klug, and G. Hgg, "European recommendations for surface electromyography," *Roessingh Research and Development, Enschede*, 1999.

[38] P. Veltink, H. Kortier, H. Schepers, V. Sluiter, R. Brookhuis, T. Lammerink, and R. Wiegerink, "Powerglove, concepts and current results," 2012.

[39] R. Q. Van der Linde, P. Lammertse, E. Frederiksen, and B. Ruiter, "The hapticmaster, a new high-performance haptic interface," in *Proc. Eurohaptics*, 2002, Conference Proceedings, pp. 1–5.

[40] Thomson Industries, Inc., "Lead screws, ball screws and ball splines," p. 181, 2014. [Online]. Available: http://www.thomsonlinear.com/downloads/screws/Leadscrews_Ballscrews_Splines_cten.pdf

[41] Haydon Kerk Motion Solutions, Inc., "Linear motion catalog and design guide," pp. 14–15, 2013. [Online]. Available: http://www.haydonkerk.com/Portals/0/pdf/Catalog/2013_Haydon_Kerk_Catalog.zip

[42] Nook Industries, Inc., "Precision screw assemblies," pp. 6–17. [Online]. Available: http://www.nookindustries.com/Content/media/NOOK-Screw-Catalog.pdf

[43] Kruger Ventilation, "Critical speed of shafts," pp. 1–5, 1998. [Online]. Available: http://www.krugerfan.com/brochure/publications/Tbn017.pdf

[44] C. D. Fryar, Q. Gu, and C. L. Ogden, "Anthropometric reference data for children and adults: United states, 2007-2010," *National Center for Health Statistics Vital and Health Statistics*, vol. 11, pp. 1–40, 2012.

[45] A. Tzeren, *Human body dynamics: classical mechanics and human movement.* Springer, 2000.

[46] Thomson Industries, Inc., "Lead screws, ball screws and ball splines," p. 18, 2014. [Online]. Available: http://www.thomsonlinear.com/downloads/screws/Leadscrews_Ballscrews_Splines_cten.pdf

[47] Nook Industries, Inc., "Precision screw assemblies," pp. 66–67. [Online]. Available: http://www.nookindustries.com/Content/media/NOOK-Screw-Catalog.pdf

[48] E. Gernaat, *Magnetische Toepassingen in de voertuigentechniek*. Steele Consulting, 2007.

[49] K&J Magnetics, Inc., "The k&j magnetic gap calculator." [Online]. Available: http://www.kjmagnetics.com/gap.calculator.asp

[50] Supermagnete.nl, "Catalogus supermagnete.nl," pp. 1–77, 2014. [Online]. Available: http://www.supermagnete.nl/catalog.pdf

[51] Electronics and Electrical Engineering Laboratory, National Instutute of Standards and Technology, *Measurements for Competitiveness in Electronics*. DIANE Publishing Company, 1994.

[52] ITACA. (2014) 5.1 the magnetisation curve. [Online]. Available: http://www.itacanet.org/basic-electrical-engineering/part-5-magnetic-materials/

[53] K&J Magnetics, Inc., "The original k&j magnet calculator." [Online]. Available: http://www.kjmagnetics.com/calculator.asp

[54] ——, "The k&j plate thickness calculator." [Online]. Available: http://www.kjmagnetics.com/thickness.calculator.asp

[55] D. Meek, "femm4.2," 2013. [Online]. Available: http://www.femm.info/wiki/HomePage

[56] Trespa International B.V., "Materiaaleigenschappentabel trespa meteon," pp. 1–2, 1 October 2012 2012. [Online]. Available: http://www.trespa.info/Images/codeN8001_Trespa_Materiaaleigenschappentabel_versie3%202_datum01-10-2012_tcm37-46522.pdf

[57] Plastica Plaat B.V., "Plastica massief nt technische informatie," pp. 1–7. [Online]. Available: http://www.plastica.nl/~/media/Files/PDF/Plastica_MassiefNT_technisch_1.ashx

[58] Milin B.V., "Technisch datablad mylit," p. 1, 2014. [Online]. Available: http://www.milin.nl/app/webroot/themed/milin/files/user_generated/Milyt-Technisch-datablad.pdf.pdf

[59] K. Stlne, *Hygro-Mechanics of Wood Fibre Composite Materials.* Lund University, 2009. [Online]. Available: http://www.byggmek.lth.se/fileadmin/byggnadsmekanik/publications/tvsm1000/web1022.pdf

[60] eFunda, Inc., “Simply supported rectangular plate with point load.” [Online]. Available: http://www.efunda.com/formulae/solid_mechanics/plates/calculators/SSSS_PPoint.cfm

[61] ——, “Simply supported rectangular plate with uniformly distributed loading.” [Online]. Available: http://www.efunda.com/formulae/solid_mechanics/plates/calculators/SSSS_PUniform.cfm

[62] V. Hayward and O. R. Astley, *Performance measures for haptic interfaces.* Springer, 1996, pp. 195–206.